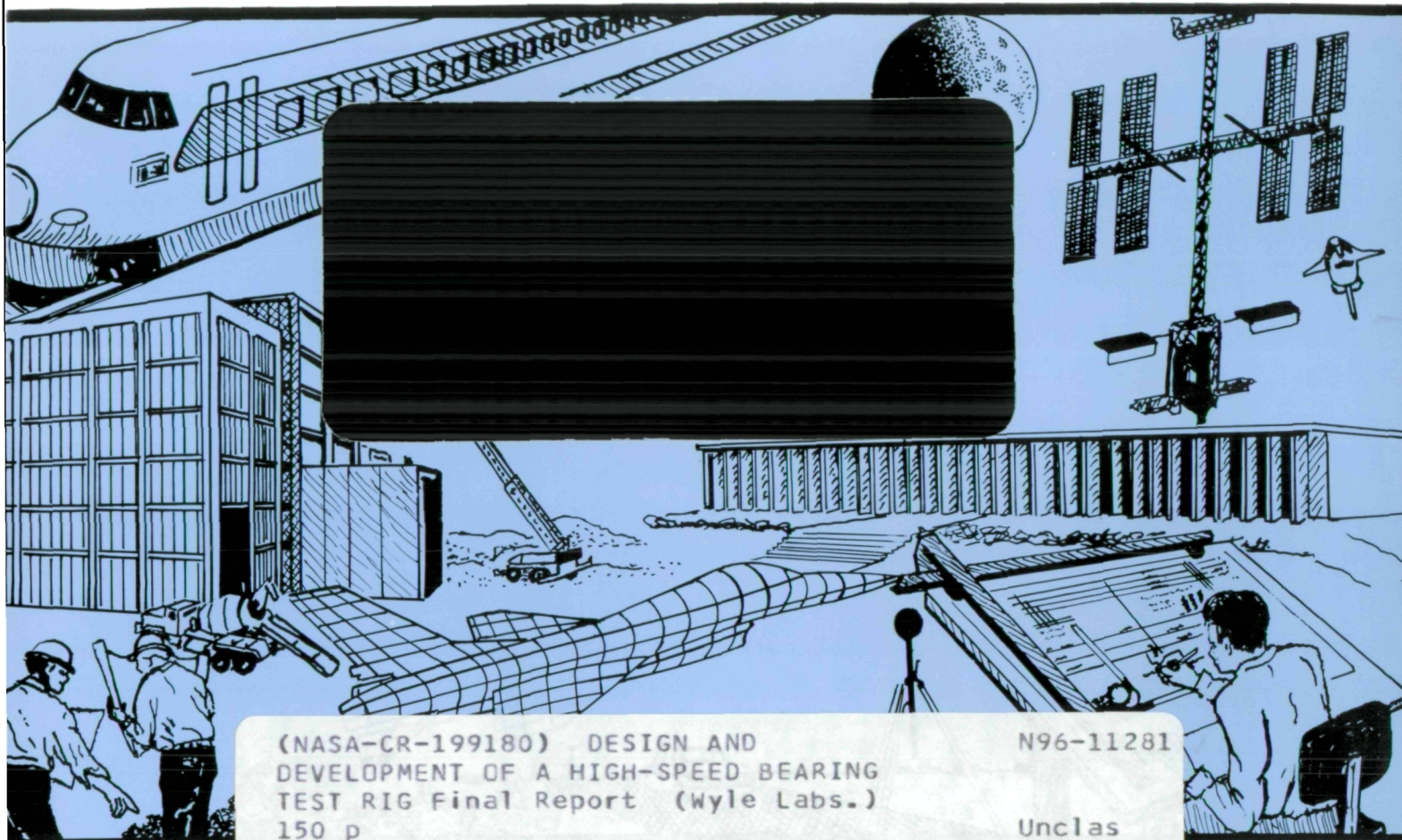


NASA-CR-199180

WYLE
LABORATORIES

ORIGINAL CONTAINS
COLOR ILLUSTRATIONS



(NASA-CR-199180) DESIGN AND
DEVELOPMENT OF A HIGH-SPEED BEARING
TEST RIG Final Report (Wyle Labs.)
150 p

N96-11281

Unclas

G3/09 0064559

Engineering Report

**WYLE LABORATORIES - ENGINEERING
TECHNICAL REPORT 61820-01**

**DESIGN AND DEVELOPMENT
OF A
HIGH-SPEED BEARING TEST RIG**

by

J. A. Cockburn

**An interim report of
work performed under contract NAS8-38095**

for

**NATIONAL AERONAUTICS AND SPACE ADMINISTRATION
GEORGE C. MARSHALL SPACE FLIGHT CENTER
MARSHALL SPACE FLIGHT CENTER, ALABAMA 35812**

June 1995

wyle
laboratories

TABLE OF CONTENTS

	Page
1.0 INTRODUCTION	1
2.0 SURVEY OF PREVIOUS WORK	3
2.1 Rolling Element Bearing Test Rigs	3
2.1.1 SSME Simulators	4
2.1.2 Bearings with Known Defects	5
2.1.3 Basic Research Rigs	6
2.2 Oil Film Bearing Test Rigs	8
3.0 TEST RIG DESIGN DESCRIPTION	11
3.1 Desired Test Rig Characteristics	11
3.2 Description of the Test Rig Design	15
3.2.1 Test Bearing Driveshaft Assembly	15
3.2.2 Test Bearing Housing	17
3.2.3 Layshaft Assembly	17
3.2.4 Drive Motor and Motor Controller	18
3.2.5 Lubrication Module	18
3.2.6 Inertia Mass	19
3.2.7 Baseframe Assembly	20
3.3 Instrumentation	20
3.4 Test Rig Bearings	21
4.0 CONCLUDING REMARKS	22
REFERENCES	24
APPENDIX A Bearing Test Rig Survey Data	
APPENDIX B Selected Bibliography of Oil-Film Bearing Experimental Studies	
APPENDIX C Design Drawings and Parts Breakdown for the High-Speed Bearing Test Rig	
APPENDIX D DC Drive Motor and DC Controller - Technical Literature	
APPENDIX E Central Lubrication Module - Technical Literature	
APPENDIX F Instrumentation Details - Technical Literature	

1.0 INTRODUCTION

This interim report describes the work accomplished to date on the development of a high-speed test rig to be used for compiling an experimental data base of bearing signatures for bearings with known faults. The development of the test rig is part of a much larger program entitled "Detection of Degradation in Turbomachinery Bearings," being conducted for the NASA Marshall Space Flight Center under contract number NAS8-38095. The ultimate objective of the program is to develop a reliable method for the detection of degradation in bearings, particularly the onset of incipient failure, through the use of instrumentation and signature analysis techniques.

Originally, the program was aimed at angular contact ball bearings of the type used in the Space Shuttle Main Engine (SSME) turbopumps. An extensive literature review was conducted to evaluate previous experimental studies of rolling element bearing dynamics, in particular the details of the test rig design, the operating conditions for the bearings, and the type of instrumentation adopted. Based upon the results of this literature review, a test rig design concept was developed for testing rolling element bearings under radial and axial loads at speeds up to 30,000 RPM.

Shortly after this initial concept design was formulated, there was some transfer of emphasis by NASA from rolling element bearings to fluid-film bearings in SSME turbopump applications. As a result of this shift in emphasis, work on the development of the test rig design was put on hold and a review of experimental work with oil-film bearing test rigs and squeeze film damper test rigs was conducted. The primary aim of this review was to identify the most important fluid-film bearing test rig characteristics so as to incorporate these into a re-design of the original test rig. The ultimate objective of the test rig now under development is to be able to perform bearing tests for both rolling element bearings and fluid-film bearings using the same basic test apparatus.

The current bearing test rig design can be adapted to test oil-film bearings as well as rolling element bearings. This is achieved by mounting the test bearing in one of two special test housings, either of which can be mounted onto a common test shaft which can be driven up to 30,000 RPM. The test bearing housing for the rolling element bearings can accommodate proximity displacement transducers, accelerometers, thermocouples, and acoustic emission sensors. The test bearing housing for the fluid-film bearings can accommodate the same instrumentation, and in addition can accommodate Bourdon tube-type transducers for measuring oil film pressures around the bearing circumference.

One area of concern in developing the concept design for the test rig was the requirement to be able to circulate cryogenic fluid through the test bearings during performance test runs. Previous experimental studies of rolling element and fluid-film bearings have reported results for a range of different fluids (in addition to oil), such as: water, Freon 113, LN₂, LOX, and RP-1 kerosene. The experiments performed with LN₂ as the fluid medium involved long chill-down periods for the apparatus prior to each test run to ensure liquid flow rather than gaseous flow through the test bearing. These chill-down periods were in excess of 2 hours. The actual flow rates during test runs were as high as 4.6 lb/sec in order to simulate SSME operating conditions. It is estimated that the 2 hour chill-down periods consumed approximately 700 lb of LN₂, and that a typical test run consumed a further 200 lb to 300 lb of LN₂. In testing which involves cryogenic fluids, the chill-down period is essential so as to prevent the fluid medium from changing to a gas as it flows through the bearing during testing. Thus, it can be seen that prohibitive amounts of cryogenic fluid are required in order to accomplish this type of testing and at the same time obtain meaningful results.

An alternative to cryogenic fluids, however, is to use a fluid such as water, which has a kinematic viscosity not too far removed from the kinematic viscosity of LOX (typically 16 ft²/sec for water versus 3 ft²/sec for LOX). Other test fluids which have been considered are Kerosene (39 ft²/sec), Freon 12 (3.29 ft²/sec), Freon 113 (7 ft²/sec) and RPI (39 ft²/sec). Thus the Reynolds Number ($Re = VL/\gamma$) for the actual LOX flow conditions can be simulated fairly closely by using water as the test medium. A more detailed discussion of previous testing involving these alternative lubricants is presented in Section 2.0 "Survey of Previous Work."

Following the survey of previous experimental work in Section 2.0, a complete description of the bearing test rig design is presented in Section 3.0. This description includes complete mechanical details as well as a description of the proposed instrumentation to be adopted for bearing investigations.

2.0 SURVEY OF PREVIOUS WORK

2.1 Rolling Element Bearing Test Rigs

An extensive review of the available literature was conducted in order to take advantage of promising mechanical design and instrumentation concepts adopted during previous bearing test programs. Of special interest were previous studies involving bearing health monitoring instrumentation or bearing fault diagnosis techniques. The experimental studies described in the literature generally fell into one of the following categories:

- (1) Bearing experimental studies involving direct simulation of SSME turbopump bearing operating conditions. These investigations were conducted using test rigs modeled directly after the SSME turbopump geometry, using actual turbopump bearings, large available quantities of cryogenic fluid, and prime movers capable of providing operating speeds up to 30,000 RPM.
- (2) Simple bearing test rigs developed exclusively for fault monitoring and diagnostic investigations. These test rigs were used for testing bearings with known defects, usually at low speeds.
- (3) Basic research rigs developed for fundamental experimental studies of bearing behavior over a wide range of operating conditions, not necessarily related to fault diagnosis studies.

For each bearing test rig surveyed, the following characteristics were noted:

- Experiment objectives
- Test bearing type
- Details of prime mover
- Maximum test speed and technique for achieving high rpm
- Bearing test loads (axial and radial)
- Method used to apply loads
- Type of instrumentation and summary of measurements
- Any other relevant information

A detailed description of these different classes of experimental test rig is presented in the following paragraphs. In addition, a brief summary of these test rigs is presented in Appendix A.

2.1.1 SSME Simulators

Gleeson et al (Reference 1) investigated the transfer of film lubrication from the bearing cage retainer to the ball/race interfaces. The test rig was operated up to 28,400 RPM using a 50 HP variable speed electric motor and a step-up gearbox. The test ball bearings were 45 mm bore and axial bearing loads of 800 lb were applied. Actual measurements were limited to outer race temperatures. During the test runs, the bearings were cooled by LN_2 , though no tests were actually conducted at cryogenic temperatures.

Keba and Beatty (Reference 2) reported results from two different bearing testers built for operation in LOX. Experiment objectives were to examine bearing wear and the adequacy of cooling provided by the LOX flow, as well as the study of local vaporization of the coolant. Ball bearings of 57 mm bore and 85 mm bore were tested up to 30,000 RPM and 5300 RPM respectively under axial pre-loads ranging from 500 lb to 4500 lb. Instrumentation was provided to measure LOX coolant flow rates through the test bearings, LOX pressures, shaft speeds, and axial bearing loads. Flow rates for the LOX coolant ranged from 3 to 18 lb/sec.

Hampson et al (Reference 3) used fiber optic deflectometers (up to 6 per bearing) to measure outer race radial deflections caused by ball passage during operation. The test rig consisted of a high pressure bearing monitor tester, capable of simulating high-pressure oxidizer turbopump conditions of speed, axial load, and coolant flow rates; namely, 30,000 RPM, 500 lb, and 30 gal/min of LN_2 respectively. Other instrumentation consisted of accelerometers on the bearing housings and pressure and temperature probes upstream and downstream of the test bearings to monitor LN_2 coolant conditions. The fiber optic deflectometers, manufactured by MTI of Latham, NY, provide an electrical signal which is proportional to the bearing race surface deflection.

Dolan et al (Reference 4) reported on bearing thermal limit tests conducted in LN_2 using the NASA/MSFC Bearing and Seal Materials Tester (BSMT) installed in a remotely operated test stand. A diesel engine coupled to a speed-increaser gearbox provided test speeds up to 30,000 RPM. Test bearings were 57 mm bore ball bearings, and axial preloads ranging from 300 lb to 2500 lb were applied. Experimental measurements consisted of bearing temperatures, LN_2 flow rates and pressures, as well as post-test physical inspection of the bearings. A 2-hour chill period was imposed prior to each test run, and during the actual test runs, the flow rate of LN_2 was 4.6 lb/sec. This test rig was also used by Jolly et al (Reference 5) to investigate the performance of a prototype acoustic emission coupler. The acoustic coupler was installed in the bearing housing such that the instrument probe was in contact with the outer surface of the ball

bearing outer race. The experimental results indicated that the acoustic coupler design could be used in the high noise, cryogenic environment of the test rig, and would be able to detect increased bearing noise due to worn or damaged bearings. There was some concern, however, that cavitation noise could possibly mask the bearing noise although no cavitation actually occurred during these experiments.

2.1.2 Bearings with Known Defects

Experiments using ball bearings with intentionally introduced defects were reported by Tandon & Nakra (Reference 6). A two-microphone sound intensity technique was used to examine the change in the intensity frequency spectrum due to the defects. 15 mm bore bearings were tested at speeds up to 1500 RPM with radial loads of 220 lb. The noise from the drive motor and support bearings was shielded using Plexiglas panels lined with absorbing foam. The test results showed that detectability of an outer race defect was much better than that of an inner race or ball defect. This was probably due to shielding effects, since the two-microphone probe was placed 100 mm away from the test bearing in a radial direction.

The use of an acoustic emission technique for bearing health monitoring studies was reported by Hawnan and Galinaitis (Reference 7). Two-inch bore ball bearings were loaded axially to 2400 lb at speeds up to 5700 RPM in a low-speed ball bearing test rig. Acoustic emissions were measured using patented Point Contact Transducers (PCT's) developed by United Technologies Research Center. The PCT's were mounted through the bearing housings so that the sensing elements were held in firm contact with the outer race. An accelerometer was mounted to the bearing housing immediately over the test bearing location for signal comparison purposes. Bearings containing carefully controlled defects were subjected to short test runs while data was acquired and digitized from both the acoustic emission probes and the accelerometer. The ability to detect small defects through acoustic emission monitoring was clearly demonstrated as a result of these experiments.

Experiments using a proximity transducer technique for bearing health monitoring were carried out by Kim (Reference 8) using 15 mm bore ball bearings with controlled defects in both inner and outer races. The test bearings were subjected to radial loads up to 900 lb at test speeds of 2450 RPM. An eddy current proximity transducer, similar to that originally used by Bently and Harker (Reference 9) was adopted for this experimental study. The probe monitored the elastic deformation of the outer race as each rolling element passed the probe sensing surface. It was demonstrated that this measurement technique could detect inner race damage as well as outer race damage. A comparison with other detection methods such as the "shock pulse method,"

"kurtosis analysis," "cepstrum analysis" and a high-frequency resonance technique was also presented.

Experimental studies using a low-speed ball bearing test rig housed within a soundproof enclosure were reported by Igarashi et al (References 10 and 11). The radial vibration velocity of the bearing outer ring was monitored during test runs on single row, deep groove, ball bearings under axial loads at speeds up to 1800 RPM. Multiple dents were deliberately introduced to the bearing races prior to the test runs. The velocity transducer was of the moving coil converter type. A condenser microphone was used to acquire sound pressure levels at various points around the test bearing while the test bearings with known defects were operated under load.

An earlier study of the detection of incipient failure in bearings was reported by Balderston (Reference 12). A test rig based upon a standard lubricant tester was used to investigate angular contact ball bearings with known defects while operating at speeds up to 10,000 RPM. Accelerometer transducers were mounted on the bearing housing over the test bearing and the data was recorded on a 14-channel tape recorder. Analysis of the data was carried out by using a reduced playback speed in conjunction with a power spectrum analyzer. Direct correlation of the severity of defects with signal amplitudes was observed within specific bandwidths.

2.1.3 Basic Research Rigs

A high-speed (12,000 RPM maximum) bearing test rig for investigating angular contact ball bearings was reported by Falcon and Andrew (Reference 13). Inductive displacement transducers embedded in the outer race were used to measure race deflections under each ball for 55 mm bore bearings subjected to axial loads up to 3000 lb at speeds up to 12,000 RPM. The bearing test rig consisted of a spindle mounted vertically in support bearings and carrying a housing for the test bearing. The housing was loaded axially relative to the spindle, either by means of dead weights or hydraulically via oil pressure. The test spindle was driven by an electric motor through a flat belt and pulley arrangement. Three inductive displacement transducers were installed around the outer race, 10 degrees apart, in order to measure the deflections caused by each ball. Contact angles were deduced from the measurements of the sub-surface displacements in the race, and these angles were then compared to predicted values from a number of different theories.

A high-speed roller bearing test rig capable of operating up to 3 million DN was described by Bowen and Murphy (Reference 14). The test rig was powered by an industrial engine driving

through a step-up gearbox. Maximum test speed was 26,100 RPM and the test bearings were 115 mm bore roller bearings, loaded with a 600 lb radial load. The investigation was carried out to evaluate the performance of hollow cylindrical rollers at high speeds. Instrumentation and measurements consisted of thermocouples to measure the bearing outer race and lubricant temperatures, a torque sensor between the motor and gearbox, and post-test measurement of wear in the test bearings. The test shaft was supported at each end by 55 mm bore slave bearings with the test bearing and housing assembly located at the approximate mid-point between the slave bearings.

A test rig utilizing optical measurements to determine the local oil film thickness in cylindrical roller bearings was developed by Pemberton and Cameron (Reference 15). This test rig was a low-speed roller bearing test rig driven by a 3 HP electric motor at speeds up to 3,000 RPM. A specially designed sapphire window was installed in the outer race of a 65 mm bore cylindrical roller bearing. A Xenon laser and flash lamp were used for observation of the oil film, and the oil film characteristics were viewed by a microscope and recorded via a 35 mm camera as well as a video recorder. One of the main purposes of this experimental study was to examine the oil inlet boundary at the edge of the roller and the effects of oil starvation. Other instrumentation included thermocouples to measure oil temperature, a magnetic pick-up to measure cage speed, and a fiber optic scanner to detect the passage of individual rollers.

A high speed roller bearing test rig used for studies at DN values in excess of 1 million was reported by Markho, Smith and Lalor (Reference 16). This bearing test rig was a sophisticated research facility with provisions for the measurement of cage and roller speeds, bearing torque, bearing load, and bearing ring temperatures. An AC motor driving through a two-stage flat belt and pulley system produced a rotational speed of 22,500 RPM in the 63.5 mm bore cylindrical roller test bearing. A full complement of instrumentation was incorporated into the research rig, and this included load cells for measuring radial load and friction torque, inductive displacement transducers for measuring inner and outer ring motions, magnetic pickup for measuring cage speed, laser doppler anemometer for measuring roller surface velocity, thermocouples for outer ring temperatures and lubricant temperatures, infrared radiation thermometer for inner ring temperatures, and a photoelectric transducer for measuring the speed of the test shaft.

Gupta, Dill and Bandow (Reference 17) investigated angular contact ball bearings operating at 2 million DN (100 mm bore, 20,000 RPM rotational speed). The test rig was driven by a 50 HP electric motor having a variable speed drive, connected to a step-up gearbox. Proximity probes were arranged to measure both radial and axial displacements of the bearing cage, and

thermocouples were located on the inner and outer races in the oil supply jets and in the oil scavenge ports. Angular velocity of the bearing cage was measured by using two photonic sensors, arranged 180 degrees apart, which were focused on a grid pattern etched into the rim of the cage. In addition, a magnetic pickup was used to measure shaft speed, and a thin section of the driveshaft between the support bearing and the test bearing was instrumented with strain gages to measure shaft bending and axial loads as well as shaft torsion. The experimental results were compared with theoretical predictions of the dynamic of angular contact ball bearings obtained from the "DREB" and "RAPIDREB" computer programs developed by Gupta (Reference 18).

A laboratory bearing test rig to study wear and failure mechanisms in high speed roller bearings was reported by Savaskan and Veinot (Reference 19). The test rig was designed to allow long duration wear testing of three bearings simultaneously. After test runs of 720 hours duration, wear of the cylindrical roller bearings was monitored by using ferrography and atomic adsorption oil analysis. Test bearings of 25 mm bore were driven at 26,000 RPM with a nominal radial load applied. The test shaft was driven by a 15 HP AC motor through a flat belt speed increaser having a 15 to 1 step-up ratio. Instrumentation consisted of strain gages on the driveshaft to sense radial load, fiber optic light guides to measure rotational speeds of the shaft and the bearing cages, and thermocouples to measure bearing outer race and lubricating oil temperatures. Wear debris particles collected from the bearings by ferrography were studied with scanning electron microscopy.

2.2 Oil Film Bearing Test Rigs

Previous experimental studies involving oil-film bearings and squeeze film dampers were reviewed extensively for their applicability to the present test rig design. Of particular interest were high-speed test rigs (20,000 - 30,000 RPM) and the type of instrumentation adopted. An extensive bibliography of this previous experimental work is presented in Appendix B.

One highly notable test rig for testing journal bearings at high speeds was reported by Woolacott and Cooke (Reference 20). The test bearings were run at speeds up to 35,000 RPM under steady loads, and measurements of oil temperatures at different oil flow rates and bearing loads were obtained. The rig was powered by a 75 HP Thyatron controlled DC motor driving through a 40 to 1 step-up gearbox, giving a test bearing speed range of 5,000 to 60,000 RPM. Measurements of journal attitude and eccentricity were obtained using inductive transducers. Pressure tappings connected to calibrated Bourdon-type pressure gages were used to monitor oil pressures in the oil inlet region and around the oil groove in the test bearing.

The use of on-rotor instrumentation and slip ring telemetry in a fluid film journal bearing test rig was described by Read and Flack (Reference 21) and Flack et al (Reference 22). The on-rotor instrumentation consisted of a high frequency pressure transducer, two eddy current displacement probes and a copper-constantan thermocouple, all imbedded in the shaft. The data from these transducers was amplified with on-shaft amplifiers and transmitted to ground-mounted equipment via slip rings. The ground-mounted instrumentation included 4 static pressure taps in the bearing surface, 10 thermocouples mounted at the bearing surface at different circumferential locations, 12 eddy current probes to monitor relative displacement between bearing and rotor, a rotameter to measure oil flow rates, 2 load cells for bearing load measurements and a torque monitor mounted on the bearing housing to determine power loss in the test bearing. The extensive external instrumentation allowed for detailed comparison with the on-shaft instrumentation.

The application of a non-contacting fiber optic probe to measure displacements in a squeeze film damper was described by Tichy (Reference 23). The probe operated by reflecting a transmitted light beam off the surface for which the displacement was to be measured. The change in intensity of the reflected light signal was proportional to the change in displacement. In situ calibration of the fiber optic probe was required. A high speed oil-film bearing rig using Freon 113 as the working fluid was reported by Murphy and Wagner (Reference 24). The high density Freon derivative was adopted because of its hydrodynamic similarity to cryogenic turbopump propellants. The test speed was 22,700 RPM, and rotor dynamic coefficients were determined for a pair of hydrostatic radial bearings. Eddy current displacement probes imbedded in the stator were used to measure the orbital pattern of the rotor motion.

A high speed bearing test rig used for testing combined hydrostatic/hydrodynamic bearings with hot water as the working fluid was developed by Kurtin et al (Reference 25). Such hybrid bearings have been proposed to replace the rolling element bearings used in the SSME high pressure turbopump. By adopting water at 54°C as the working fluid, high Reynolds numbers (up to 16,500) were achieved for the flow in the bearing land areas without having to resort to the use of cryogenic fluids. The rotational speed of the test shaft was 25,000 RPM, obtained by using a step-up gearbox with a 125 HP electric motor as the prime mover. Instrumentation included eddy current type proximity sensors for the measurement of bearing relative position, strain gage-type pressure transducers for the measurement of supply annulus pressure and bearing recess pressures, a turbine flow meter to measure flow rate through the bearing, and a strain-gage load cell and loading yoke to determine static bearing loads and the force

measurements necessary to calculate frictional torque. In addition, thermocouples were provided for determining fluid temperatures at various locations within the bearing, and accelerometers were used to derive dynamic coefficients for the bearing. During the test runs it was possible to induce cavitation damage in the bearing recesses.

3.0 TEST RIG DESIGN DESCRIPTION

3.1 Desired Test Rig Characteristics

As a result of the survey of previous work, and discussions with NASA/MSFC, a set of test rig design requirements was formulated, as follows:

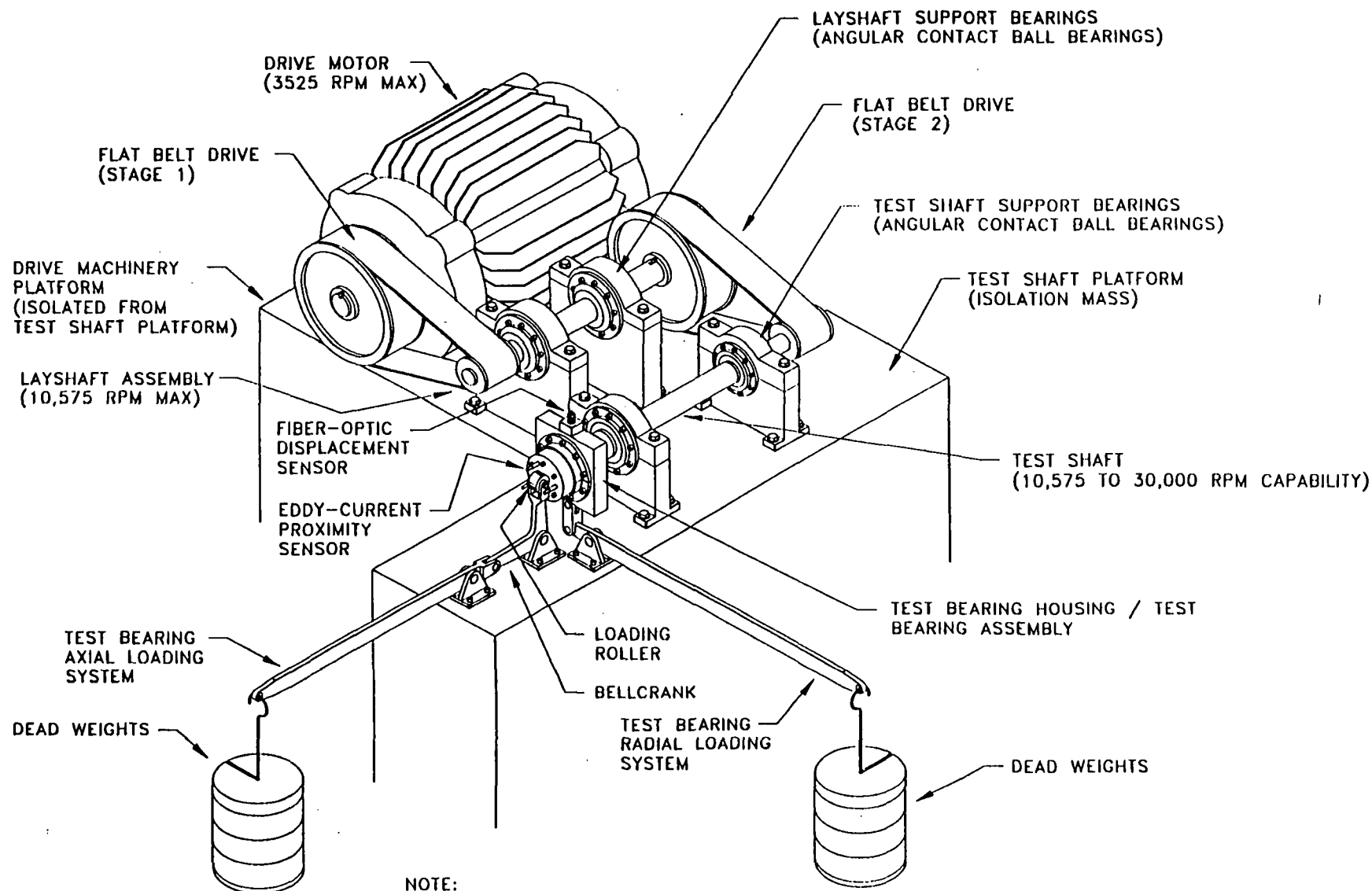
- Ball bearings with a 45 mm bore angular contact were selected as the test bearings.
- The basic test rig should be capable of operation up to at least 30,000 RPM. Bearing tests will thus be conducted at the same DN values as the SSME turbopump end bearings, i.e., approximately 1.35 million.
- An electric motor and two-stage flat belt drive system was adopted as the preferred method of achieving the necessary high rotational speed of the test shaft. This approach is simple, cost-effective, and minimizes extraneous vibrations input to the test bearing. Speed control of the electric motor to within a close tolerance was also considered desirable.
- Radial and axial test loads should be applied to the test bearing housing through deadweights and lever arms. This simplifies the test rig and avoids the necessity for hydraulic cylinders and a hydraulic power supply. Assuming a ten to one mechanical advantage, the required test weights for axial and radial loading of the 45 mm bore test bearing will be less than 100 lb for most test runs.
- The test bearing housing should be designed to accommodate an extensive complement of instrumentation. Types of instrumentation that should be accommodated during the test program includes the following:
 - *Proximity displacement transducers for measuring bearing outer race and cage motions.* The proximity transducers may be inductive or eddy current type. Typical sensitivity for this type of transducer is 60 mV/mil, DC to 10 kHz. Inductive displacement transducers were used by Falcon and Andrew (Reference 13) and Markho et al (Reference 16) in angular contact and roller bearing studies, respectively. Eddy current proximity transducers were used by Kim (Reference 8) to detect damage in both inner and outer races of ball bearings.
 - *Fiber optic displacement transducers for measuring deflections of the bearing outer race.* Typical sensitivity for this type of transducer is 50 mV/mil, DC to 70 kHz. Fiber optic sensors (as well as proximity displacement transducers) were used

successfully by Gupta et al (Reference 17) to measure radial and axial cage motions and cage rotational speed in angular contact ball bearings.

- *Accelerometers for monitoring the vibrations transmitted to the external surface of the test bearing housing.*
 - *Thermocouples for measuring inlet and outlet oil temperatures in the vicinity of the contact area.*
 - *Acoustic emission sensor mounted to the external surface of the test bearing housing.*
 - *Photoelectric detector or similar device for measuring test shaft speed.*
- The test bearing housing should be designed to accept the flow of cryogenic fluid, such as LN₂, during bearing test programs. This will provide an option for testing bearings with known faults under low temperature conditions as well as ambient temperature conditions.

A preliminary concept for the bearing test rig is illustrated in Figure 1. An electric drive motor is coupled to an intermediate shaft, or layshaft, through a flat belt. The layshaft, which is supported in pedestal bearings, in turn drives the test shaft via a second flat belt. This two stage step-up drive system provides an overall speed ratio of around 9 to 1, so that for a 3500 RPM electric motor, the test shaft rotational speed will be 30,000 RPM or greater. The test shaft is supported in pedestal bearings, and the test bearing is contained within a special bearing housing which fits over the end of the driveshaft as shown. Axial and radial loading of the test bearing is accomplished through the use of deadweights and lever arms as shown in Figure 1.

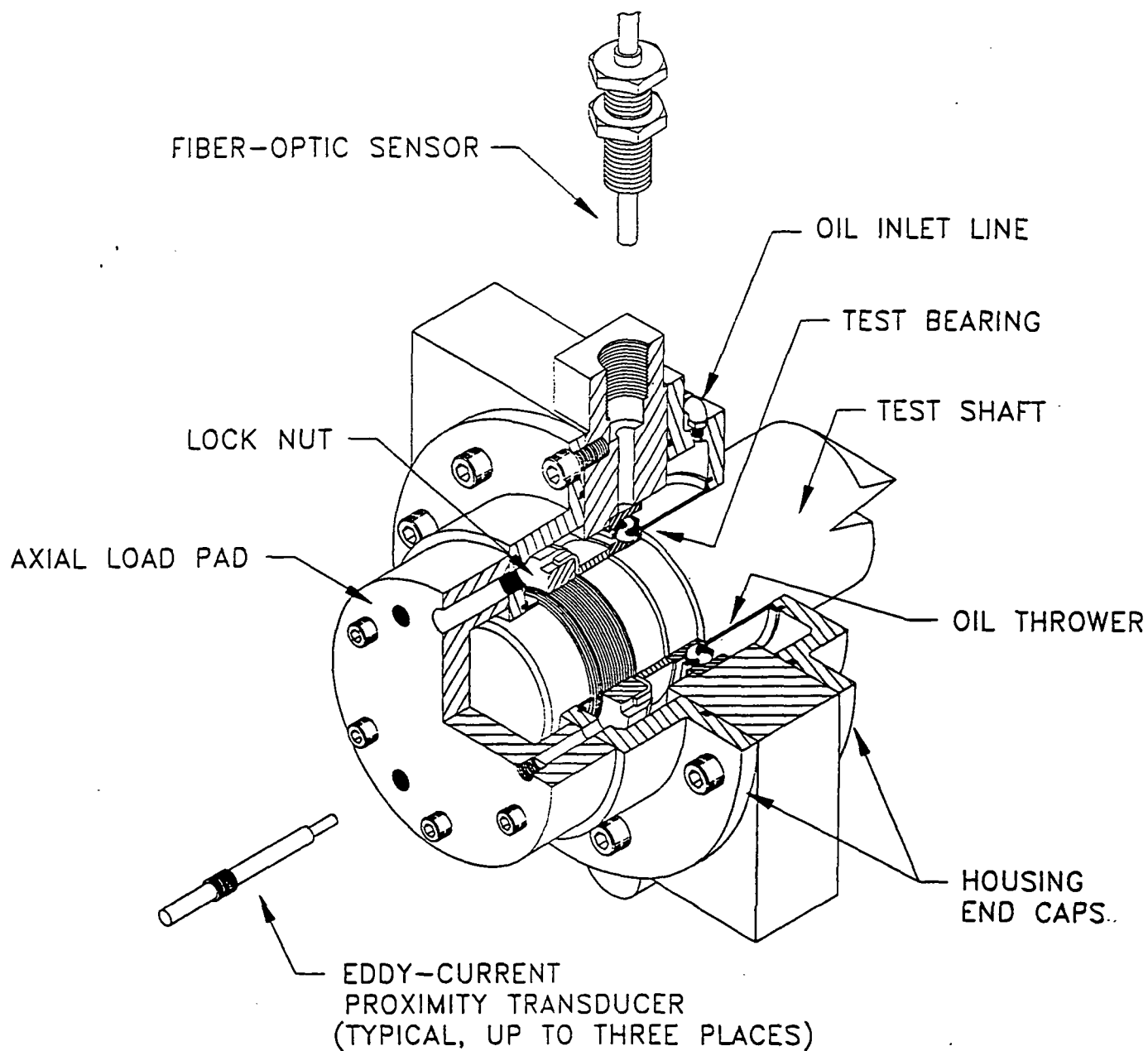
A preliminary concept for the test bearing housing is shown in Figure 2. The housing is designed to apply an initial axial preload to the bearing upon final assembly. Axial loads are superimposed on the preload by the deadweights and lever arms. The housing is designed to accept eddy-current proximity displacement transducers, and a fiber optic displacement transducer, as shown in Figure 2. In addition, the test bearing housing may accept acoustic emission transducers, accelerometers, and thermocouple feedthroughs.



NOTE:
OIL SUPPLY AND SCAVENGE LINES
TO/FROM LAYSHAFT BEARINGS, TEST
SHAFT SUPPORT BEARINGS AND TEST
BEARING HOUSING NOT SHOWN.

WYLE LABORATORIES	BASIC TURBOMACHINERY BEARING TEST RIG
-----------------------------	--

Figure 1. Preliminary Concept for Bearing Test Rig



\82180\ISO-2
RCR 2/25/92

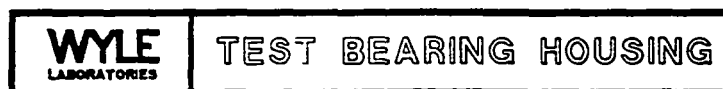


Figure 2. Preliminary Concept for Test Bearing Housing

3.2 Description of the Test Rig Design

The high-speed bearing test rig consists of a test bearing driveshaft assembly which is mounted on a heavy inertia mass. This inertia mass is in turn supported by a large baseframe (approximately 6 ft x 5 ft) mounted on casters. The inertia mass weighs approximately 1300 lb and provides a sufficiently rigid platform for the high speed test shaft. The test shaft is belt driven from an adjacent layshaft assembly which is also supported by the large baseframe. The layshaft is powered by a 50 HP DC electric motor mounted on the baseframe assembly. The drive from the motor to the layshaft is also through a flat belt. A motor controller is also mounted on the baseframe assembly adjacent to the DC motor. Motor speed is adjustable from zero to 3500 RPM with speed regulation to 0.01 percent.

Design details of the high speed bearing test rig are documented on the drawings contained in Appendix C. A listing of these drawings is as follows:

- | | |
|---------------------------|---|
| • SK61820-1000 (3 sheets) | "High Speed Bearing Test Rig"
(Top Assembly Drawing) |
| • SK61820-100 (4 sheets) | "Test Bearing Driveshaft Assembly" |
| • SK61820-101 (1 sheet) | "Driveshaft" |
| • SK61820-111 (1 sheet) | "Test Housing" |
| • SK61820-200 (2 sheets) | "Layshaft Assembly" |
| • SK61820-201 (1 sheet) | "Layshaft" |
| • SK61820-300 (1 sheet) | "Inertia Mass Assembly" |
| • SK61820-400 (1 sheet) | "Baseframe Weldment" |

A complete breakdown of the individual parts for the high speed bearing test rig is also contained in Appendix C.

A brief description of the major components is presented in the following paragraphs.

3.2.1 Test Bearing Driveshaft Assembly

The driveshaft assembly which is described on drawing SK61820-100 (see Appendix C), consists of a 316 stainless steel shaft supported by two preloaded pairs of back-to-back angular contact ball bearings. The support bearings are housed in a rigid mild steel housing, and each bearing is individually lubricated from a central lubrication module. The driveshaft housing is bolted to a 3/4 in. thick steel plate which forms the top surface of the inertia mass. The bearing to be tested is mounted on one end of the driveshaft as shown in the assembly drawing

(SK61820-100, sheet 1). The test bearing is fitted into a test housing which rides on the end of the shaft. The inner race of the angular contact test bearing is held in place by the locknut on the end of the driveshaft. The test bearing is preloaded axially by the end cover on the test housing which applies the necessary preload through an accurately machined spacer (find number 25 of Drawing No. SK61820-100).

The material selection for the driveshaft (316 stainless steel) was based upon the need for high impact strength at low temperatures (e.g. 110 ft lb Izod at -320°F) as well as a satisfactory fatigue endurance limit (38,000 lb/in² minimum for 316 stainless). By selecting this grade of stainless steel it will be possible to run bearing tests at ambient temperature and at very low temperatures (using LN₂ to chill the test bearings) without having to change driveshaft materials. At one stage during the design, a thermal isolation section was considered for the driveshaft. This was essentially a nonmetallic thermal isolator fitted between two sections of the steel driveshaft to isolate the test bearing housing from the rest of the driveshaft. This option was discarded in favor of the stainless steel shaft because of the difficulties in maintaining concentricity between the driveshaft segments and the uncertainties concerning the strength and other physical properties of the nonmetallic section.

The test bearing housing has provisions for applying axial and radial loads to the bearing under test. The radial loads are applied by hanging deadweights on a ten-to-one lever arm which activates a loading clevis attached to the base of the test bearing housing, the line of action of the radial load being through the centerline of the test bearing. Axial loads are similarly applied by hanging deadweights on a ten-to-one lever arm which activates a bell crank and applies an axial load to the test housing end cover via a crowned roller.

The test bearing driveshaft is driven by a "Habasit" flat belt from the layshaft, the slightly crowned aluminum alloy drive pulley being clamped to the end of the driveshaft through a "Trantorque" bushing. The flat drive belts manufactured by Habasit Belting Incorporated are thin, lightweight high-strength belts capable of very high tangential belt speeds, up to 18,000 ft/min. The maximum speed capability of the driveshaft is 31,500 RPM for the present pulley diameters and a maximum drive motor speed of 3500 RPM.

Final lubrication details for the pairs of angular contact ball bearings are not shown on Drawing No. SK61820-100. Because of funding constraints, the central lubrication module was not purchased under the present contract. Final design details for the installation of the lubrication nozzles were, therefore, not included in the assembly drawing. However, the driveshaft

housing has been scarred to accept the lubrication nozzles, and the required machining operations (drilling, reaming, tapping) are considered to be routine.

3.2.2 Test Bearing Housing

The test bearing housing, which is described on Drawing No. SK61820-111, is constructed from 316 stainless steel. The housing is bored to accept 45 mm bore x 85 mm outside diameter angular contact ball bearings as standard test bearings. A series of inlet and outlet ports is provided to accommodate the flow of LN_2 and GN_2 through the test bearing when running tests at near cryogenic temperatures. Also shown on Drawing No. SK61820-111 is the machining required to accept a typical proximity displacement transducer (in this case a Bently Nevada Model 7200) and a typical acoustic emission transducer. Due to funding constraints on the present program, final instrumentation for the bearing test rig was not selected. Therefore, the final machining of the test bearing housing to accept the instrumentation complement is not shown.

3.2.3 Layshaft Assembly

The layshaft assembly, described on drawing No. SK61820-200, consists of a medium carbon steel shaft (AISI 1045) supported by a pair of single row deep groove ball bearings. The support bearings are housed in a rigid mild steel housing (similar to the driveshaft housing described above), and each bearing is lubricated from a central distribution module. The layshaft housing is bolted to a 3/4 in. thick steel plate which is mounted to a support stand assembly which in turn is attached to the baseframe. Final lubrication details for the two ball bearings are not shown on Drawing No. SK61820-200. Due to funding constraints, the central lubrication module was not purchased under the present contract. Final design details for installation of the lubrication nozzles were, therefore, not included in the assembly drawing. However, the layshaft housing has been scarred to accept the lubrication nozzles, and the required machining (i.e. drilling, reaming, tapping) is basically routine.

The layshaft has a 2.75 in. diameter driven pulley attached at one end and a 5.75 in. diameter driving pulley attached at the other end. Both pulleys, which are slightly crowned and fabricated from aluminum alloy, are clamped to the layshaft through "Trantorque" bushings. The maximum speed capability of the layshaft is 10,950 RPM for the present pulley diameters and a maximum drive motor speed of 3500 RPM.

3.2.4 Drive Motor and Motor Controller

The drive motor selected for the bearing test rig is a Reliance DC motor rated at 50 HP at 3500 RPM, 460 volts, Force Ventilated Enclosure with Blower, SC2512ATZ Frame. The DC drive is a Reliance 50 HP, 460 volt, Regenerative, Digital Regulator Maxpak III Drive with the following features:

- Field and Tach Loss Relays
- Motor Blower Starter and Interlock
- 0.01% Speed Regulation
- RD120-2 Tachometer, Digital Feedback
- Digital Speed Indicator mounted on cabinet door
- Wall Mounted Enclosure
- On Pilot Light mounted and wired
- Off Pilot Light mounted and wired
- Speed Pot mounted and wired
- Start Push-button mounted and wired to door
- Stop Push-button mounted and wired to door
- Forward/Reverse Selector Switch mounted and wired
- Run/Jog Selector Switch mounted and wired
- E-Stop Push-button, Mushroom Head mounted and wired
- Dynamic Braking

The installation of the drive motor and motor controller is shown on Drawing No. SK61820-1000. Technical literature describing these two components is contained in Appendix D.

3.2.5 Lubrication Module

The ball bearings specified for the bearing test rig are manufactured by SKF USA Inc. Because of the very high rotational speeds planned for this test rig, SKF were contacted for a recommendation concerning lubrication of the driveshaft support bearings and the layshaft support bearings. It was recommended that oil spot lubrication be adopted, and specifically that a centralized "Oil + Air" lubrication system manufactured by Vogel Lubrication, Inc. should preferably be utilized. The principle of the Vogel oil + air system is that a sufficient sequence of oil droplets is delivered to the friction points within the bearing. The air is used only to transport the small metered oil quantity from the metering unit. Once the oil droplet arrives at the friction point (i.e. nozzle outlet) the air escapes. This system is not an oil mist lubrication system. The chief advantages of this type of lubrication system are as follows:

- Attainment of high-speed parameters for anti-friction bearings (up to approximately 1,500,000 DN)
- Always fresh lubricant at the friction point
- Small consumption of lubricant, approximately 10 percent of an oil mist lubrication system
- Oil selection from a wide viscosity range possible
- Use of oils with EP and adhesive additives
- Elimination of grease replacement times
- Simplified bearing seals are possible
- No oil mist, therefore cleaner components
- Bearing temperatures are lower
- Each bearing is supplied with the required oil quantity at pre-programmed intervals

Manufacturers' literature for the oil + air system is contained in Appendix E. It should be noted that the Lubrication Module has not been shown on the top assembly drawing (SK61820-1000). Due to funding constraints, this unit has not been purchased as part of the bearing test rig. However, the compact nature of the lubrication module (approximately 16 in. wide x 15 in. high x 6 in. deep) will make it a straightforward operation to mount this equipment adjacent to the driveshaft assembly and the layshaft assembly. Details of the actual lubrication nozzles have not been included in the assembly drawings, though the driveshaft and layshaft housings have been scarred to accept the final configuration of lubrication nozzle. A Vogel standard data sheet for an oil + air nozzle is also included in Appendix E.

3.2.6 Inertia Mass

The inertia mass details are contained on Drawing No. SK61820-300. The inertia mass is basically a large concrete block approximately 30 in. long x 18 in. wide x 23 in. high, reinforced with 2 in. x 2 in. x 1/4 in. mild steel angle around all edges and the base. Steel plates 3/4 in. thick are attached to the top surfaces of the inertia mass, and these plates are drilled and tapped to accept the hold-down bolts for the driveshaft housing and the bearing load application hardware. This structure provides a rigid platform for the test bearing driveshaft, and should assist in providing a stable, vibration-free mounting surface. The total weight of the inertia mass is estimated to be approximately 1300 lb. Lifting lugs are provided for hoisting the mass into place onto the base frame assembly.

3.2.7 Baseframe Assembly

The baseframe assembly consists of a baseframe weldment (see Drawing No. SK61820-400) mounted on swivel casters. The baseframe weldment is approximately 66 in. x 54 in. in plan form and it consists of 3 in. x 7.1 lb/ft MC mild steel channel members. Sufficient internal channel members have been included in the design to provide the necessary rigidity. The baseframe also incorporates vertical column members, approximately 40 in. high, welded directly to the baseframe. These vertical members provide the necessary support for the DC motor controller assembly which is basically a wall-mounted enclosure, approximately 27 in. wide x 38 in. high x 15 in. deep. The installation of the motor controller can be seen on Drawing No. SK61820-1000.

3.3 Instrumentation

The test bearing housing design is relatively massive in order to accommodate inlet and outlet ports for the cryogenic fluid, and also to accommodate a wide range of instrumentation. Recommended instrumentation includes the following:

- Proximity displacement transducers
- Fiber optic displacement transducers
- Accelerometers
- Thermocouples
- Acoustic emission sensors

Typical fiber optic displacement transducers include the KD-300 FOTONIC sensor manufactured by MTI Instruments, and PHILTEC fiber optic displacement sensors manufactured by Philtec, Inc. The displacement probe sensitivity for fiber optic sensors can be as high as 2 mV/microinch over small deflection ranges (e.g. 3 mils). Eddy current proximity transducers manufactured by Bently Nevada can also provide sensitivities as high as 2 mV/microinch deflection over a range of 8 mils.

Technical literature for these transducers, provided by MTI Instruments, Philtec, and Bently Nevada, is presented in Appendix F. Also included in this appendix is technical literature for acoustic emission transducers developed by Verde Geoscience. These ultrasonic transducers accurately measure the compressional and shear wave velocities and attenuations of materials under stress. The transducers may be used in either (a) a matched pair mode where one is used to transmit and the other transducer receives the signal through the material under test, or (b) a single transducer mode where the transducer works in a pulse-echo mode. Full details of this transducer design are provided in Appendix F.

The use of acoustic emission transducers to detect impending failure in rolling element bearings has been reported by Rogers (Reference 26) and by Yoshioka and Fujiwara (Reference 27). Rogers described two separate phenomena, (a) the detection of incipient failure of rolling element bearings by kurtosis (i.e., the fourth statistical moment of acceleration response data, or "peakiness" of the acceleration data), and (b) the location of fatigue cracks in slowly rotating bearings by acoustic emission. As part of this work, a slewing crane on a gas production platform was instrumented with acoustic emission sensors to evaluate and monitor sub-critical fatigue crack propagation in the slew ring bearing. Dunegan Endevco 3000 series acoustic emission source location equipment was used to make the wave propagation and signal characterization measurements on the slew ring bearing.

Reference 27 describes an acoustic emission source locating system composed of a single channel acoustic emission instrument, a magnetic detector and a locator. The acoustic emission instrument detected acoustic emissions from the test bearing (a 25 mm bore thrust ball bearing), the magnetic detector determined the position of the balls in the raceway, and the locator defined the ball positions at the time of the acoustic emission. Experimental results showed that the acoustic emission source locating system could precisely locate failure positions on the bearing race. Details of the acoustic emission transducer were not reported.

3.4 Test Rig Bearings

Initially, the test rig design incorporated hydrodynamic oil-film bearings as the support bearings for the test drive shaft. However, because of the very large power losses associated with these oil film bearings at high rotational speeds (typically 20 to 30 HP total for two radial bearings and one thrust bearing at 30,000 RPM) and concerns regarding loss of lubricant flow at high speeds, it was decided to adopt precision angular contact ball bearings instead. The test driveshaft is supported by a pair of 35 mm bore ball bearings at one end, and a pair of 30 mm bore ball bearings at the other end. Each pair of ball bearings is arranged back-to-back with a spacer between. Limiting speeds for these bearing pairs are 36,000 RPM for the 35 mm bore, and 40,500 RPM for the 30 mm bore bearings. The layshaft bearings are supported by 40 mm bore single row deep groove ball bearings (one at each end). The recommended speed limit for these bearings is 13,000 RPM, which is well above the design maximum of approximately 11,000 RPM for the layshaft.

The initial test bearing size for the high speed bearing rig is 45 mm bore x 85 mm outside diameter (SKF 7209C). This bearing was selected because of its similarity to the SSME turbopump bearing geometry and the fact that it is readily available and relatively inexpensive.

This page intentionally left blank.

4.0 CONCLUDING REMARKS

The design of the high speed bearing test rig has been based upon the results of an extensive literature survey to evaluate previous bearing test rigs and instrumentation. The present design has the flexibility to test rolling element bearings at very low temperatures as well as at ambient temperatures. This is achieved by providing internal porting in the test bearing housing and supplying a flow of liquid nitrogen directly to the inlet ports. Downstream of the test bearing, gaseous nitrogen is allowed to vent directly from the housing. Although the test rig is designed primarily for testing angular contact ball bearings, it is a simple matter to test cylindrical roller bearings or oil-film bearings by modifying the test bearing housing or by fabricating a second test bearing housing to accept the oil-film bearing design. Test loads would be applied in exactly the same way, and much of the instrumentation utilized for rolling element bearings may be used for the oil-film test bearings. The test bearing housing is of relatively massive design to enable a full complement of instrumentation to be mounted in close proximity to the bearing under test. The test rig design allows for very accurate speed control (to within 0.01 percent) during the performance of testing, and lubrication of all shaft support bearings is achieved using a centralized oil injection system which meters precise quantities of oil directly to the friction points within each bearing.

Fabrication of the actual bearing test rig is incomplete at this time because of funding constraints on the program. The original contract scope of work has been modified to reflect a major reduction in contract funding. As a result of this contract modification, fabrication of the bearing test rig can be only partially completed. The completed test rig items include the following:

- Test Bearing Driveshaft Assembly - Drawing No. SK61820-100
- Layshaft Assembly - Drawing No. SK61820-200
- Inertia Mass Assembly - Drawing No. SK61820-300

Test rig components that cannot be supplied under the present contract funding are listed on the following page:

Top Assembly Drawing SK61820-1000

<u>Item</u>	<u>Qty.</u>	<u>Part Number</u>	<u>Description</u>
4	1	SK61820-400	Baseframe Weldment
5	1		Drive Motor, Reliance, 50 H.P.
6	1		Motor Controller, Reliance, Digital Regulator MaxPak III
7	1	SK61820-1001	Motor Pulley
9	4		Bolt
10	4		Washer
11	2		Tensioner Bolt
12	39		Bolt
13	78		Washer
14	39		Nut
15	1	6248N14	Belt Guard (McMaster-Carr or equiv.)
16	1	6248N13	Belt Guard (McMaster-Carr or equiv.)
17	4	5010T432	Caster Assembly (McMaster-Carr)
18	1		Lubrication Module (Vogel or equiv.)

Despite the fact that all of the test rig components cannot be purchased/fabricated at the present time, the test rig design documentation has been fully completed (see Appendix C). Thus, the bearing test rig could be completed at some future date if funding was restored to the program.

REFERENCES

1. Gleeson, et al, "Evaluation of Self-lubricating Insert Materials and the BASIC Retainer," NASA CP-3092, 1990.
2. Keba, J. E., and R. F. Beatty, "Rocketdyne LOX Bearing Tester Program," Conference on Advanced Earth-to-Orbit Propulsion Technology, Marshall Space Flight Center, Alabama, May 1988.
3. Hampson, M. E., J. J. Collins, M. R. Randall, and S. Barkhoudarian, "SSME Bearing Health Monitoring Using a Fiberoptic Deflectometer," Conference on Advanced Earth-to-Orbit Propulsion Technology, Marshall Space Flight Center, Alabama, May 1986.
4. Dolan, F. T., H. G. Gibson, J. L. Cannon, and J. C. Cody. "Cryogenic, High Speed, Turbopump Bearing Cooling Requirements," Conference on Advanced Earth-to-Orbit Propulsion Technology, Marshall Space Flight Center, Alabama, May 1988.
5. Jolly, N. D. et al. "Development of an Acoustic Monitor to Detect Incipient Bearing Failure," NASA Conference Publication No. 2436, 1986.
6. Tandon, N., and B. C. Nakra, "The Application of the Sound-Intensity Technique to Defect Detection in Rolling-Element Bearings," *Applied Acoustics*, Vol. 29, 1990, pp. 207-217.
7. Hawman, M. W., and W. S. Galinaitis, "Acoustic Emission Monitoring of Rolling Element Bearings," 1988 Ultrasonics Symposium, *IEEE Proc.*, Vol. 2, pp. 885-889.
8. Kim, P. Y. "Proximity Transducer Technique for Bearing Health Monitoring," *J. Propulsion*, Vol. 3, No. 1, 1987, pp. 84-89.
9. Bently, D. E. and Harker, R. G. "Cost Effective Continuous Monitoring of General Purpose Rotating Machinery," Proceedings of the Seventh Machinery Dynamics Seminar, National Research Council, Canada, Oct. 1982.
10. Igarashi, T., and S. Yabe. "Studies on the Vibration and Sound of Defective Rolling Bearings - Ball Bearings with One Defect," Bulletin of the JSME, Vol. 26, No. 220, Oct. 1983.
11. Igarashi, T., and J. Kato. "Studies on the Vibration and Sound of Defective Rolling Bearings - Ball Bearings with Multiple Defects," Bulletin of the JSME, Vol. 28, No. 237, March 1985.
12. Balderston, H. L. "The Detection of Incipient Failure in Bearings," *Materials Evaluation*, June 1969, pp. 121-128.
13. Falcon, K. C., and C. Andrew. "Angular Contact Ball Bearings: Track Position at High Speeds," *Proc. of Institution of Mechanical Engineers 1969-1970*, Vol. 184, Part 1, No. 19, pp. 351-369.
14. Bowen, W. L., and T. W. Murphy. "High Speed Testing of the Hollow Roller Bearing," Trans. of ASME, *Journal of Lubrication Technology*, Vol. 103, Jan. 1981, pp. 1-5.

15. Pemberton, J. C., and A. Cameron. "Optical Study of the Lubrication of a 65-mm Cylindrical Roller Bearing," *Industrial Lubrication and Tribology*, May/June 1981, pp. 84-94.
16. Markho, P. H., B. V. Smith, and M. J. Lalor. "An Advanced Apparatus for the Study of Roller and Cage Slip in High-Speed Roller Bearings," Transactions of the ASME, *Journal of Lubrication Technology*, Vol. 103, Jan. 1981, pp. 46-54.
17. Gupta, P. K., J. F. Dill, and H. E. Bandon. "Dynamics of Rolling Element Bearings—Experimental Validation of the DREB and RAPIDREB Computer Programs," Transactions of the ASME, *Journal of Tribology*, Vol. 107, Jan. 1985, pp. 132-137.
18. Gupta, P. K. "Dynamics of Rolling Element Bearings, Parts I to IV," ASME Journal of Lubrication Technology, Vol. 101, 1979, pp. 293-326.
19. Savaskan, T., and D. E. Veinot. "On the Wear and Failure of High Speed Roller Bearings," *WEAR*, Vol. 116, No. 3, May 1987, pp. 361-380.
20. Woolacott, R. G., and W. L. Cooke. "Thermal Aspects of Hydrodynamic Journal Bearing Performance at High Speeds," Brochure Instr. Med. Engrs. Vol. 181, Part 3, 1966-67.
21. Read, L. J., and R. D. Flack. "Temperature, Pressure and Film Thickness Measurements for an Offset Half Bearing," *WEAR*, Vol. 117, 1987, pp. 197-210.
22. Flack, R. D., G. J. Kostrzewsky and D. V. Taylor. "A Hydrodynamic Journal Bearing Test Rig with Dynamic Measurement Capabilities," Paper No. 92-TC-4E-3, presented at the ASME/STLE Tribology Conference, Oct. 19-21, 1992.
23. Tichy, J. A. "Measurements of Squeeze-Film Bearing Forces and Pressures, Including the Effect of Fluid Inertia," ASLE Transactions, Vol. 28, No. 4, 1984, pp. 520-526.
24. Murphy, B. T., and M. N. Wagner. "Measurement of Rotodynamic Coefficients for a Hydrostatic Radial Bearing," Transactions of the ASME, Vol. 113, July 1991.
25. Kurtin, K. A., D. Childs, L. San Andres, and K. Hale. "Experimental Versus Theoretical Characteristics of a High-Speed Hybrid Bearing," Transactions of the ASME, Vol. 115, Jan. 1993.
26. Rogers, L. M. "The Application of Vibration Signature Analysis and Acoustic Emission Source Location to On-Line Condition Monitoring of Anti-Friction Bearings." *Tribology International*, April 1979.
27. Yoshioka, T., and T. Fujiwara. "A New Acoustic Emission Source Locating System for the Study of Rolling Contact Fatigue." *WEAR*, Vol. 81, 1982.

APPENDIX A
BEARING TEST RIG SURVEY DATA

SSME SIMULATORS

Bearing Test Rig Survey: SSME Simulators

Author(s), Title, and Year:

Gleeson, et al. "Evaluation of Self-lubricating Insert Materials and the BASIC Retainer," NASA CP-3092, 1990.

Type of Experimental Apparatus:

SSME-related bearing tester with LN₂ cooling.

Experiment Objectives:

Evaluation of transfer film lubrication from ball cage to ball/race interfaces. Endurance test at high speed.

Test Bearing Type:

Ball bearing, 45-mm HPOTP bearing fitted with a self-lubricating retainer (BASIC retainer).

Prime Mover Details:

50-hp variable-speed electric motor driving through a step-up gearbox with 8-to-1 ratio.

Maximum Test Speed: 28,400 rpm

Axial Bearing Load: 800 lb

Radial Bearing Load: None

Load Application Device: No details presented

Instrumentation and Measurements:

Temperature of outer race was measured (no details of transducers given). Experiment consisted mainly of an endurance test to confirm that transfer film lubrication took place. Testing confirmed that both PTFE and bronze were transferred from the retainer to the balls.

Additional Remarks:

Test bearing cooled via liquid nitrogen (LN₂). All tests run at ambient temperature. The insert material in the bearing retainer was "SALOX" material (60 percent bronze, 40 percent PTFE).

Bearing Test Rig Survey: SSME Simulators (Continued)

Author(s), Title, and Year:

Keba, J. E., and R. F. Beatty. "Rocketdyne LOX Bearing Tester Program," Conference on Advanced Earth-to-Orbit Propulsion Technology. Marshall Space Flight Center, Alabama, May 1988.

Type of Experimental Apparatus:

Two SSME-related bearing testers:

- (1) SSME low pressure LOX bearing tester
- (2) SSME high pressure LOX bearing tester

Experiment Objectives:

Examination of bearing wear and adequacy of cooling effects from LOX. Also study the local vaporization of coolant

Test Bearing Type:

Ball bearings, 57-mm bore (high pressure bearing tester) and 85-mm bore (low pressure bearing tester)

Prime Mover Details:

Electric motor (horsepower rating and gearbox details not given)

Maximum Test Speed:

30,000 rpm (high pressure tester), 5300 rpm (low pressure tester)

Axial Bearing Load:

500 lb to 4500 lb (low pressure tester)
1100 lb (high pressure tester)

Radial Bearing Load:

None

Load Application Device:

Pressurized piston acting on outer race (pressurized via LOX). Belleville springs utilized for initial preloads.

Instrumentation and Measurements:

- LOX coolant flow rates through test bearings
- Shaft rotational speed
- LOX pressures
- Axial loads via strain gaged ring.

Additional Remarks:

Liquid oxygen (LOX) flows through test bearings. A gaseous nitrogen (GN₂) purged buffer seal prevents gaseous oxygen (GOX) leakage to atmosphere.

Bearing Test Rig Survey: SSME Simulators (Continued)

Author(s), Title, and Year:

Hampson, M.E., J.J. Collins, M. R. Randall, and S. Barkhoudarian. "SSME Bearing Health Monitoring Using a Fiberoptic Deflectometer," Conference on Advanced Earth-to-Orbit Propulsion Technology, Marshall Space Flight Center, May 1986.

Type of Experimental Apparatus:

High pressure bearing monitoring tester

Experiment Objectives:

Investigation of bearing health monitoring using fiberoptic deflectometers and comparison with accelerometer data

Test Bearing Type:

Two ball bearings (16-ball turbine end configuration, used in high pressure oxidizer turbopump)

Prime Mover Details:

No details given

Maximum Test Speed:

30,000 rpm

Axial Bearing Load:

550 lb

Radial Bearing Load:

None

Load Application Device:

LN₂ pressurized piston

Instrumentation and Measurements:

- Fiberoptic deflectometers used to measure outer race deflections caused by ball passage (six per bearing)
- Accelerometers located on bearing housings (3-axis)
- Pressure and temperature probes upstream and downstream of bearings monitored LN₂ coolant conditions

Additional Remarks:

Fiberoptic deflectometer probe (manufactured by MTI, Latham, N.Y.) utilizes reflected light from bearing outer race surface. Probe tip is 0.125 inches in diameter by 3 inches long.

Bearing Test Rig Survey: SSME Simulators (Concluded)

Author(s), Title, and Year:

Dolan, F. T., H. G. Gibson, J. L. Cannon, and J. C. Cody. "Cryogenic, High Speed, Turbopump Bearing Cooling Requirements," Conference on Advanced Earth-to-Orbit Propulsion Technology, Marshall Space Flight Center, Alabama, May 1988.

Type of Experimental Apparatus:

MSFC bearing and seal materials tester (BSMT)

Experiment Objectives:

Numerous studies to examine bearing thermal limits and verify computer model

Test Bearing Type:

Ball bearings, 57-mm bore

Prime Mover Details:

Diesel engine (455 hp) coupled to speed-increaser gearbox (22 to 1 ratio) driving a quill shaft

Maximum Test Speed:

30,000 rpm

Axial Bearing Load:

300 lb nominal (2500 lb maximum)

Radial Bearing Load:

None

Load Application Device:

Pressurized piston

Instrumentation and Measurements:

Bearing temperatures, LN₂ flow rates and pressures, parametric studies and investigation of subcooling conditions, post-test inspection of bearings, and characterization of wear.

Additional Remarks:

Bearing tester thoroughly chilled with cryogenic for more than two hours prior to testing.

BEARINGS WITH KNOWN DEFECTS

Bearing Test Rig Survey: Bearings with Known Defects

Author(s), Title, and Year:

Tandon, N., and B. C. Nakra. "The Application of the Sound-Intensity Technique to Defect Detection in Rolling-Element Bearings," *Applied Acoustics*, Vol. 29, 1990, pp. 207-217.

Type of Experimental Apparatus:

Low-speed spindle with radially loaded test bearing

Experiment Objectives:

Application of sound-intensity technique to detect defects in raceways and balls

Test Bearing Type:

Ball bearing, 15-mm bore. Defects placed in raceways and balls by spark erosion method

Prime Mover Details:

DC motor direct drive to spindle housed in ball bearings at each end

Maximum Test Speed:

1500 rpm

Axial Bearing Load:

None

Radial Bearing Load:

220 lb maximum

Load Application Device:

Deadweight on lever arm

Instrumentation and Measurements:

Sounding intensity probe, i.e., a two-microphone probe assembly (two 1/2-inch-diameter condenser microphones, 12-mm separation). Narrow-band plot of sounding intensity using a dual-channel FFT analyzer.

Additional Remarks:

Defect diameters: 0.006, 0.01, and 0.02 inch. Defect depths: 0.002, 0.004, and 0.006 inch. Sound intensity peaks observed due to system structural resonances. Peaks due to bearing defects observed above 5 kHz. Detection of inner ring defects difficult. Also, detection of defects at low speeds difficult.

Bearing Test Rig Survey: Bearings with Known Defects (Cont'd)

Author(s), Title, and Year:

Hawman, M. W., and W. S. Galinaitis. "Acoustic Emission Monitoring of Rolling Element Bearings," 1988 Ultrasonics Symposium, *IEEE Proc.*, Vol. 2, pp. 885-889.

Type of Experimental Apparatus:

Low-speed ball bearing test rig

Experiment Objectives:

To investigate the use of acoustic emission transducers in monitoring bearing health

Test Bearing Type:

Ball bearing, 2.0-inch bore, 12-ball configuration

Prime Mover Details:

Electric motor

Maximum Test Speed:

5700 rpm

Axial Bearing Load:

2400 lb

Radial Bearing Load:

None

Load Application Device:

Axial piston with hydraulic fluid

Instrumentation and Measurements:

- Acoustic emission measured with patented point-contact transducers (PCTs) developed by United Technologies Research Center
- PCTs mounted on each bearing in contact with outer surface of outer race
- Accelerometer attached to bearing housing (over the test bearing)
- Bearing defects carefully controlled. Scratch in outer race was gradually increased in width and depth

Additional Remarks:

Acoustic emission (AE) pulses easily identifiable for scratch widths above 0.02 inches. Vibration data did not indicate a defect until size of defect reached 0.065-inch wide. AE monitoring allowed strong indication of small defects located on opposite side of the bearing from the AE transducer.

Bearing Test Rig Survey: Bearings with Known Defects (Cont'd)

Author(s), Title, and Year:

Kim, P. Y. "Proximity Transducer Technique for Bearing Health Monitoring," *J. Propulsion*, Vol. 3, No. 1, 1987, pp. 84-89.

Type of Experimental Apparatus:

Low-speed ball bearing test rig

Experiment Objectives:

Evaluation of proximity transducer in detection of incipient failure

Test Bearing Type:

Ball bearing (SKF 6002), 15-mm bore

Prime Mover Details:

No details given

Maximum Test Speed:

2450 rpm

Axial Bearing Load:

None

Radial Bearing Load:

900 lb maximum

Load Application Device:

Deadweight and lever arm

Instrumentation and Measurements:

Eddy current proximity transducer (sensing deflection of outer race). Prove sensitivity approximately 2 volts per 0.001 inch.

Additional Remarks:

Test bearings contained defects in both inner and outer races. Measured deflection of outer race used to monitor defects in both inner and outer races. Computerized automatic monitoring system was demonstrated. A favorable comparison with other methods, such as the shock pulse method, kurtosis analysis and high frequency resonance technique, was presented.

Bearing Test Rig Survey: Bearings with Known Defects (Cont'd)

Author(s), Title, and Year:

Igarashi, T., J. Kato and S. Yabe. "Studies on the Vibration and Sound of Defective Rolling Bearings," *Bulletin of JSME*, Vol. 26, No. 220, 1983, pp. 1791-1798; *Bulletin of JSME*, Vol. 28, No. 237, 1985, pp. 492-499.

Type of Experimental Apparatus:

Low-speed ball bearing test rig in soundproof enclosure

Experiment Objectives:

Measurement of sound radiated and vibrational velocity of outer race of ball bearings with defects.

Test Bearing Type:

Ball bearing (single row, deep groove)

Prime Mover Details:

Electric motor

Maximum Test Speed:

1800 rpm

Axial Bearing Load:

7 lb nominal

Radial Bearing Load:

None

Load Application Device:

Deadweight on cable over pulleys

Instrumentation and Measurements:

- Condenser microphone measurements over an arc of 100-mm radius
- Velocity pickup at outer ring of bearing
- Accelerometer attached to outer surface of bearing outer ring

Additional Remarks:

Bearing Test Rig Survey: Bearings with Known Defects (Concluded)

Author(s), Title, and Year:

Balderston, H. L. "The Detection of Incipient Failure in Bearings," *Materials Evaluation*, June 1969, pp. 121-128.

Type of Experimental Apparatus:

Medium-speed ball bearing test rig

Experiment Objectives:

Investigation of vibration acceleration data for bearings with controlled defects in inner race, outer race, ball cage, and balls

Test Bearing Type:

Angular contact ball bearings

Prime Mover Details:

Electric motor

Maximum Test Speed:

10,000 rpm

Axial Bearing Load:

No details

Radial Bearing Load:

No details

Load Application Device:

No details

Instrumentation and Measurements:

- Accelerometers placed on outer bearing housing
- Accelerometer data recorded at high tape speed and played back at reduced speed (16-to-1 reduction). Spectrum analyzer range: 20-20 kHz
- Vibrational frequencies in the range of 10 kHz to 90 kHz examined in this way
- Data analysis was able to detect acoustic emissions

Additional Remarks:

"Burst"-type acoustic emissions and "continuous"-type acoustic emissions were clearly identified during this study.

BASIC RESEARCH RIGS

Bearing Test Rig Survey: Basic Research Rigs

Author(s), Title, and Year:

Falcon, K. C., and C. Andrew. "Angular Contact Ball Bearings: Track Position at High Speeds," *Proc. of Institution of Mechanical Engineers 1969-1970*. Vol. 184, Part 1, No. 19, pp. 351-369.

Type of Experimental Apparatus:

High-speed ball bearing test rig

Experiment Objectives:

Measurement of ball track position and comparison with theory

Test Bearing Type:

Angular contact ball bearing, 55-mm bore

Prime Mover Details:

5-hp electric motor with speed increase via flat belts and pulleys

Maximum Test Speed:

12,000 rpm

Axial Bearing Load:

3000 lb maximum test load

Radial Bearing Load:

None

Load Application Device:

Hydraulic pressure

Instrumentation and Measurements:

- Inductive displacement transducers embedded in outer race to measure race deflections under each ball. (Outer race machined to allow displacement transducer tip to be inserted into race to within 0.04 inch of the track surface.)
- Magnetic pickup measuring test shaft speed

Additional Remarks:

Bearing Test Rig Survey: Basic Research Rigs (Continued)

Author(s), Title, and Year:

Bowen, W. L., and T. W. Murphy. "High Speed Testing of the Hollow Roller Bearing," *Trans. of ASME Journal of Lubrication Technology*, Vol. 103, Jan. 1981, pp. 1-5.

Type of Experimental Apparatus:

High-speed roller bearing test rig for operation up to three million DN

Experiment Objectives:

Performance and endurance testing of cylindrical roller bearing with hollow rollers

Test Bearing Type:

Hollow cylindrical roller bearing, 115-mm bore

Prime Mover Details:

120-hp industrial V-8 engine driving a 12-to-1 step-up gearbox

Maximum Test Speed:

26,100 rpm

Axial Bearing Load:

None

Radial Bearing Load:

600 lb

Load Application Device:

Hydraulic cylinder applying radial load to test bearing housing

Instrumentation and Measurements:

- Thermocouples measuring bearing outer race and lubricant temperatures
- Torque sensor between motor and gearbox
- Post-test measurement of wear

Additional Remarks:

Test shaft supported at each end by 55-mm slave bearings with the test bearing and housing assembly located at the approximate mid-point between slave bearings. Endurance testing up to 1000 hours performed on test bearing.

Bearing Test Rig Survey: Basic Research Rigs (Continued)

Author(s), Title, and Year:

Pemberton, J. C., and A. Cameron. "Optical Study of the Lubrication of a 65-mm Cylindrical Roller Bearing," *Industrial Lubrication and Tribology*, May/June 1981, pp. 84-94.

Type of Experimental Apparatus:

Low-speed cylindrical roller bearing test rig

Experiment Objectives:

Optical study of the lubrication of a cylindrical roller bearing via interferometry

Test Bearing Type:

Cylindrical roller bearings, 65-mm bore

Prime Mover Details:

3-hp electric motor

Maximum Test Speed:

3000 rpm

Axial Bearing Load:

None

Radial Bearing Load:

Not specified

Load Application Device:

Hydraulic pressure to bearing housing

Instrumentation and Measurements:

- Window cut into outer race of bearing to allow optical examination of oil film thickness through a sapphire insert
- Xenon flash lamp, Xenon laser (pulse rate up to 50 per second), microscope with 35-mm camera and video attachments
- Thermocouples measuring oil temperature and sapphire window surface temperature
- Photodiode and strips of adhesive reflecting tape to determine rotational speed
- Magnetic pickup activated by rollers to measure cage speed
- Fiberoptic "skanner" to detect individual rollers and reference mark on cage

Additional Remarks:

- Dovetailed slot machined in bearing outer race and sapphire window let into machined slot
- Apparatus used to study inlet boundary and the effects of oil starvation, including oil globules formed after lubricant cutoff

Bearing Test Rig Survey: Basic Research Rigs (Continued)

Author(s), Title, and Year:

Markho, P. H., B. V. Smith and M. J. Lalor. "An Advanced Apparatus for the Study of Roller and Cage Slip in High-Speed Roller Bearings," Transactions of the ASME, *Journal of Lubrication Technology*, Vol. 103, Jan. 1981, pp. 46-54.

Type of Experimental Apparatus:

High-speed roller bearing test rig for studies at DN values in excess of one million

Experiment Objectives:

Measurement of cage and roller motions in lightly loaded bearings

Test Bearing Type:

Cylindrical roller bearings, 63.5-mm bore

Prime Mover Details:

A.C. motor driving two-stage flat belt and pulley system

Maximum Test Speed:

22,500 rpm

Axial Bearing Load:

Lightly loaded; not specified

Radial Bearing Load:

270 lb

Load Application Device:

Axial load applied via pneumatic piston. Radial load applied to test bearing housing via worm and wheel jack

Instrumentation and Measurements:

- Laser doppler anemometer for measuring roller surface velocity
- Inductive displacement transducers for measuring inner and outer ring motions
- Infra-red radiation thermometer for inner ring temperatures
- Thermocouples for outer ring temperatures and lubricant temperatures
- Magnetic pickup for measuring cage speed
- Photoelectric transducer for measuring test shaft speed
- Load cells for determining radial load and friction torque

Additional Remarks:

- Test bearing mounted in housing and attached to end of hydrostatic spindle
- Study investigated the effect of bearing load on the level of slip in the bearing
- Significant variation in roller speed observed as it travels around bearing

Bearing Test Rig Survey: Basic Research Rigs (Continued)

Author(s), Title, and Year:

Gupta, P. K., J. F. Dill and H. E. Bandon. "Dynamics of Rolling Element Bearings—Experimental Validation of the DREB and RAPIDREB Computer Programs," Transactions of the ASME, *Journal of Tribology*, Vol. 107, Jan. 1985, pp. 132-137.

Type of Experimental Apparatus:

High-speed ball bearing test rig capable of operating up to two million DN

Experiment Objectives:

Measurement of the general motion of the ball cage in an angular contact ball bearing and comparison with computer model predictions

Test Bearing Type:

Angular contact ball bearing, 100-mm bore, split inner race

Prime Mover Details:

50-hp electric motor with variable-speed drive and 9.25-to-1 ratio step-up gearbox

Maximum Test Speed:

20,000 rpm (30,000 rpm maximum)

Axial Bearing Load:

250 lb

Radial Bearing Load:

0 to 250 lb

Load Application Device:

Pressurized piston

Instrumentation and Measurements:

- Magnetic pickup for shaft speed
- Radial and axial proximity probes (Bently probes) for displacement measurement (four radial and four axial probes)
- Two photonic sensors to determine angular velocity of cage
- Thermocouples on bearing inner and outer races, in oil supply jets, scavenge ports and oil sump
- Torque measurement

Additional Remarks:

- Test shaft housed in three bearings (the test bearing and two support bearings)
- Extensive calibration procedure devised to compensate for proximity sensor sensitivity to temperature
- Drive shaft instrumented with strain gages to measure bending, axial and torsional loads on shaft

Bearing Test Rig Survey: Basic Research Rigs (Concluded)

Author(s), Title, and Year:

Savaskan, T., and D. E. Veinot. "On the Wear and Failure of High Speed Roller Bearings," *WEAR*, Vol. 116, No. 3, May 1987, pp. 361-380.

Type of Experimental Apparatus:

High-speed ball bearing test rig

Experiment Objectives:

Study of wear and failure mechanisms of high-speed roller bearings

Test Bearing Type:

Single-row, cylindrical roller bearings, 25-mm bore

Prime Mover Details:

15-hp, A.C. motor with belt drive speed increaser (15-to-1 step-up)

Maximum Test Speed:

26,000 rpm

Axial Bearing Load:

None

Radial Bearing Load:

375 lb nominal

Load Application Device:

Mechanical displacement of bearing housings relative to one another (test shaft carried in three bearings)

Instrumentation and Measurements:

- Strain gages on shaft to convert shaft deflection to radial bearing load
- Fiberoptic light guides used to measure rotational speeds of shaft and bearing cages
- Thermocouple and digital thermometers measuring bearing outer race and lubricating oil temperatures
- Analysis of oil samples using ferrography and atomic absorption analysis. Wear debris collected from bearings was studied with scanning electron microscopy using energy-dispersive x-ray analysis

Additional Remarks:

- The three test bearings were lubricated separately. Oil flow rate to each bearing was independently controlled to study effects of supply rate on wear
- Test rig operated for 15 hours per day to accumulate more than 700 hours of bearing operation

APPENDIX B

**SELECTED BIBLIOGRAPHY OF OIL-FILM BEARING
EXPERIMENTAL STUDIES**

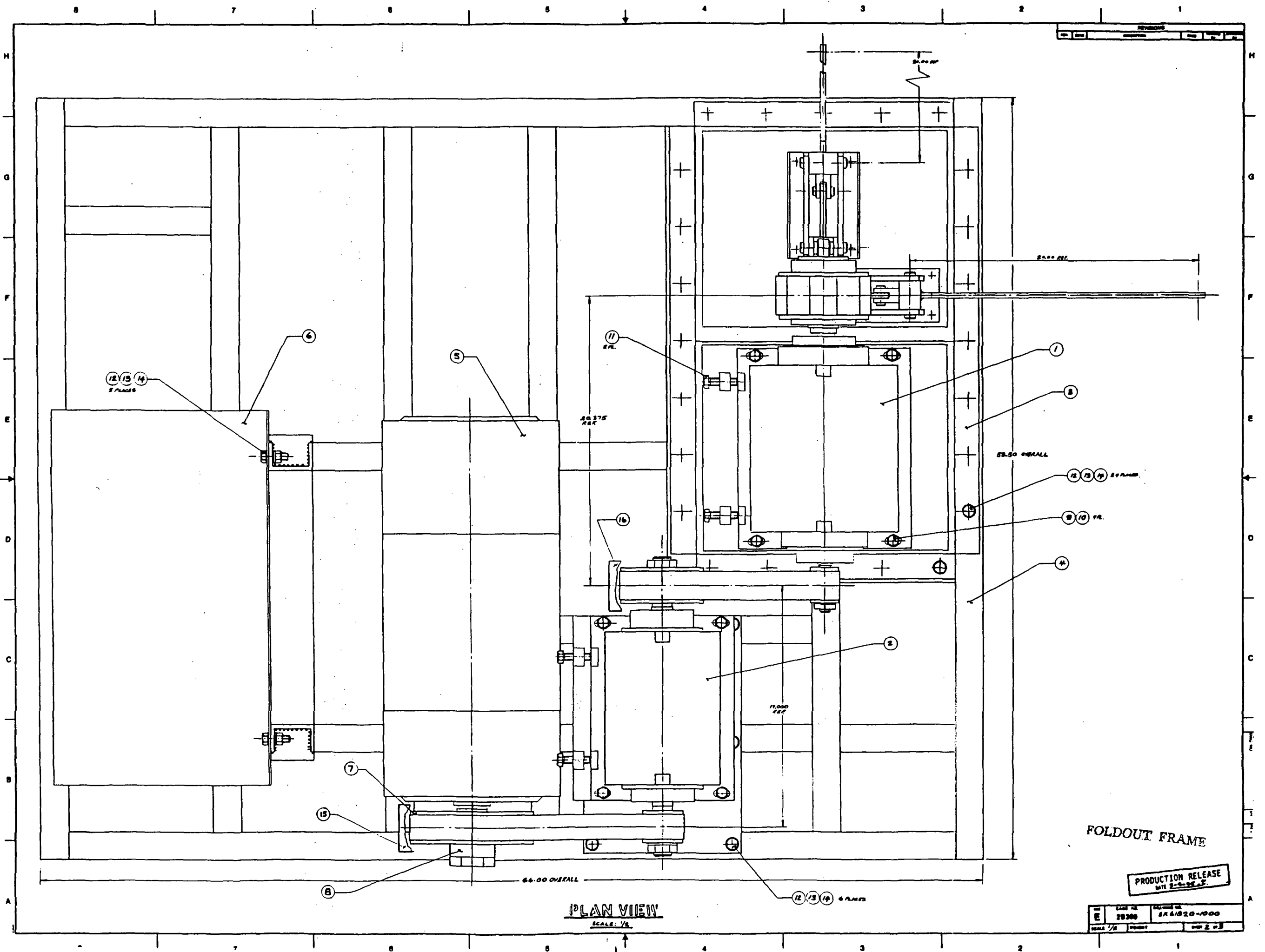
BIBLIOGRAPHY

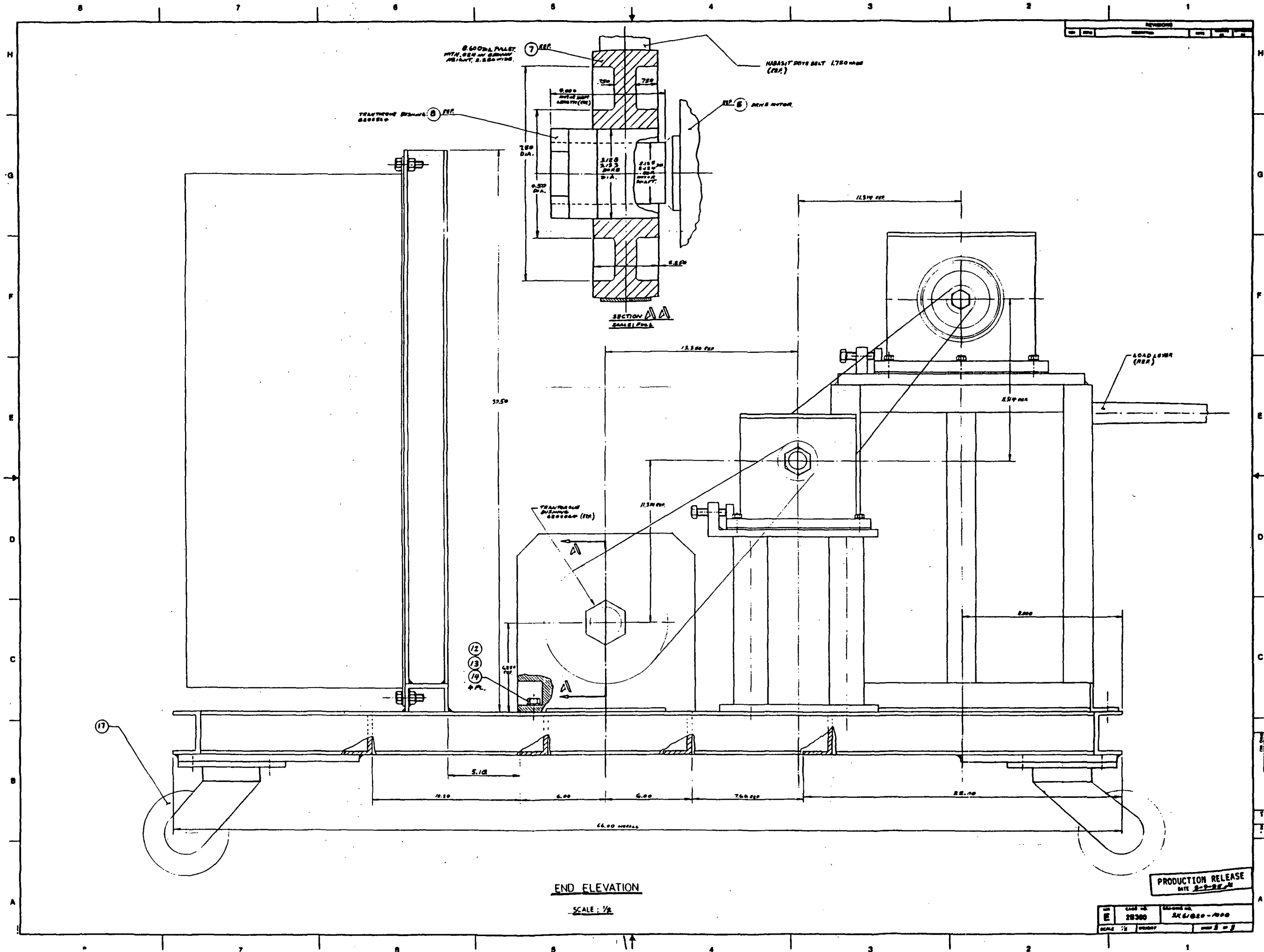
- Carl, T. E. "An Experimental Investigation of a Cylindrical Journal Bearing Under Constant and Sinusoidal Loading." *Proceedings of the Institution of Mechanical Engineers*, Vol. 178, Part 3N, 1963-64.
- Rafique, S.O. "Failure of Plain Bearings and Their Causes." *Proceedings of the Institution of Mechanical Engineers*, Vol. 178, Part 3N, 1963-64.
- Mitchell, J. R., R. Holmes, and H. Van Ballegooyen. "Experimental Determination of a Bearing Oil-Film Stiffness." *Proceedings of the Institution of Mechanical Engineers*, Vol. 180, Part 3K, 1965-66.
- Woolacott, R. G., and W. L. Cooke. "Thermal Aspects of Hydrodynamic Journal Bearing Performance at High Speeds." *Proceedings of the Institution of Mechanical Engineers*, Vol. 181, Part 3, 1966-67.
- Azzoni, A., et al. "Experimental Studies on the Shaft Dynamics of Large Turbogenerators for an Improved Surveillance." Paper C185/76, I. Mech. E. 1976.
- Bannister, R. H. "A Theoretical and Experimental Investigation Illustrating the Influence of Non-Linearity and Misalignment on the Eight Oil Film Force Coefficients." Paper C219/76, I. Mech. E. 1976.
- Goodwin, G., and R. Holmes. "On The Continuous Monitoring of Oil-Film Thickness in an Engine Bearing." *Proceedings of the Institution of Mechanical Engineers*, Vol. 192, 1978.
- Higa, S., T. Matsuura, and T. Someya. "Experiments on the Dynamic Characteristics of Large Scale Journal Bearings." Paper C284/80, I. Mech. E., 1980.
- Cookson, R. A., and S. S. Kossa. "Theoretical and Experimental Investigation into the Effectiveness of Squeeze-Film Damper Bearings without a Centralizing Spring." Paper C304/80, I. Mech. E., 1980.
- Holmes, R., and M. Dogan. "Investigation of a Rotor Bearing Assembly Incorporating a Squeeze-Film Damper Bearing." *Journal of Mechanical Engineering Science*, Vol. 24, No. 3, 1982.
- Tichy, J. A. "Measurements of Squeeze-Film Bearing Forces and Pressures, Including the Effect of Fluid Inertia." *ASLE Transactions*, Vol. 28, No. 4, 1984, pp. 520-526.
- Cappel, K. L, and G. L. von Pragenau. "Damping Seal Tester Progress and Initial Test Results." NASA Conference Publication No. 2437, 1986.
- Read, L. J., and R. D. Flack. "Temperature, Pressure and Film Thickness Measurements for an Offset Half Bearing." *WEAR*, Vol. 117, 1987, pp. 197-210.
- Ku, C. P., and J. A. Tichy. "An Experimental and Theoretical Study of Cavitation in a Finite Submerged Squeeze Film Damper." *Journal of Tribology*, Vol. 112, 1990.
- Goggin, D. G., J. K. Scharrer, and R. F. Beatty. "Hydrostatic Damper for the Space Shuttle Main Engine High Pressure Oxidizer Turbopump." *Journal of Tribology*, Vol. 112, Jan. 1990.

- Palazzolo, A. B., et al. "Vibration Dampers for Cryogenic Turbomachinery." NASA Conference Publication No. 3092, 1990.
- Murphy, B. T., and M. N. Wagner. "Measurement of Rotordynamic Coefficients for a Hydrostatic Radial Bearing." Transactions of the ASME, Vol. 113, July 1991.
- Flack, R. D., G. J. Kostrzewsky, and D. V. Taylor. "A Hydrodynamic Journal Bearing Test Rig with Dynamic Measurement Capabilities." Paper presented at the ASME/STLE Tribology Conference, San Diego, CA, Oct. 1992.
- Arauz, G. L., and A. San Andres. "Experimental Pressures and Film Forces in a Squeeze Film Damper." Transactions of the ASME, Vol. 115, Jan. 1993.
- Kurtin, K. A., et al. "Experimental Versus Theoretical Characteristics of a High-Speed Hybrid (Combination Hydrostatic and Hydrodynamic) Bearing." Transactions of the ASME, Vol. 115, Jun. 1993.

APPENDIX C

**DESIGN DRAWINGS AND PARTS BREAKDOWN
FOR THE HIGH-SPEED BEARING TEST RIG**





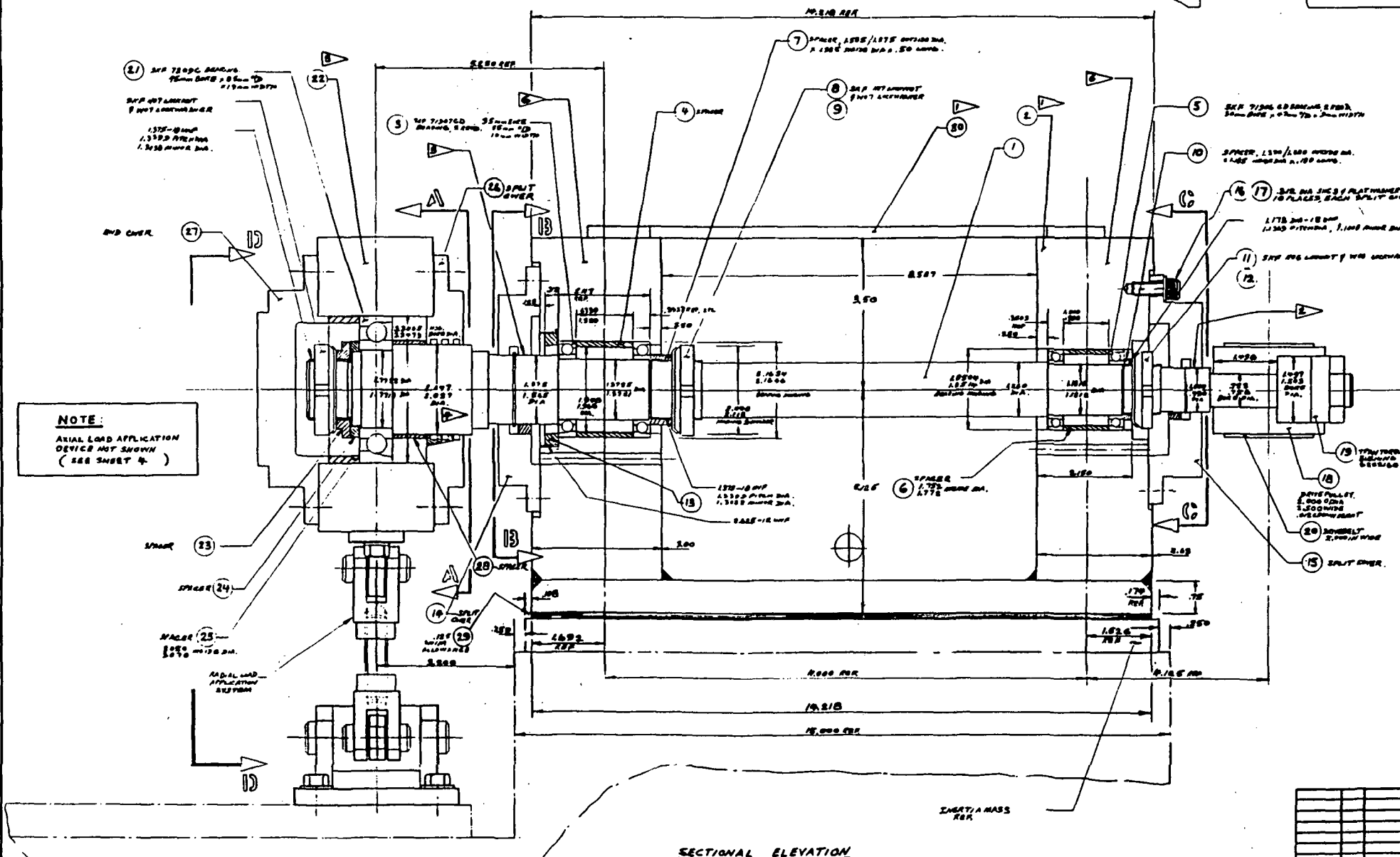
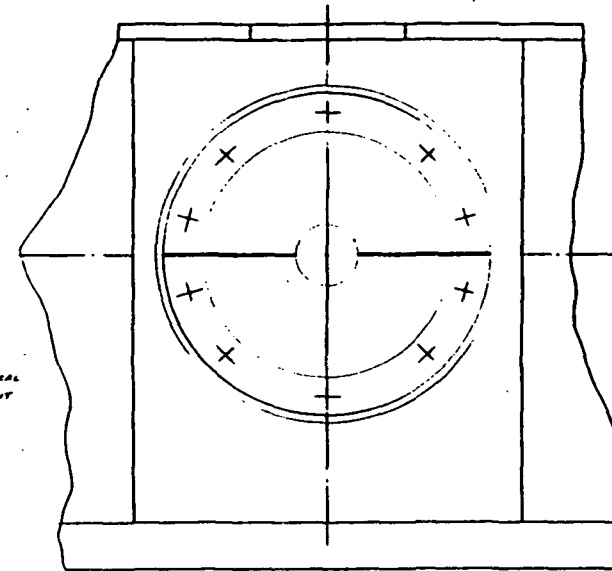
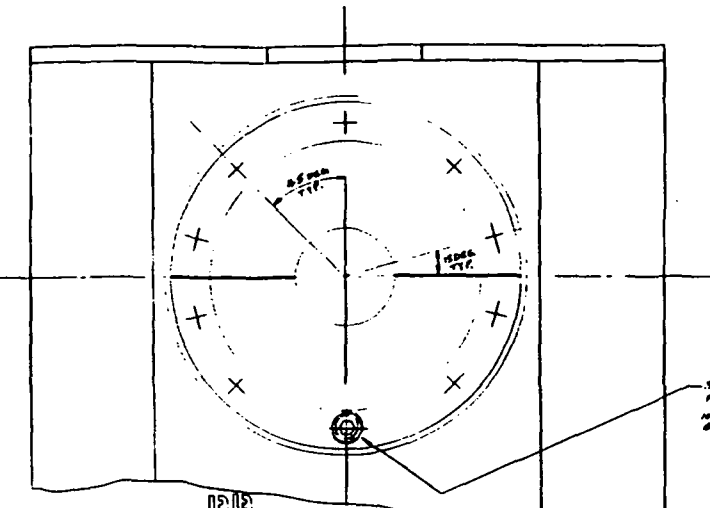
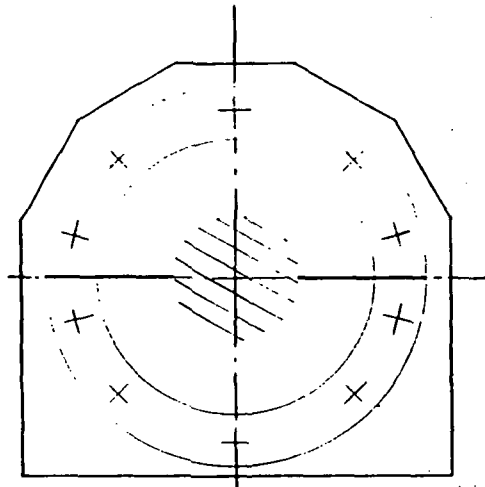
FOLDOUT FRAME

FOLDOUT FRAME

END ELEVATION
SCALE: 1/8"

PRODUCTION RELEASE
DATE 3-2-88

UN	CD	CD	CD
E	28300	2461020-1000	
SCALE	1/8"	UNLESS	NOTED



NOTE:
AXIAL LOAD APPLICATION
DEVICE NOT SHOWN
(SEE SHEET 4)

VIEW 000
STATE: CUBA

NOTES

[illegible]

PRODUCTION RELEASE

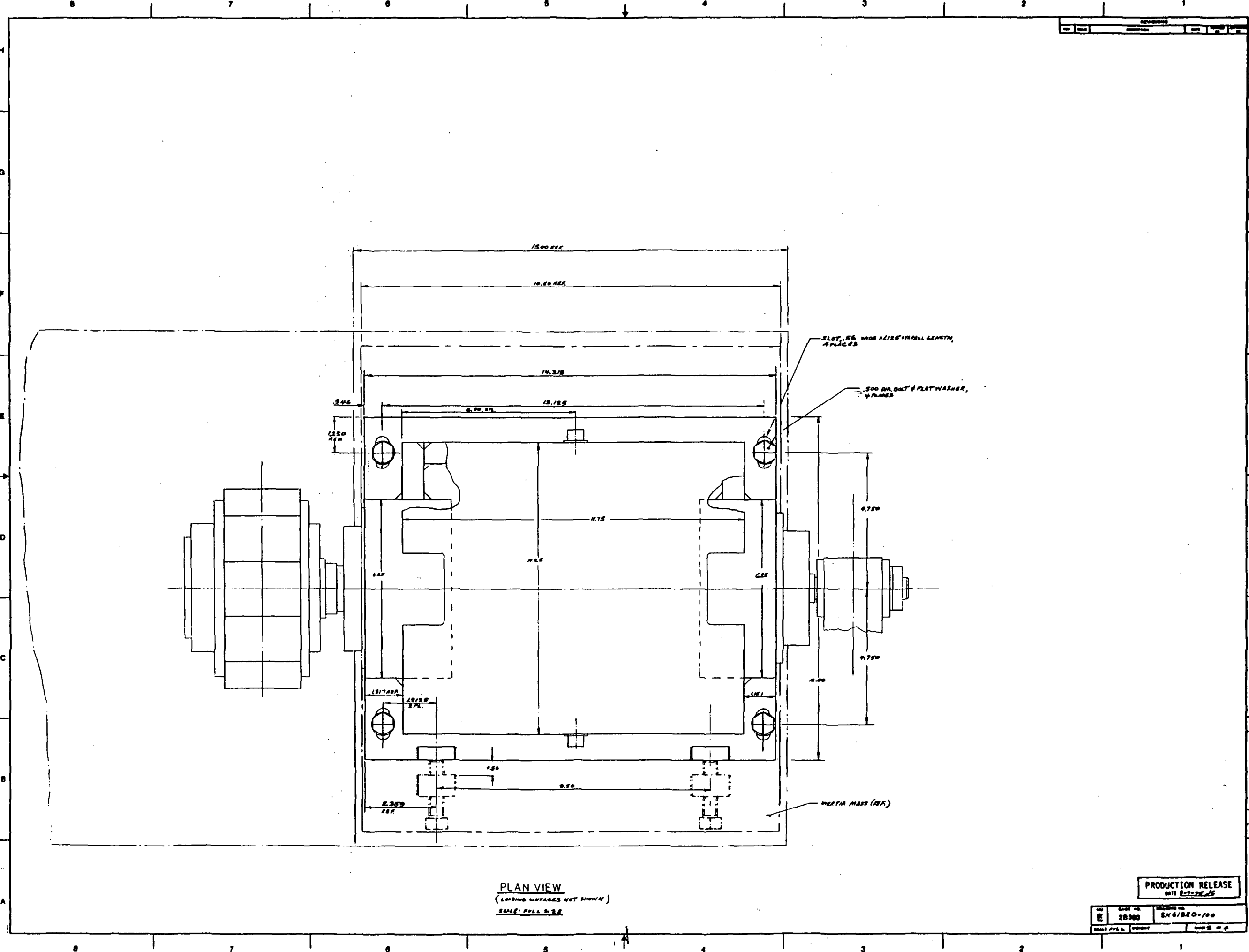
[illegible]

**ORIGINAL PAGE IS
OF POOR QUALITY**

FOLDOUT FRAME

FOLDDOUT FRAME

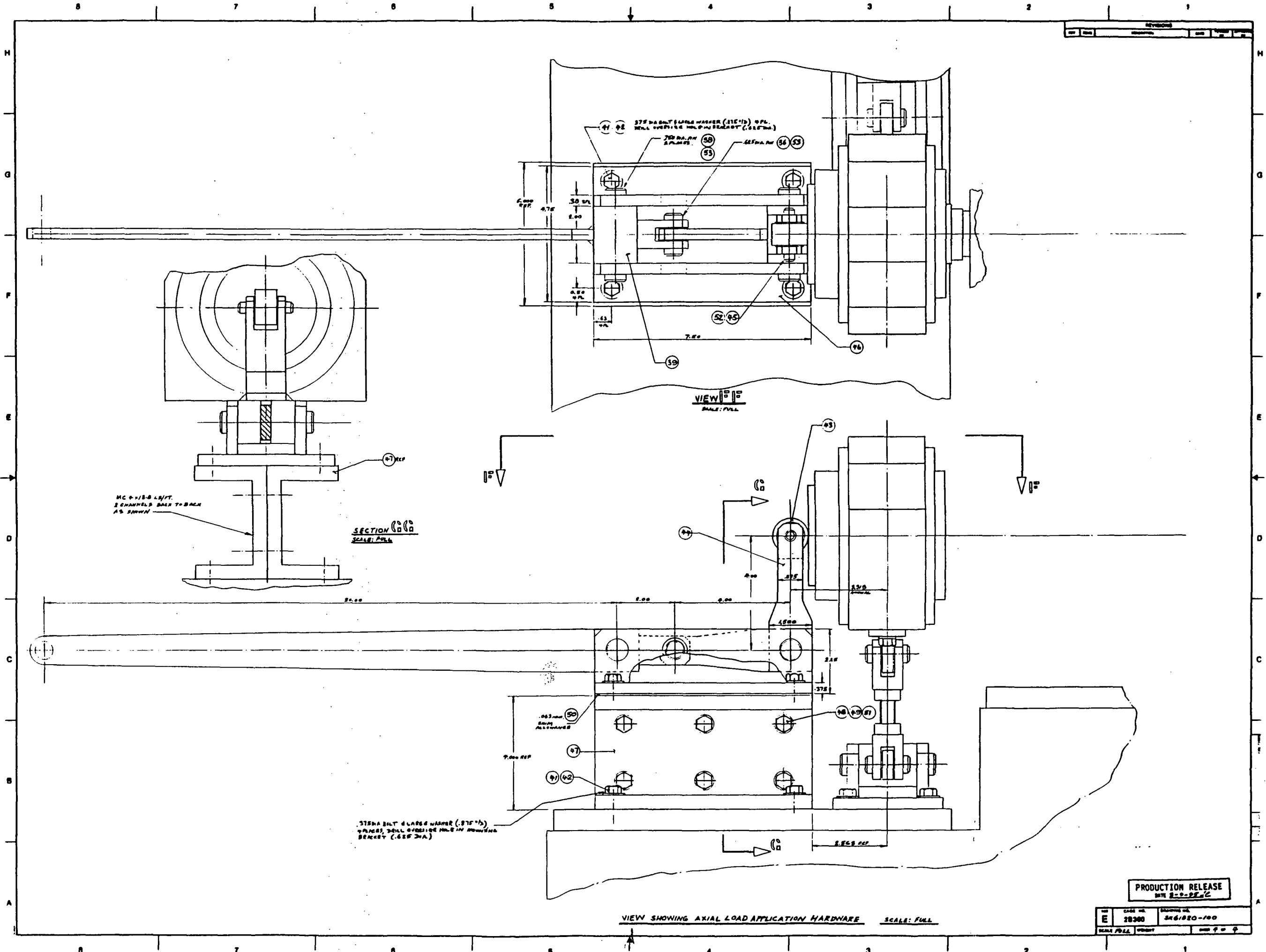
C-5



FOLDOUT FRAME

C-8

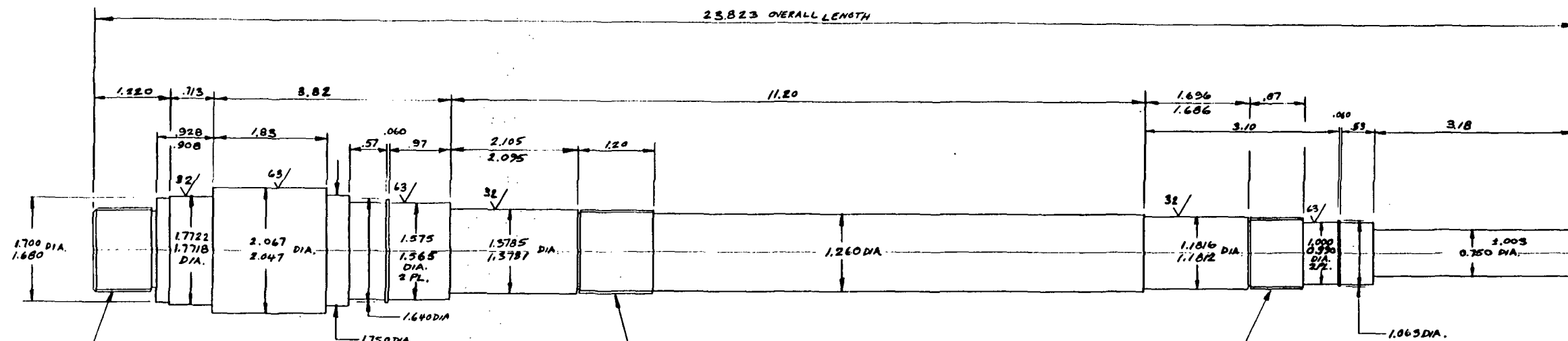
FOLDOUT FRAME



DWG. NO.	REV	DATE	REVISED BY	APPROVED BY
REVISIONS				
REV.	DESCRIPTION	DATE	REVISED BY	APPROVED BY

NOTES

1. SURFACE FINISH $\sqrt{125}$ UNLESS NOTED OTHERWISE.



PRODUCTION RELEASE
DATE 5-2-95, 10

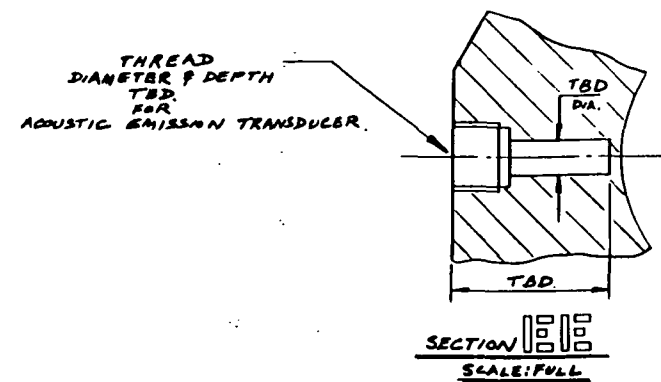
B/L	REV	CC	NO.	DATE

CONTRACT NO. NASB 58095		WYLE SCIENTIFIC SERVICES LABORATORIES GROUP		EASTERN TEST AND ENGINEERING OPERATIONS HUNTSVILLE, ALABAMA	
APPROVED		DATE		TEST BEARING DRIVESHAFT	
PROJECT ENGR	7-14-74				
DRAWN	7-14-74				
CHECKED					
WITNESS					
MATERIAL					
316 STAINLESS STEEL					
PER UNS 591600					
FINISH					
SIZE	D	PCN NO.	28360	DRAWING NO.	SK61820-101
SCALE	FULL	WEIGHT		SHEET	1 OF 1

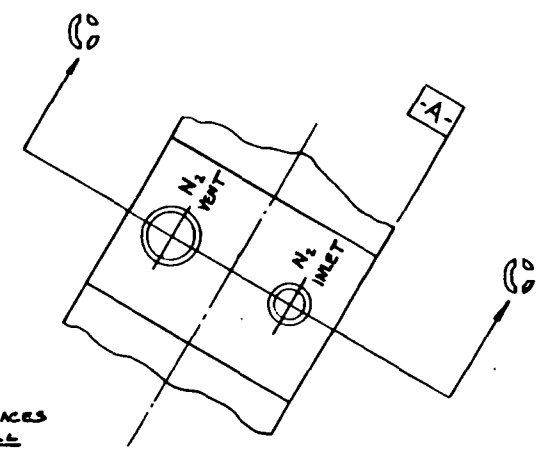
FOLDOUT FRAME

FOLDOUT FRAME

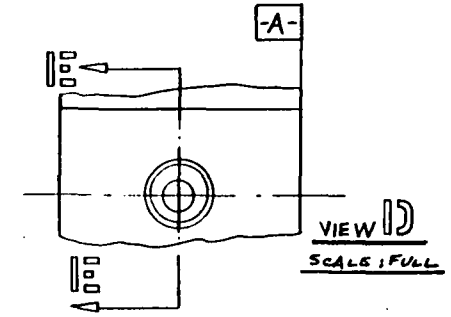
DWG. NO.	REV	1
REVISIONS		
REV.	DESCRIPTION	DATE
REV.	REVISED BY	APPROVED BY



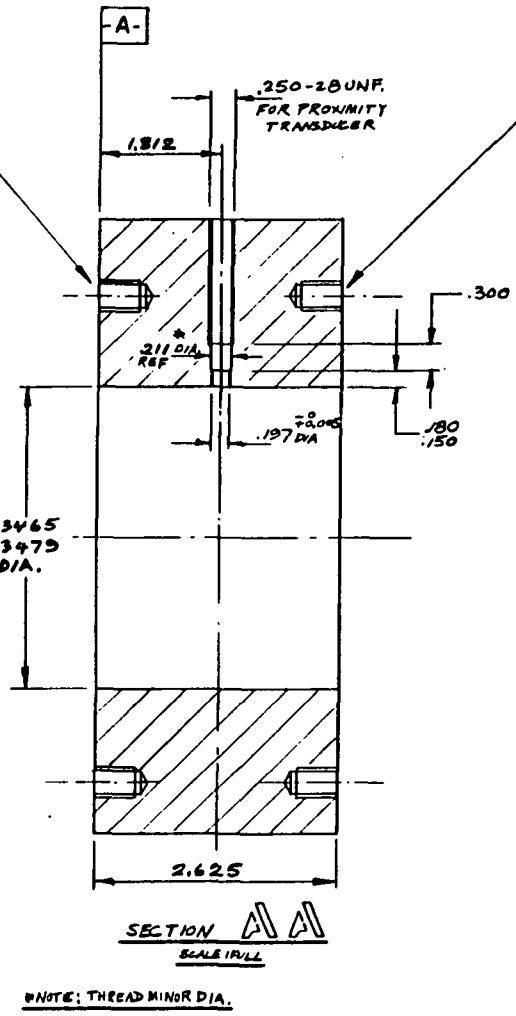
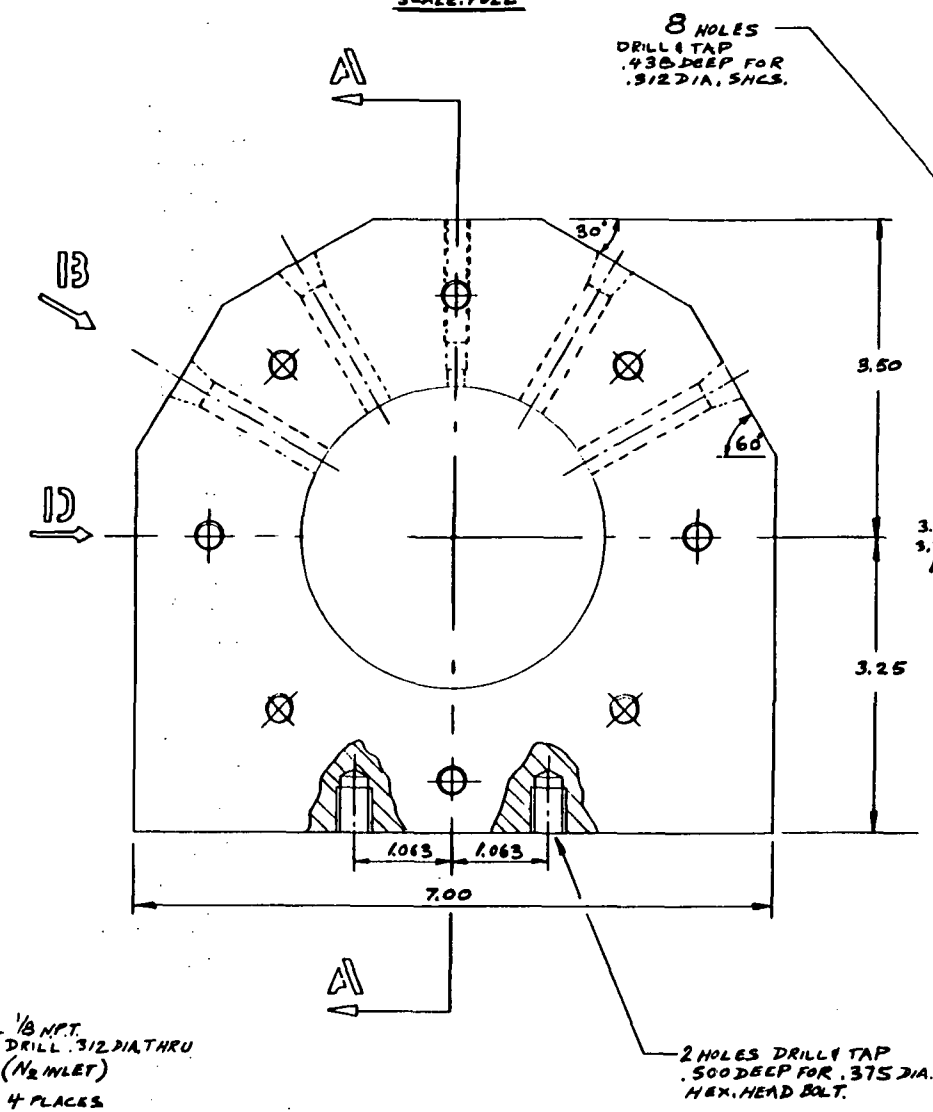
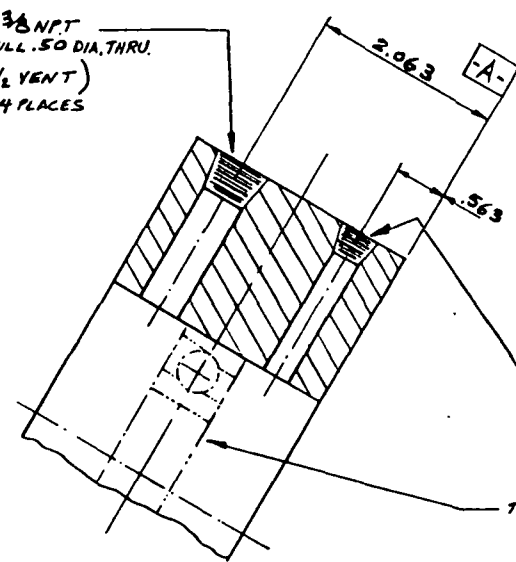
VIEW 13
TYPICAL, 4 PLACES
SCALE: FULL



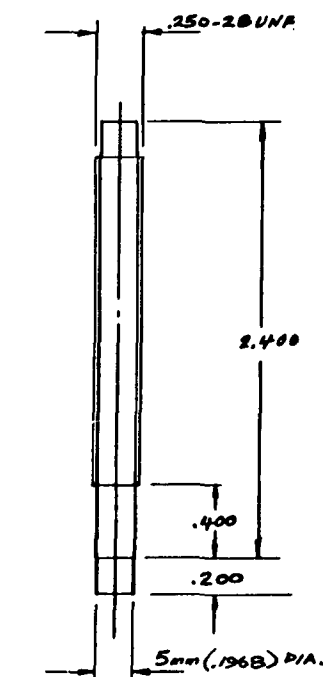
VIEW 12
SCALE: FULL



3/8 NPT
DRILL .50 DIA. THRU.
(N₂ VENT)
4 PLACES



10 HOLES
DRILL & TAP
.438 DEEP FOR
.312 DIA. SHCS.

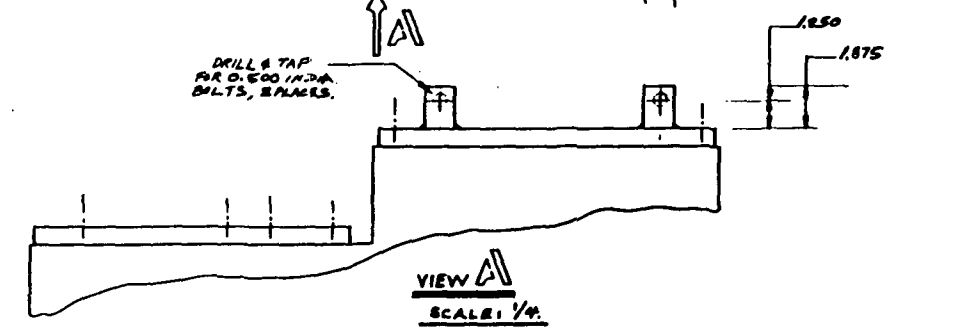
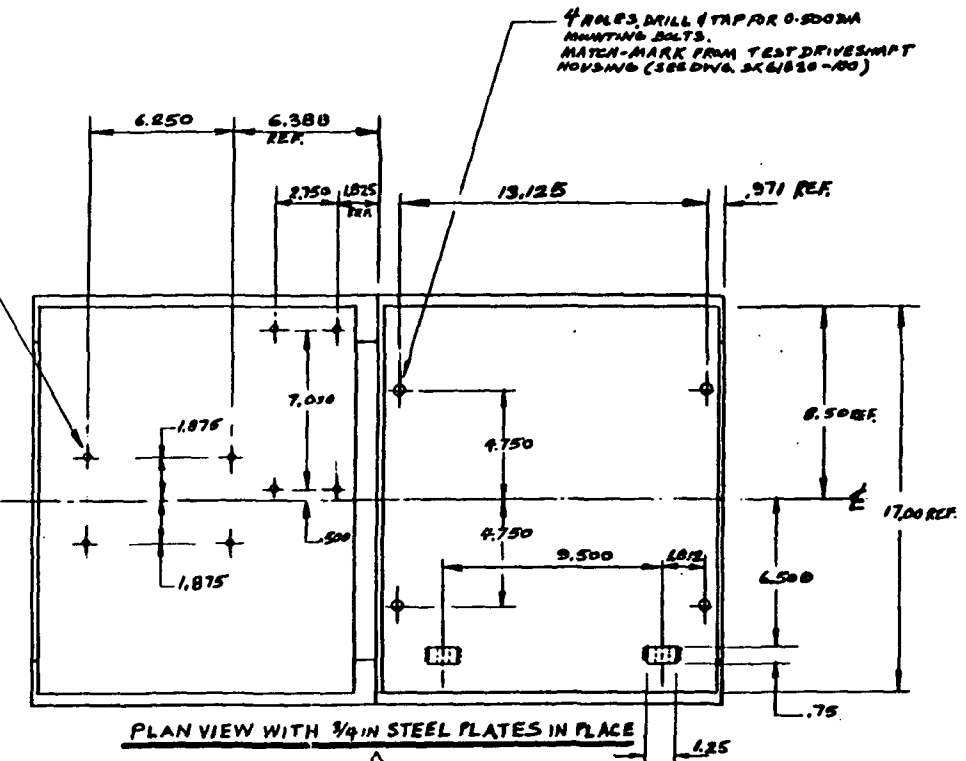
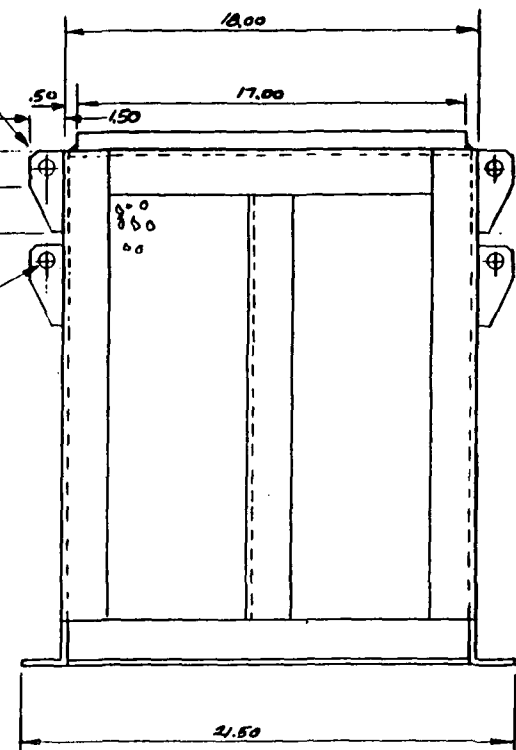
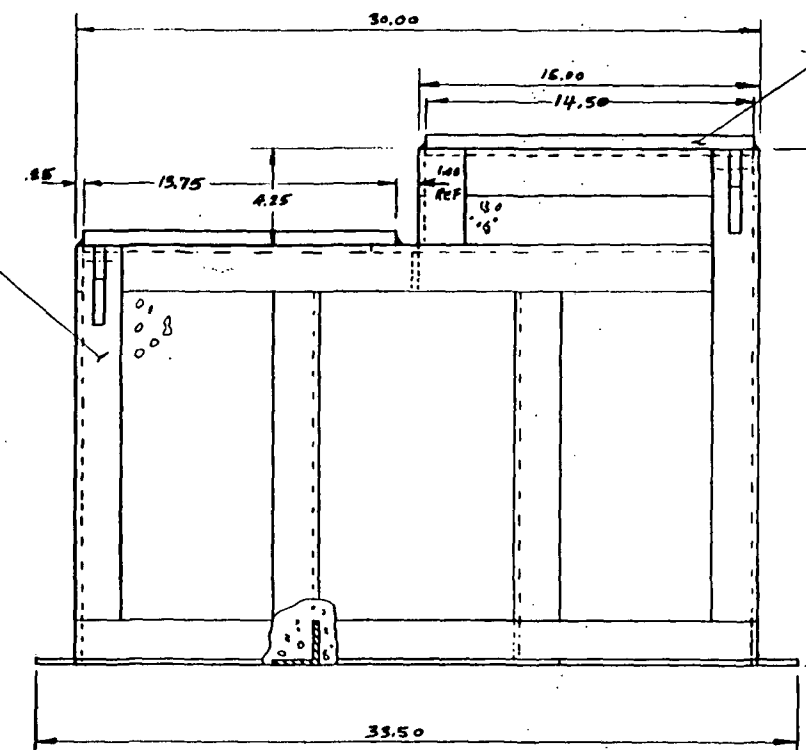
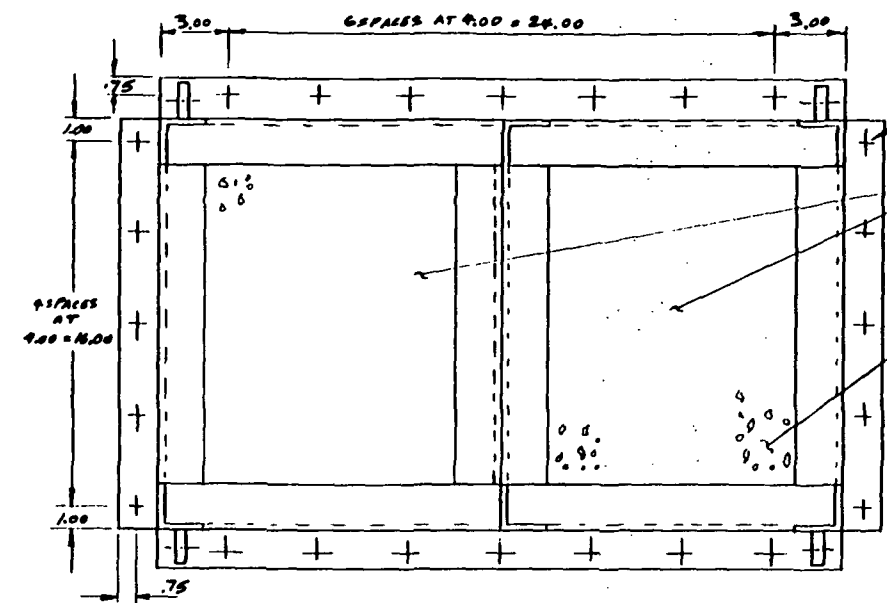


PRODUCTION RELEASE
DATE 3-2-88 JLC

UNLESS OTHERWISE SPECIFIED DIMENSIONS ARE IN INCHES TOLERANCES ON: FRACTIONS DECIMALS ANGLES ± .005 ± .005 ± .005 MATERIAL 316 STAINLESS STEEL 63/600 FINISH	CONTRACT NO. NASB-58025 APPROVED DATE PROJECT ENGR. 1/2/84 8-2-84 DRAWN 1/2/84 8-2-84 CHECKED STRESS MATERIALS THERMAL SAFETY QUALITY PROGRAM ENGR. ELECTRICAL	WYLE SCIENTIFIC SERVICES & SYSTEMS LABORATORIES GROUP EASTERN TEST AND ENGINEERING OPERATIONS HUNTSVILLE, ALABAMA TEST HOUSING SIZE D PCH NO. 28360 DRAWING NO. 5K61820-111 SCALE FULL WEIGHT SHEET 1 OF 1	REV. CC NO. DATE B/L REV. CC NO. DATE



DWG. NO.	SH	REV	1
REVISIONS			
REV.	DESCRIPTION	DATE	APPROVED BY



PRODUCTION RELEASE
DATE 2-2-95 J/C

--	--	--	--	--	--	--	--	--	--	--	--	--	--	--	--	--	--	--	--	--	--	--	--	--	--	--	--	--	--	--	--	--	--	--	--	--	--	--	--	--	--	--	--	--	--	--	--	--	--	--	--	--	--	--	--	--	--	--	--	--	--	--	--	--	--	--	--	--	--	--	--	--	--	--	--	--	--	--	--	--	--	--	--	--	--	--	--	--	--	--	--	--	--	--	--	--	--	--	--	--	--	--	--	--	--	--	--	--	--	--	--	--	--	--	--	--	--	--	--	--	--	--	--	--	--	--	--	--	--	--	--	--	--	--	--	--	--	--	--	--	--	--	--	--	--	--	--	--	--	--	--	--	--	--	--	--	--	--	--	--	--	--	--	--	--	--	--	--	--	--	--	--	--	--	--	--	--	--	--	--	--	--	--	--	--	--	--	--	--	--	--	--	--	--	--	--	--	--	--	--	--	--	--	--	--	--	--	--	--	--	--	--	--	--	--	--	--	--	--	--	--	--	--	--	--	--	--	--	--	--	--	--	--	--	--	--	--	--	--	--	--	--	--	--	--	--	--	--	--	--	--	--	--	--	--	--	--	--	--	--	--	--	--	--	--	--	--	--	--	--	--	--	--	--	--	--	--	--	--	--	--	--	--	--	--	--	--	--	--	--	--	--	--	--	--	--	--	--	--	--	--	--	--	--	--	--	--	--	--	--	--	--	--	--	--	--	--	--	--	--	--	--	--	--	--	--	--	--	--	--	--	--	--	--	--	--	--	--	--	--	--	--	--	--	--	--	--	--	--	--	--	--	--	--	--	--	--	--	--	--	--	--	--	--	--	--	--	--	--	--	--	--	--	--	--	--	--	--	--	--	--	--	--	--	--	--	--	--	--	--	--	--	--	--	--	--	--	--	--	--	--	--	--	--	--	--	--	--	--	--	--	--	--	--	--	--	--	--	--	--	--	--	--	--	--	--	--	--	--	--	--	--	--	--	--	--	--	--	--	--	--	--	--	--	--	--	--	--	--	--	--	--	--	--	--	--	--	--	--	--	--	--	--	--	--	--	--	--	--	--	--	--	--	--	--	--	--	--	--	--	--	--	--	--	--	--	--	--	--	--	--	--	--	--	--	--	--	--	--	--	--	--	--	--	--	--	--	--	--	--	--	--	--	--	--	--	--	--	--	--	--	--	--	--	--	--	--	--	--	--	--	--	--	--	--	--	--	--	--	--	--	--	--	--	--	--	--	--	--	--	--	--	--	--	--	--	--	--	--	--	--	--	--	--	--	--	--	--	--	--	--	--	--	--	--	--	--	--	--	--	--	--	--	--	--	--	--	--	--	--	--	--	--	--	--	--	--	--	--	--	--	--	--	--	--	--	--	--	--	--	--	--	--	--	--	--	--	--	--	--	--	--	--	--	--	--	--	--	--	--	--	--	--	--	--	--	--	--	--	--	--	--	--	--	--	--	--	--	--	--	--	--	--	--	--	--	--	--	--	--	--	--	--	--	--	--	--	--	--	--	--	--	--	--	--	--	--	--	--	--	--	--	--	--	--	--	--	--	--	--	--	--	--	--	--	--	--	--	--	--	--	--	--	--	--	--	--	--	--	--	--	--	--	--	--	--	--	--	--	--	--	--	--	--	--	--	--	--	--	--	--	--	--	--	--	--	--	--	--	--	--	--	--	--	--	--	--	--	--	--	--	--	--	--	--	--	--	--	--	--	--	--	--	--	--	--	--	--	--	--	--	--	--	--	--	--	--	--	--	--	--	--	--	--	--	--	--	--	--	--	--	--	--	--	--	--	--	--	--	--	--	--	--	--	--	--	--	--	--	--	--	--	--	--	--	--	--	--	--	--	--	--	--	--	--	--	--	--	--	--	--	--	--	--	--	--	--	--	--	--	--	--	--	--	--	--	--	--	--	--	--	--	--	--	--	--	--	--	--	--	--	--	--	--	--	--	--	--	--	--	--	--	--	--	--	--	--	--	--	--	--	--	--	--	--	--	--	--	--	--	--	--	--	--	--	--	--	--	--	--	--	--	--	--	--	--	--	--	--	--	--	--	--	--	--	--	--	--	--	--	--	--	--	--	--	--	--	--	--	--	--	--	--	--	--	--	--	--	--	--	--	--	--	--	--	--	--	--	--	--	--	--	--	--	--	--	--	--	--	--	--	--	--	--	--	--	--	--	--	--	--	--	--	--	--	--	--	--	--	--	--	--	--	--	--	--	--	--	--	--	--	--	--	--	--	--	--	--	--	--	--	--	--	--	--	--	--	--	--	--	--	--	--	--	--	--	--	--	--	--	--	--	--	--	--	--	--	--	--	--	--	--	--	--	--	--	--	--	--	--	--	--	--	--	--	--	--	--	--	--	--	--	--	--	--	--	--	--	--	--	--	--	--	--	--	--	--	--	--	--	--	--	--	--	--	--	--	--	--	--	--	--	--	--	--	--	--	--	--	--	--	--	--	--	--	--	--	--	--	--	--	--	--	--	--	--	--	--	--	--	--	--	--	--	--	--	--	--	--	--	--	--	--	--	--	--	--	--	--	--	--	--	--	--	--	--	--	--	--	--	--	--	--	--	--	--	--	--	--	--	--	--	--	--	--	--	--	--	--	--	--	--	--	--	--	--	--	--	--	--	--	--	--	--	--	--	--	--	--	--	--	--	--	--	--	--	--	--	--	--	--	--	--	--	--	--	--	--	--	--	--	--	--	--	--	--	--	--	--	--	--	--	--	--	--	--	--	--	--	--	--	--	--	--	--	--	--	--	--	--	--	--	--	--	--	--	--	--	--	--	--	--	--	--	--	--	--	--	--	--	--	--	--	--	--	--	--	--	--	--	--	--	--	--	--	--	--	--	--	--	--	--	--	--	--	--	--	--	--	--	--	--	--	--	--	--	--	--	--	--	--	--	--	--	--	--	--	--	--	--	--	--	--	--	--	--	--	--	--	--	--	--	--	--	--	--	--	--	--	--	--	--	--	--	--	--	--	--	--	--	--	--	--	--	--	--	--	--	--	--	--	--	--	--	--	--	--	--	--	--	--	--	--	--	--	--	--	--	--	--	--	--	--	--	--	--	--	--	--	--	--	--	--	--	--	--	--	--	--	--	--	--	--	--	--	--	--	--	--	--	--	--	--	--	--	--	--	--	--	--	--	--	--	--	--	--	--	--	--	--	--	--	--	--	--	--	--	--	--	--	--	--	--	--	--	--	--	--	--	--	--	--	--	--	--	--	--	--	--	--	--	--	--	--	--	--	--	--	--	--	--	--	--	--	--	--	--	--	--	--	--	--	--	--	--	--	--	--

EOLDOUT FRAME

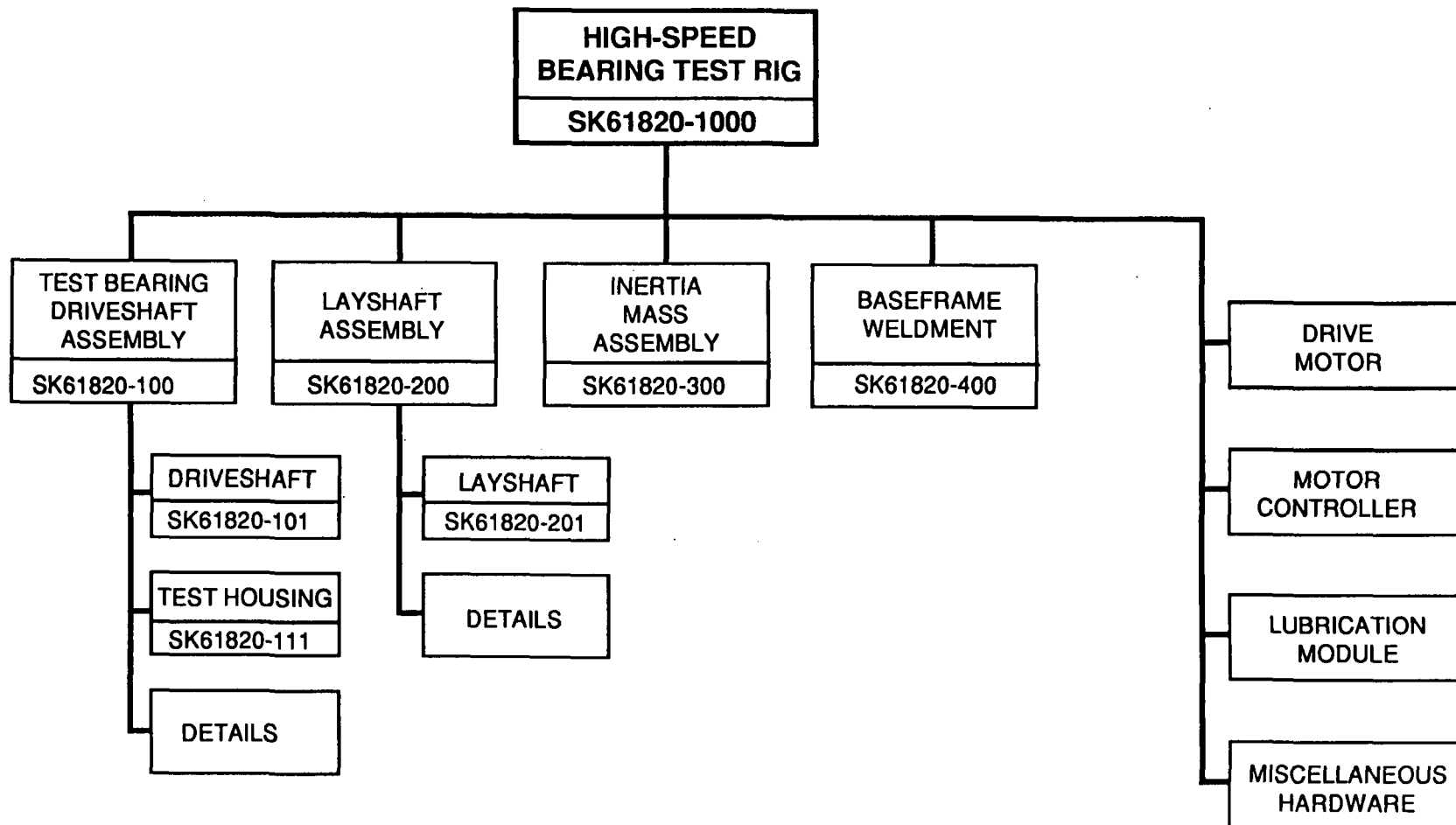
EOLDOUT FRAME

**PARTS LIST
FOR
HIGH-SPEED BEARING
TEST RIG**

May 1995

Contract No. NAS 8-38095

wyle
laboratories



DRAWING TREE FOR HIGH-SPEED BEARING TEST RIG

Drawing Number	Item	Qty.	Part Number	Description	Remarks
SK61820-1000 High-Speed Bearing Test Rig	1	1	SK61820-100	Test Bearing Driveshaft Assembly	See breakdown below
	2	1	SK61820-200	Layshaft Assembly	See breakdown below
	3	1	SK61820-300	Inertia Mass Assembly	--
	4	1	SK61820-400	Baseframe Weldment	--
	5	1		Drive Motor	
	6	1		Motor Controller	
	7	1	SK61820-1001	Motor Pulley	--
	8	1	6202564	Trantorque Bushing	
	9	4		Bolt	--
	10	4		Washer	--
	11	2		Tensioner Bolt	--
	12	39		Bolt	--
	13	78		Washer	--
	14	39		Nut	--
	15	1	6248N14	Beltguard (McMaster-Carr or equiv.)	--
	16	1	6248N13	Belt Guard (McMaster-Carr or Equiv.)	--
	17	4	5010T432	Caster Assembly (McMaster-Carr)	
	18	1		Lubrication Module (Vogel or Equiv.)	
SK61820-100 Test Bearing Driveshaft Assembly	1	1	SK61820-101	Driveshaft	See Drawing # SK61820-101
	2	1	SK61820-102	Housing	--
	3	2	SKF71907-CD	Bearing, 35 mm Bore	
	4	1	SK61820-103	Spacer	--
	5	2	SKF71906-CD	Bearing, 30 mm Bore	
	6	1	SK61820-104	Spacer	--
	7	1	SK61820-105	Spacer	--
	8	2	SKFN07	Locknut	
	9	2	SKFW07	Lockwasher	
	10	1	SK61820-106	Spacer	--
	11	1	SKFN06	Locknut	
	12	1	SKFW06	Lockwasher	
	13	1	SK61820-107	Locking Ring	--
	14	1	SK61820-108	Split Cover, Primary	--
	15	1	SK61820-109	Split Cover, Secondary	--

Drawing Number	Item	Qty.	Part Number	Description	Remarks
SK61820-100 (Continued)	16	38		Socket Head Cap Screw	--
	17	38		Flat Washer	--
	18	1	SK61820-110	Drive Pulley	--
	19	1	6202160	Trantorque Bushing	
	20	1		Drivebelt (Habasit or equiv.)	
	21	1	SKF 7209C	Test Bearing, 45 mm Bore	
	22	1	SK61820-111	Test Housing	See Drawing # SK61820-111
	23	1	SK61820-112	Spacer	--
	24	1	SK61820-113	Spacer	--
	25	1	SK61820-114	Spacer	--
	26	1	SK61820-115	Split Cover, Test Housing	--
	27	1	SK61820-116	End Cover	--
	28	1	SK61820-117	Spacer, Locating	--
	29	A.R.	SK61820-118	Shim	--
	30	1	SK61820-119	Top Cover	--
	31	1	SK61820-120	Loading Bracket	--
	32	2		Bolt	--
	33	2		Washer	--
	34	2	SK61820-121	Loading Clevis	--
	35	1	SK61820-122	Threaded Rod	--
	36	3	98306D491	Pin, 5/8 in. dia. x 1-1/4 Grip (McMaster-Carr or equiv.)	--
	37	1	SK61820-123	Link	--
	38	4	98306 A562	Pin, 3/4 in. dia. x 3.0 Grip (McMaster-Carr or equiv.)	--
	39	2	SK61820-124	Load Lever	--
	40	1	SK61820-125	Bracket	--
	41	12		Bolt	--
	42	12	MS51412-6A	Oversize Washer, 3/8 Bore x 7/8 o/dia.	--
	43	1	CCYR-1 1/4-S	Roller	
	44	1	SK61820-126	Bellcrank	--
	45	1	98306 A273	Pin, 3/8 in. dia. x 1-1/2 Grip (McMaster-Carr or equiv.)	--
	46	1	SK61820-127	Bracket	--
	47	2	SK61820-128	Channel	--
	48	6		Bolt	--
	49	12		Washer	--
	50	A.R.	SK61820-129	Shim	--

Drawing Number	Item	Qty.	Part Number	Description	Remarks
SK61820-100 (Continued)	51	6		Nut	--
	52	1	92391 D054	Hairpin Cotter, 3/8 dia. pin (McMaster-Carr or equiv.)	--
	53	7	92391 D064	Hairpin Cotter, 5/8 dia & 3/4 dia pins (McMaster-Carr or equiv.)	--
	54	TBD		Lubrication Nozzle	
	55	2		Plug, 1/2 in NPT (MS20913-4 or equiv.)	--
SK61820-200 Layshaft Assembly	1	1	SK61820-201	Layshaft	See Drawing #SK61820-201
	2	1	SK61820-202	Housing	--
	3	2	SKF61908	Bearing, 40 mm Bore	
	4	1	SK61820-203	Spacer	--
	5	1	SK61820-204	Spacer	--
	6	2	SKF N08	Locknut	
	7	2	SKF W08	Lockwasher	
	8	1	SK61820-205	Locking Ring	--
	9	1	SK61820-206	Large Pulley	--
	10	1	SK61820-207	Small Pulley	--
	11	2	6202320	Trantorque Bushing	
	12	1	SK61820-208	Split Cover, Long	--
	13	1	SK61820-209	Split Cover, Short	--
	14	1		Drivebelt (Habasit or equiv.)	
	15	20		Socket Head Capscrew	--
	16	20		Washer	--
	17	4		Bolt	--
	17	4		Washer	--
	19	1	SK61820-210	Support Stand Assembly	--
	20	2		Tensioner Bolt	--
	21	1	SK61820-211	Top Cover	--
	22	A.R.		Shim	--
	23	2		Lubrication Nozzle	--
	24	2		Plug, 1/2 in NPT (MS20913-4 or equiv.)	

APPENDIX D

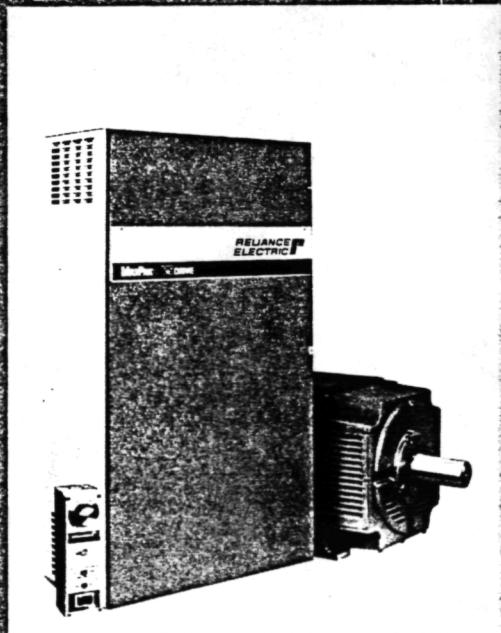
**DC DRIVE MOTOR AND DC CONTROLLER -
TECHNICAL LITERATURE**

**RELIANCE
ELECTRIC**

Special
capabilities —

Regenerative

MAXPAK PLUS VS DRIVE MAXPAK PLUS
D-C VS DRIVE
Type S6R



- for 5 to 1500 hp applications requiring
- regeneration
 - contactorless reversing
 - super high response

RELIANCE ELECTRIC

Special capabilities

Regenerative

MAXPAK PLUS

with all of the reliability, quality,
flexibility and features you have
come to expect with **MAXPAK PLUS**

We started with the most preferred D-C drive in industry — the Reliance® MAXPAK PLUS V*S Drive — and built a line of drives for those applications requiring regeneration, contactorless reversing or extremely high response. The result is a drive every bit a MAXPAK PLUS, with the added capability of four-quadrant control.

Like every MAXPAK PLUS, these regenerative drives are furnished complete with:

A total commitment to reliability

Components designed to Reliance specifications and inspected upon receipt to unyielding tolerance levels, in-process testing, thermal cycling and computer-directed final drive test together assure shipment of Regenerative MAXPAK PLUS controllers that are every bit as good as their design.

Design coordinated Super RPM™ Motors

Regenerative MAXPAK PLUS, delivered with a matched Super RPM™ Motor, offers you a completely compatible drive package with all of the advantages of single source responsibility — every time.

Simplified installation and service

Well-positioned power terminals and ample space within the controller cabinet allow faster and simpler installation. Two complete sets of output power terminations allow easy top or bottom output power exit from the controller. A complete spare parts list, startup instructions and tightening specifications for power bus and cable fasteners are printed and mounted inside the cabinet door. And, as with every MAXPAK PLUS, construction is completely modular.

Availability from stock

Selected ratings through 150 hp, with matched Super RPM motors as well as motor and controller modification kits, are available for delivery right from our stock. Ratings from 200 through 1500 hp are available from the factory.

Real flexibility

Regenerative MAXPAK PLUS is easily modified — during manufacture, from stock at one of our V*S Sprint stock modification centers, or right in your plant using the complete line of MAXPAK PLUS prepackaged modification kits. (Kits are described in detail in Bulletin D-2638).

Compact construction in an enclosure of your choice.

Standard units through 150 hp are furnished in wall-mount NEMA 1 enclosures. NEMA 4, NEMA 12 or floor-mount enclosures are optional. Or, you can specify the controller in open panel construction for mounting in an enclosure of your own.

Useable anywhere

Operable without modification on either 50 or 60 Hz power and easily adapted for operation on any line voltage between 200 and 575V A-C. Regenerative MAXPAK PLUS satisfies drive requirements worldwide.

UL listed and CSA certified

Of course. Supplied in a Reliance cabinet, the Regenerative MAXPAK PLUS controller—even when kit is modified—is UL listed and adapts simply to CSA requirements. As an open panel controller, it is UL listed and CSA certified.

With Regenerative MAXPAK PLUS you also get:

Full regenerative capability

Two six-pulse rectifier bridges (S6R) and coordinated sequencing and control allow both motoring and regenerating operation and contactorless motor reversing.

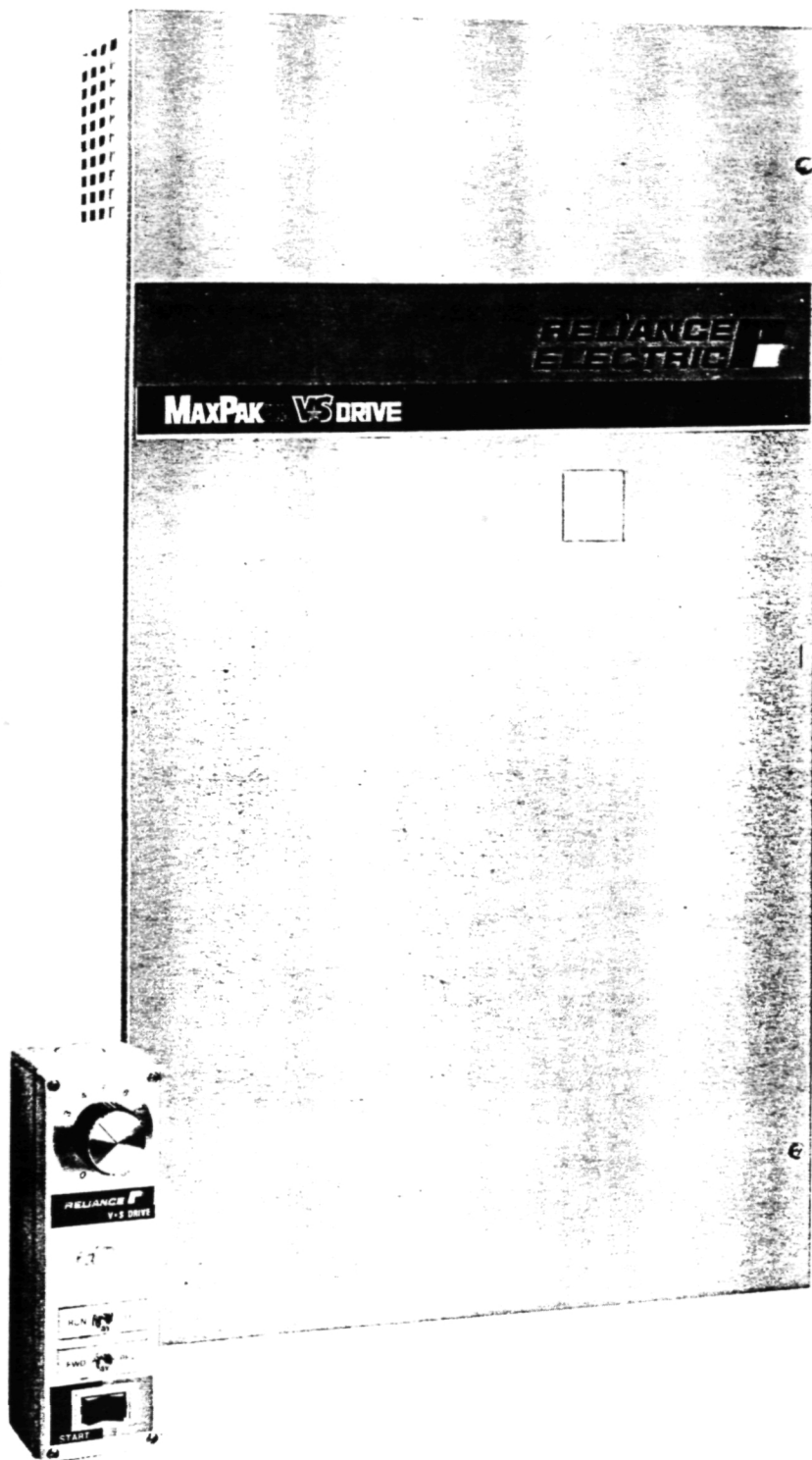
Super high performance capability

As standard, the Regenerative MAXPAK PLUS has all the response you will normally need. But when your application requires more, an automatic adaptive current loop (providing a 10:1 increase in current loop bandwidth when in discontinuous conduction) and proper selection of major loop amplifier feedback components let us give you all the response you need.

A lot in common with non-regenerative MAXPAK PLUS

Regenerative MAXPAK PLUS shares its concept, design, and many components and assemblies with non-regenerative MAXPAK PLUS. Over half of the regulator cards, all fuses, the shunt field supply and nearly all kit modifications are identical with non-regenerative MAXPAK PLUS. Minimum spare parts. Minimum personnel training. Maximum return on your drive investment.

Regenerative MAXPAK PLUS provides application and operational flexibility without complexity. Each controller consists of a power unit, regulator and armature loop disconnects for 20:1 controlled speed range, 50/60 HZ operation without modification, 5% speed regulation with 95% load change and more—all with a standard, out-of-stock package.



Basic description

Regenerative MAXPAK PLUS drives provide full four-quadrant operation with regenerative capability to the A-C power line. This, in turn, provides a reverse-torque "hold back" capability for overhauling loads, on applications requiring rapid, controlled deceleration to zero speed, or for process lines requiring progressive draw between individual sections.

Regenerative MAXPAK PLUS drives also provide motor operation in either direction of rotation — without field reversal or operation of the armature loop contactor. This contactorless reversing capability permits frequent motor reversal without causing excessive wear on relays or contactors.

Regenerative MAXPAK PLUS provides application and operational flexibility without complexity. It's all done within the electronics of the armature power unit.

Together with the complete control afforded by the fully regenerative power unit, regulator circuit options like the adaptive current loop (providing a 10:1 increase in current loop gain when in discontinuous conduction) and application-selected major loop amplifier feedback components make Regenerative MAXPAK PLUS the answer for those applications requiring super high response.

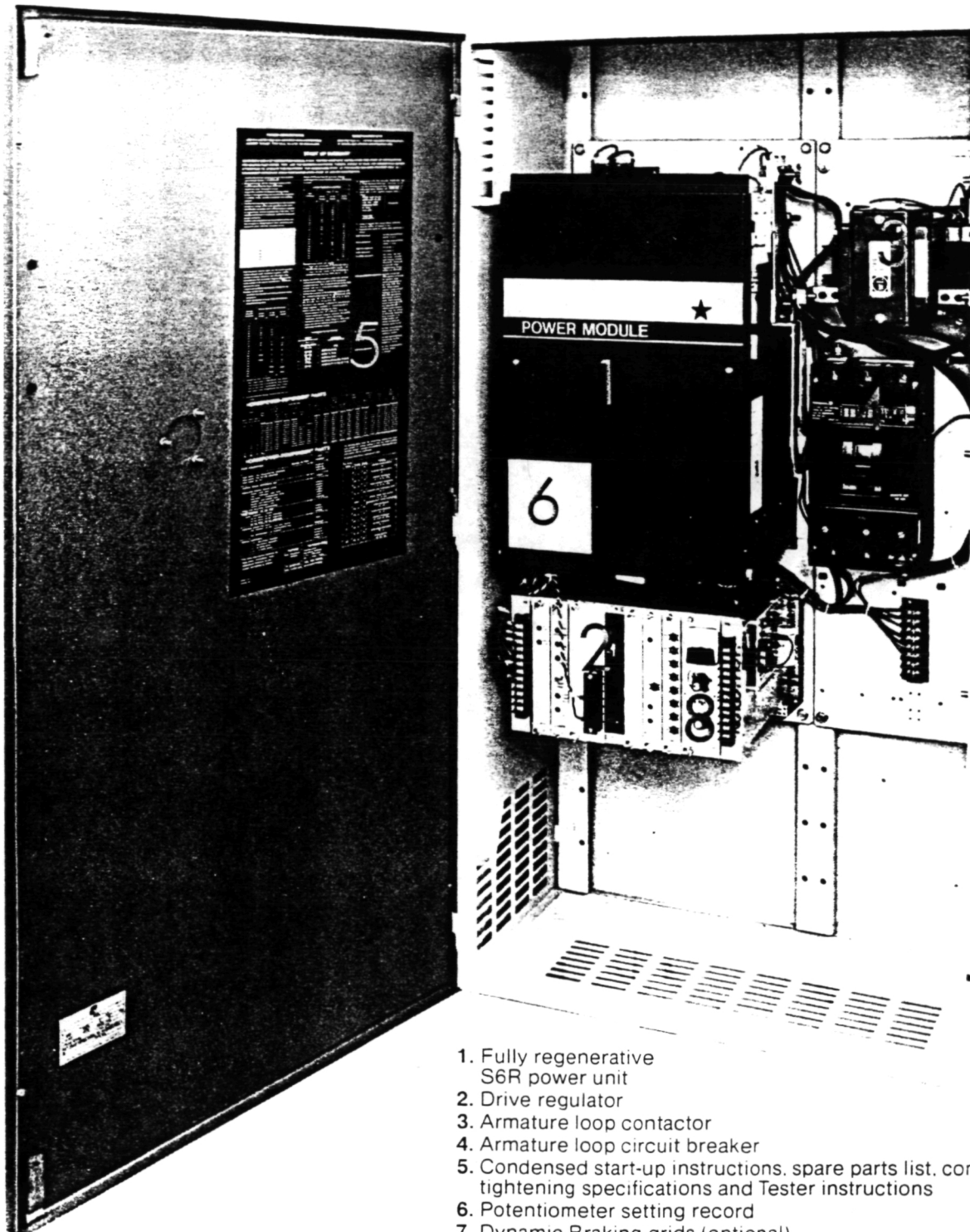
Each Regenerative MAXPAK PLUS controller consists of a power unit, regulator and armature loop disconnects. These elements provide Regenerative MAXPAK PLUS with the following capabilities:

- 20:1 controlled speed range for wide speed range applications.
- 5% speed regulation with 95% load change for minimum motor speed variation even without tachometer feedback.
- Separately adjustable rates of linear acceleration and deceleration to assure smooth starts and speed changes.
- Jog at adjustable preset speed by pushbutton or selector switch for momentary drive operation at an independently adjusted speed.
- Adjustable maximum and minimum speeds to preset machine speed limits.
- 50/60 Hz operation without modification.
- Armature loop contactor to provide positive motor disconnect.
- Fused and isolated 115V A-C supply to power pushbutton devices and regulator.
- Six-pulse power bridges assure cooler motor operation and better commutation.
- 150%, one-minute current ratings support acceleration and short term machine overload.

By simple reconnection, Regenerative MAXPAK PLUS controllers may be adapted to provide additional features.

- Speed regulation with tachometer feedback provides 1% or 0.5% regulation depending upon the tachometer used.
- Timed acceleration to and deceleration from jog speed to cushion machinery and process during jogging operation.
- Delayed contactor drop-out after jog command allows repeated jogging without contactor cycling for minimum contactor wear.
- Extended acceleration and deceleration times for applications requiring extremely slow speed changes.
- Regenerative braking to rest upon a stop command for controlled motor deceleration to zero speed.

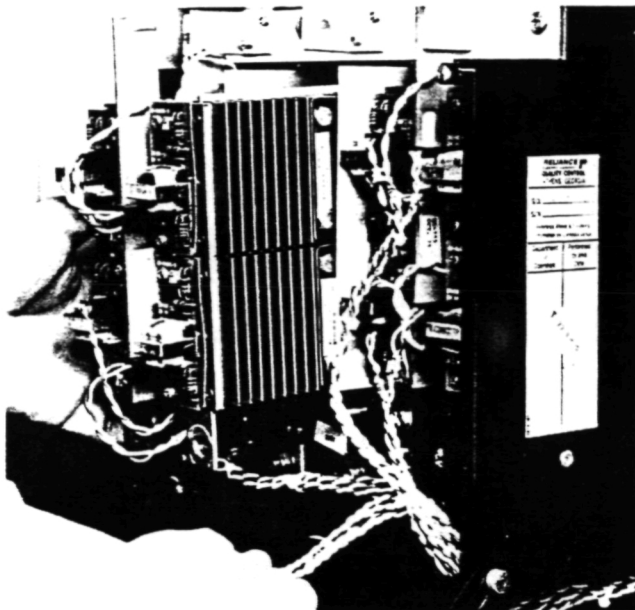
A 100 hp, 460V Regenerative MAXPAK PLUS Drive with Dynamic Braking and optional Tester Card in its compact, wall-mount cabinet.



1. Fully regenerative S6R power unit
2. Drive regulator
3. Armature loop contactor
4. Armature loop circuit breaker
5. Condensed start-up instructions, spare parts list, connector tightening specifications and Tester instructions
6. Potentiometer setting record
7. Dynamic Braking grids (optional)
8. Tester (optional)

Basic description

Power unit

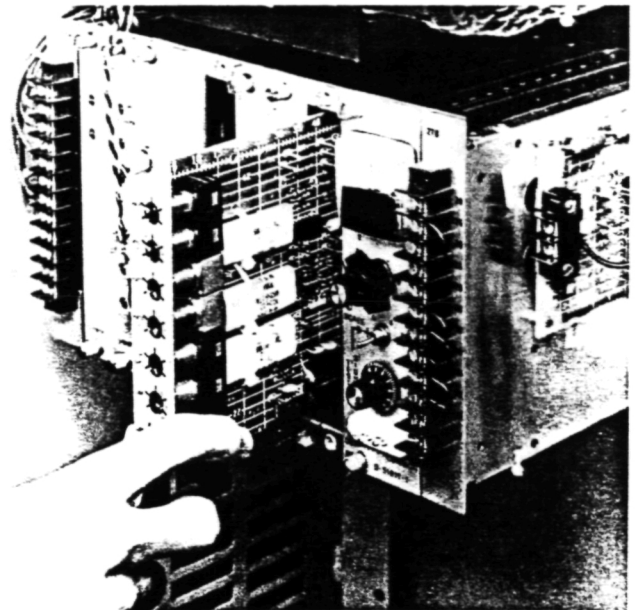


Power unit components are mounted on three identical rectifier modules — one for each phase. Bolted power connections are readily accessible. Gate leads are quickly, easily removed with plug connectors.

The Regenerative MAXPAK PLUS controller employs two independent full-wave, six-pulse, phase-controlled rectifier bridges which are connected in anti-parallel (S6R) to provide adjustable voltage armature power for adjustable speed D-C motor drive service. These rectifier bridges, each composed of six thyristors, operate directly from three-phase plant power. This power unit provides full four-quadrant capability: (1) forward motoring, (2) forward regeneration, (3) reverse motoring, (4) reverse regeneration. Through regulator selection of either the forward or reverse rectifier bridge, the direction of armature current flow can be determined. And through firing angle control, armature current flow is regulated and controlled.

Power unit construction is modular — with three identical rectifier modules. Each module contains four thyristors plus their dv/dt protective networks... gate firing circuitry... and heatsinks. Each module is easily removable and replaceable as a unit. Gate lead connections utilize quick-disconnect plugs.

Regulator



The fully modular regulator is composed of six plug-in cards. Faceplate-mounted status indicators allow easier troubleshooting and a better understanding of regulator operation. All regulator adjustments are faceplate-mounted — up front where you can see them. The optional Tester Card makes servicing even easier.

Acting in response to the setting of the operator's speed potentiometer and the instantaneous value of the major loop controlled variable — most often armature voltage or motor speed — the drive regulator selects the proper rectifier bridge and determines its firing angle.

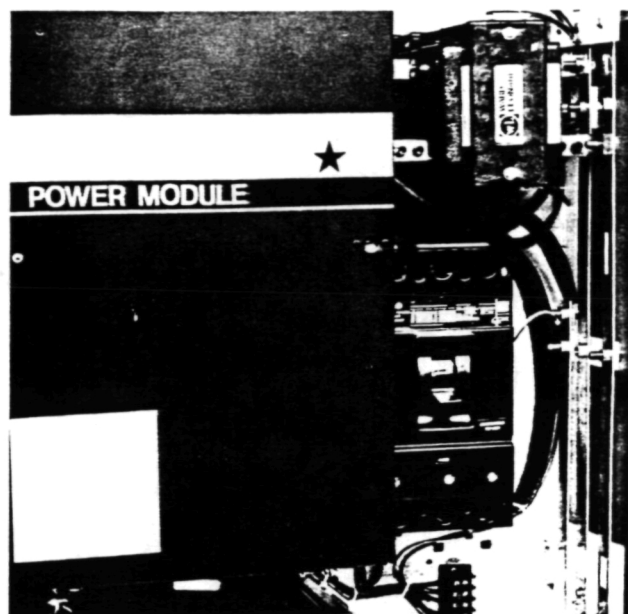
Through its static logic circuitry, the regulator sequences the drive as required for proper operation in response to operator start, stop and jog pushbuttons and interfaces with the forward/reverse selector switch. All sequencing is solid state.

By continuously monitoring motor armature current (motor torque), the regulator assures that power unit output current and delivered motor torque remain within safe limits. Current limit circuitry, motor thermal overload protection and electronic peak overcurrent protection (Instantaneous Electronic Trip) all reside within the drive regulator.

The gate pulses used to fire power unit thyristors are generated by a digital firing circuit within the regulator. This circuitry removes the possibility of thyristor-to-thyristor firing angle differences caused by component tolerances, assures balanced firing and load sharing between thyristors and removes the need for phase balance adjustments.

The regulator consists of six plug-in cards for ease of service. An optional Tester Card is available, allowing measurement of 11 regulator and power unit voltage levels for in-service drive monitoring and analysis.

Armature disconnects



The motor armature is connected to the controller through an armature loop contactor and D-C circuit breaker. Together, these devices form an armature disconnect system to assure coordinated armature connection to the Regenerative MAXPAK PLUS controller.

The drive motor is connected to the power unit through an armature contactor and armature loop circuit breaker. The contactor provides a positive disconnect between the motor and the power unit during standby periods. Although selected to interrupt 100% armature current, regulator sequencing operates this device under zero armature current conditions to assure long service life.

For protection of the complete drive, the D-C breaker in the armature loop provides a means to disconnect the motor from the power unit under unusual inverting fault conditions, such as loss of incoming A-C power during regenerative operation.

Coordinated drive protection

Regenerative MAXPAK PLUS has been designed with a complete protective system to help safeguard the drive as well as the driven machinery.

- Phase sequence and line loss interlock with indicator light assure that plant power — with the correct phase rotation — is present before the drive can start.
- A-C line and D-C load transient protection assures reliable controller operation.
- Current-limiting fuses in the A-C line protect the drive from high current faults.
- Output from the field supply is monitored, with a proper output required before drive operation is enabled. An indicating light confirms proper field supply output.
- Current limit control, with independent adjustment for positive and negative armature current flow, helps protect the drive and the driven machine from damaging current and torque levels during acceleration or deceleration, as well as from machine-induced overloads.
- A digital thermal overload circuit, with indicating light, protects the drive from long term, low level overloads.
- Electronic peak overcurrent protection (Instantaneous Electronic Trip) and indicating light provide protection against severe and sudden overloads such as those brought on by machine jam-ups.
- Armature loop circuit breaker protects both the motor and the controller in event of an inverting fault.

Performance/specifications

Service Conditions

Elevation Up to 3300 feet
(1000 meters)

Ratings

Ambient Temperature

Cabinet Models 32 to 104°F
(0 to 40°C)

Panel-Mounted Models 32 to 131°F
(0 to 55°C)

Power Input Three-phase, 230, 460 or 575 VAC

Line Frequency 48-62 Hz

Line Voltage Variation $\pm 10\%$ of nominal

Relative Humidity 0 to 95%
(without condensation)

Load Specifications

Overload Capacity 150% of full load rated armature
current for one minute

Controller Service Factor 1.0

Minimum Load for Assured Stable Operation 5%

Adjustments

Acceleration 0.5-30 seconds

Deceleration 0.5-30 seconds

Minimum Speed 0-40%

Maximum Speed 80-120%

Jog Speed 0-50%

Current Limit

Positive I_A 50-150%

Negative I_A 50-150%

Speed Regulation

Speed Regulation with 95% load change (% of motor base speed)	All Other Variables (% of motor base speed)	Tachometer Required (1)
5%	15%	None
1%	2%	5PY
0.5%	0.5%	BC-42
0.1%	0.15% (2)	RE-210

(1) Tachometer must provide direct current (D-C) output.

(2) Controller requires factory addition of precision reference supply to meet this specification.

Efficiency

Controller only Figure 1 illustrates typical controller-only efficiency vs. speed and load.

Complete drive, including motor Dependent on motor selected. Typical drive efficiency will be in the range of 85 to 93% operating at full speed, full load.

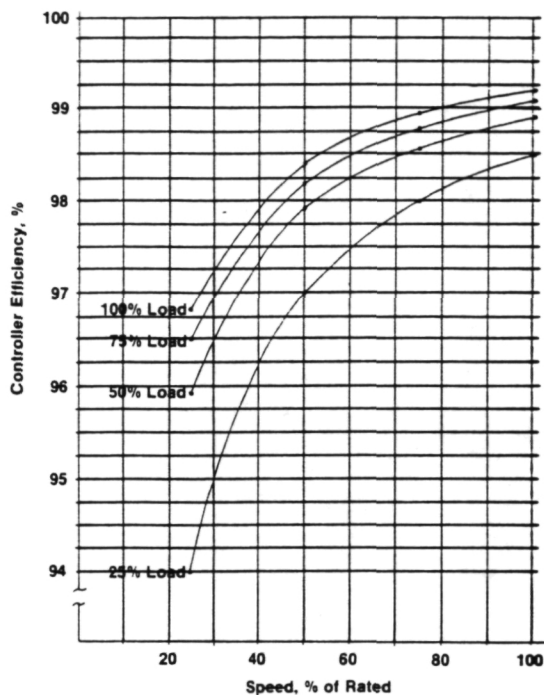


Figure 1

Displacement Power Factor

This is almost entirely a function of operating speed. Displacement power factor vs. speed is illustrated in Figure 2.

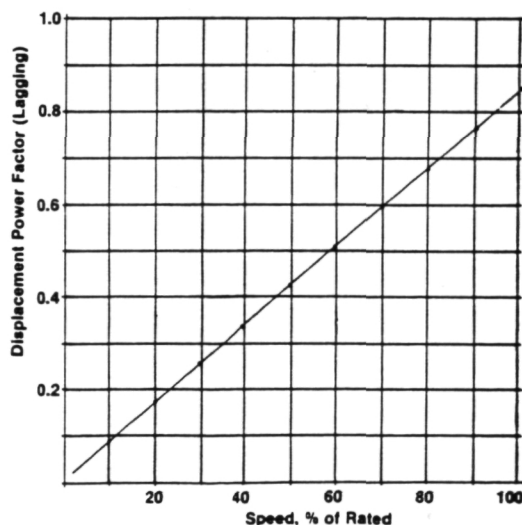
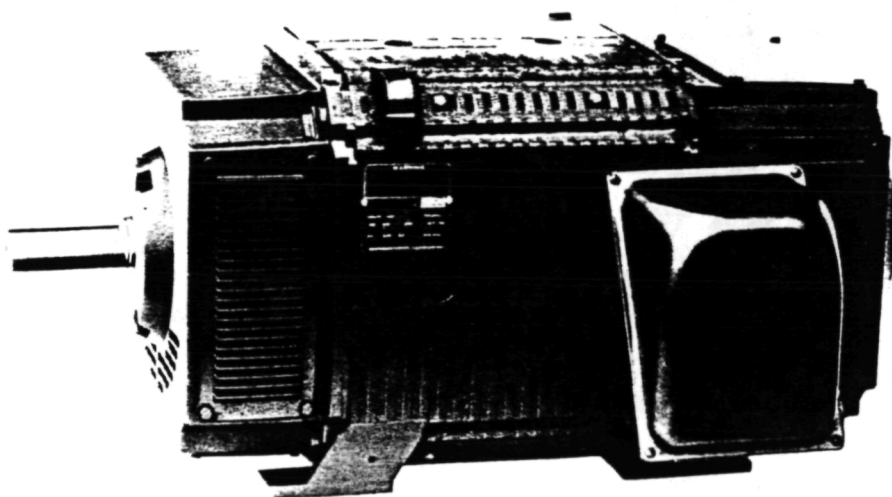


Figure 2

Controller Ratings

HP Ratings	Full Load Rated RMS A-C Line Current (Amperes)			Full Load Rated D-C Armature Current (Amperes)			Field Supply Current Capacity (Amperes)		
	230V	460V	550V	240V	500V	600V	150V	300V	240V
5	20	15	—	19	10	—	5	5	—
7½	29	18	—	29	14	—	5	5	—
10	36	21	—	38	18	—	5	5	—
15	52	30	—	56	28	—	5	5	—
20	68	37	—	74	36	—	10	5	—
25	84	44	—	93	45	—	15	5	—
30	99	50	—	110	52	—	15	5	—
40	127	64	54	144	69	57	15	10	15
50	158	79	68	178	86	72	15	15	15
60	186	91	79	212	100	86	15	15	15
75	244	116	97	265	129	107	15	15	15
100	—	152	127	—	167	139	—	15	15
125	—	180	152	—	205	171	—	15	15
150	—	219	180	—	250	208	—	15	15



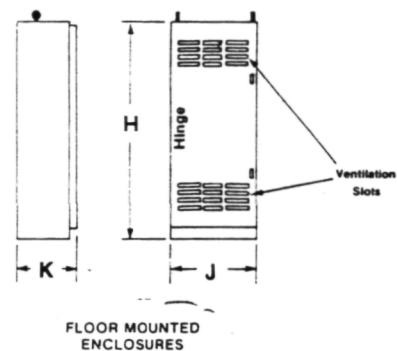
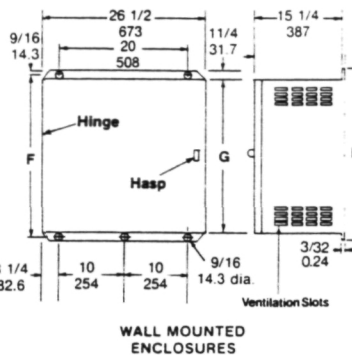
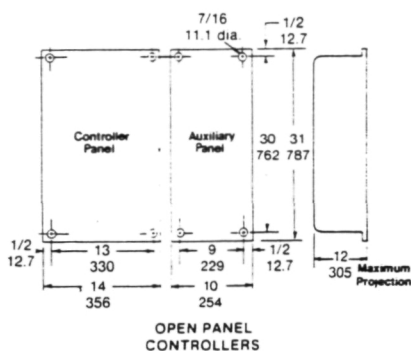
**“We build
more into
every
Reliance
motor!”**

Regenerative MAXPAK PLUS, like all V•S Drives, is design-coordinated with a dependable Reliance motor. The power-matched Super™ RPM Motor is built to take on industry's toughest jobs. The result is a completely compatible drive package with single-source responsibility.

Dimensions

Regenerative **MAXPAK PLUS**

(Inches
Millimeters)



Controller Enclosures (Optional)

HP			
230V A-C Input 240V D-C Armature	460V A-C Input 500V D-C Armature	575V A-C Input 600V D-C Armature	NEMA 1 Controller Enclosure
5 - 50	5 - 100	40 - 125	W42
60 - 75	125 - 150	150	W48

Wall Mounted Enclosures (Standard)

Size	Dimensions Inches/Millimeters			Weight
	E	F	G	
W42	44 1/2 1130	43 3/8 1102	42 1067	320 lbs. 145 kg.
W48	50 1/2 1283	49 3/8 1254	48 1219	400 lbs. 181 kg.

Floor Mounted Enclosures

Size	Dimensions Inches/Millimeters			Door Swing	Weight
	H	J	K		
FD68	68 1727	32 813	20 508	135°	600 lbs. 272 kg.
FD86	86 2184	34 864	24 610	155°	725 lbs. 330 kg.

This bulletin is not intended to provide operational instructions. Appropriate Reliance Electric instruction manuals and warning tags attached to the apparatus should be read prior to installation, operation and/or maintenance of equipment.

Straight Shunt Motor Ratings⁽¹⁾

HP	Armature Volts	Drip Proof RPM		Fan Cooled RPM	
		1750	1150	1750	1150
5	240	B1811ATZ	B1812ATZ	B1812ATZ	B2112ATZ
	500	B1811ATZ	B1812ATZ	B1812ATZ	B2112ATZ
7 1/2	240	B1811ATZ	B2111ATZ	B2112ATZ	B2511ATZ
	500	B1811ATZ	B2111ATZ	B2112ATZ	B2510ATZ
10	240	B1812ATZ	B2112ATZ	B2510ATZ	B2810ATZ
	500	B1812ATZ	B2112ATZ	B2510ATZ	B2810ATZ
15	240	B2111ATZ	B2511ATZ	B2810ATZ	B327ATZ
	500	B2111ATZ	B2511ATZ	B2810ATZ	B327ATZ
20	240	B2112ATZ	B2810ATZ	B2810ATZ	B328ATZ
	500	B2112ATZ	B2810ATZ	B2810ATZ	B328ATZ
25	240	B2510ATZ	B2810ATZ	B327ATZ	AB328ATZ
	500	B2510ATZ	B2810ATZ	B327ATZ	AB328ATZ
30	240	B2511ATZ	B2811ATZ	B328ATZ	B367ATZ
	500	B2511ATZ	B2811ATZ	B328ATZ	B367ATZ
40	240	B2810ATZ	B327ATZ	B368ATZ	B369ATZ
	500	B2810ATZ	B327ATZ	B367ATZ	B369ATZ
50	240	B2811ATZ	AB328ATZ	B368ATZ	B3610ATZ
	500	B2811ATZ	AB328ATZ	B368ATZ	B3610ATZ
60	240	B327ATZ	B367ATZ	B3610ATZ	B409ATZ
	500	B327ATZ	B368ATZ	B3610ATZ	B409ATZ
75	240	BB328ATZ	BB368ATZ	B408ATZ	B409ATZ
	500	B328ATZ	B368ATZ	B408ATZ	B409ATZ
100	500	B367ATZ	B3610ATZ	B409ATZ	B506ATZ
	500	B369ATZ	UB408ATZ	B506ATZ	B507ATZ
125	500	B369ATZ	UB408ATZ	B506ATZ	B507ATZ
	500	B3610ATZ	UB409ATZ	B507ATZ	B508ATZ
150	500	B3610ATZ	UB409ATZ	B507ATZ	B508ATZ
	500	B3610ATZ	UB409ATZ	B507ATZ	B508ATZ

1. Straight shunt D-C motors (with no series or stabilizing winding) are recommended for use with Regenerative MAXPAK PLUS controllers in order to assure full torque capability under conditions of forward regeneration and reverse motoring.

Reference Literature Regenerative MAXPAK PLUS

Product Bulletin.	D-2638
Controller Instruction Manual (Controller and all modification kits).	D-3851
Selection and Application Manual.	D-9081
Super RPM D-C Motor Product Bulletin.	C-2519
Instruction Manual.	C-3076

Reliance Electric Company • 24703 Euclid Avenue • Cleveland, Ohio 44117

RELIANCE ELECTRIC

AND GENERATORS - RPM III

ENCLOSURE: Drip-Proof Fully-Guarded, Splashproof

COOLING:

Force Ventilated with Integral Blower and Motor
Air Filtered

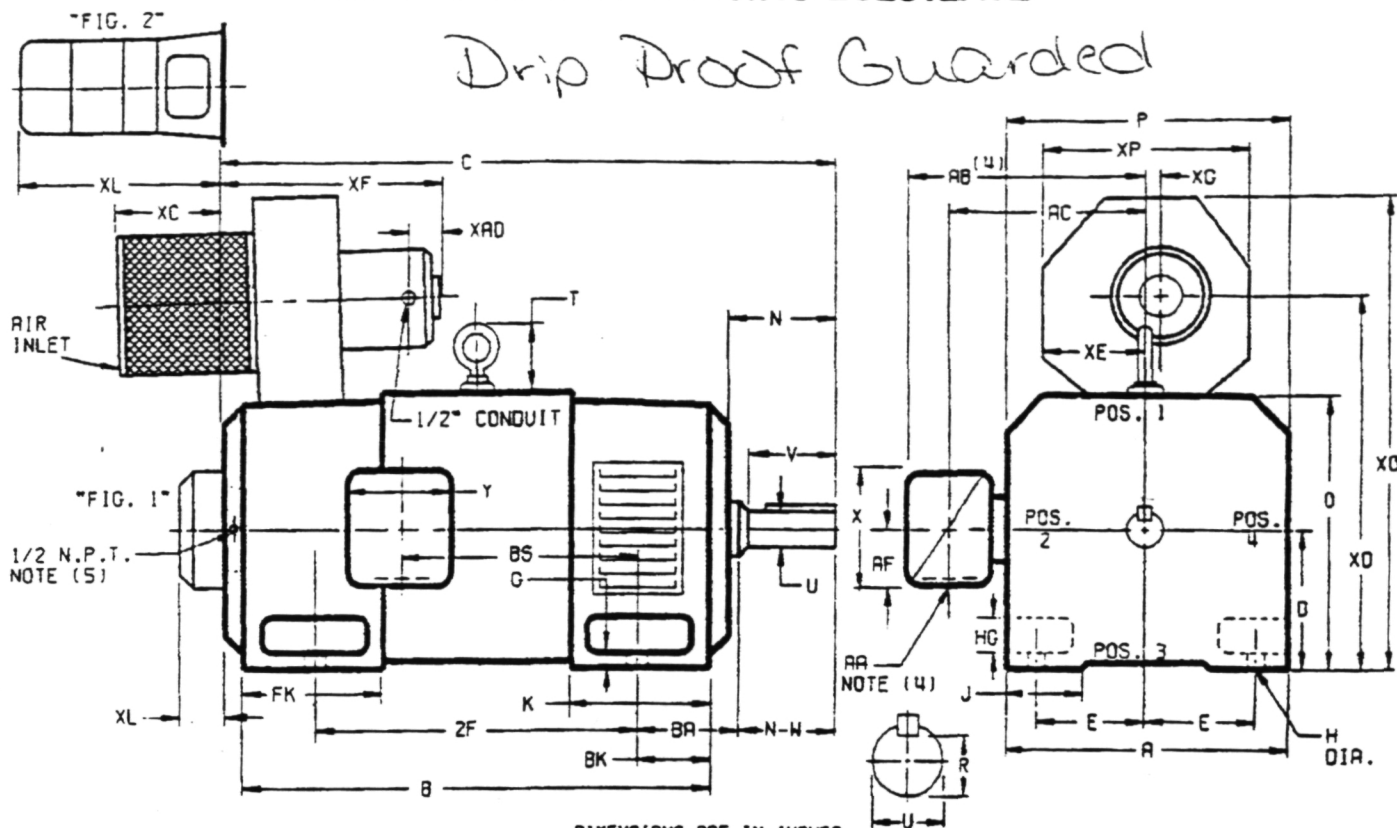
MOUNTING: Foot

METHOD OF DRIVE: Coupled or Belted

ACCESSORIES: Flange Mounted Tachometer

FRAMES SC2113ATZ THRU LC2812ATZ

Drip Proof Guarded



DIMENSIONS ARE IN INCHES

FRAME	A	D(1)	E	G	H	HQ	J	O	P	T	BA	K	FK	BK
SC2113ATZ-LC2113ATZ	10.25	5.25	4.25	.44	.44	1.38	1.75	10.44	10.31	2.56	3.50	5.19	6.81	2.38
SC2512ATZ-LC2512ATZ	12.31	6.25	5.00	.50	.56	1.62	2.00	12.50	12.44	3.06	4.25	6.06	8.00	3.00
MC2812ATZ-LC2812ATZ	13.78	7.00	5.50	.62	.56	1.88	2.75	14.00	13.94	3.38	4.75	6.75	9.19	3.50

FRAME	C	B	BS	2F	DRIVE END SHAFT AND KEY							WT. LBS.
					N	N-W	UC(1)	V	RI(3)	SO.	LGTH.	
SC2113ATZ	28.38	22.50	11.38	18.00	4.00	3.75	1.875	3.50	1.591	.500	2.50	345
MC2113ATZ	29.62	23.75	12.62	18.00	4.00	3.75	1.875	3.50	1.591	.500	2.50	370
LC2113ATZ	31.25	25.38	14.25	18.00	4.00	3.75	1.875	3.50	1.591	.500	2.50	400
SC2512ATZ	31.69	25.06	12.06	20.00	4.50	4.25	2.125	4.00	1.845	.500	3.00	535
MC2512ATZ	33.19	26.56	13.56	20.00	4.50	4.25	2.125	4.00	1.845	.500	3.00	570
LC2512ATZ	34.69	28.06	15.06	20.00	4.50	4.25	2.125	4.00	1.845	.500	3.00	610
MC2812ATZ	37.38	29.94	14.25	22.00	5.00	4.75	2.375	4.50	2.021	.625	3.50	810
LC2812ATZ	39.62	31.19	16.50	22.00	5.00	4.75	2.375	4.50	2.021	.625	3.50	885

TACH.	XL	WT. LBS.	FIG.
RE-007, RE-020	4.94	10	2
RE-045G	1.56	5	1
RE-210	15.62	35	2
BC-42	13.62	35	2
BC-46	16.06	50	2
BC-46/K460	18.75	55	2
X/P BC-42	15.25	35	2
X/P BC-46	16.44	50	2
RD-11			
RD-12	10.38	10	2
RD-51	16.94	50	2
RD-61, RD-62	9.94	10	2
SPY	11.31	17	2
TGF-2100-00-A	1.56	5	1
TGF-2100-00-D	1.56	5	1
M627, M628			
M727, M737, M738	10.69	25	2
OTMAPAR 74C	3.25	12	1
RESOLVER			
CU9-1093-020	11.44	15	2
MIAN, MIA7	3.19	25	1

FRAME	XC	XO	XE	XF	XG	XO	XP	XAD
SC2113ATZ-LC2113ATZ	3.88	15.56	5.12	14.38	.38	20.69	10.25	1.00
SC2512ATZ-LC2512ATZ	3.19	17.62	5.12	15.12	.38	22.75	10.25	1.00
MC2812ATZ-LC2812ATZ	6.38	19.12	5.12	18.12	.38	24.25	10.25	3.00

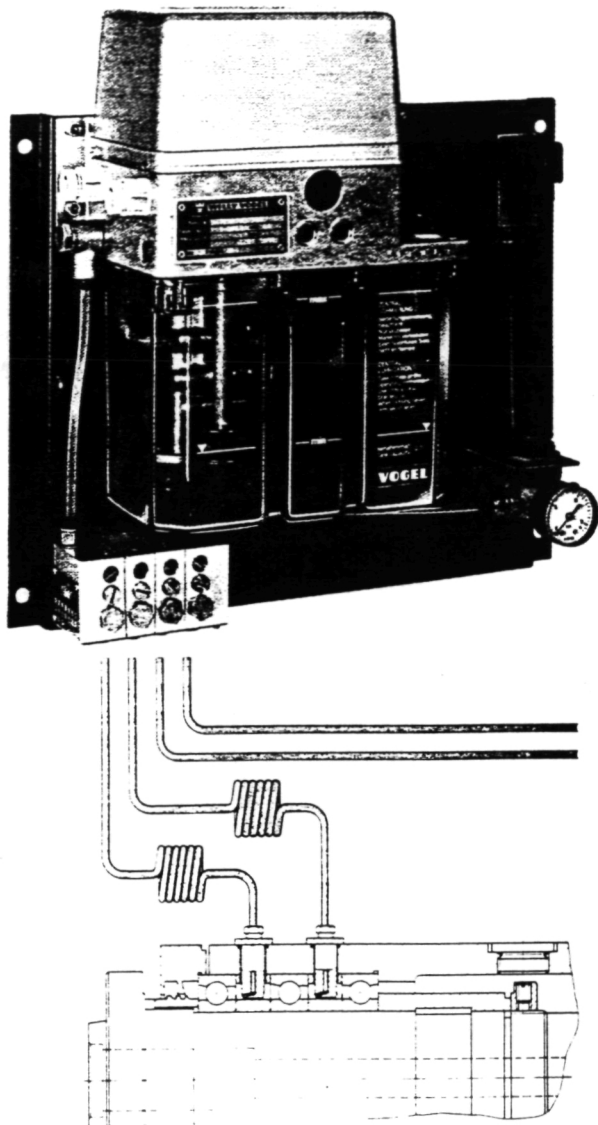
- (1) "D" DIMENSION WILL NOT BE EXCEEDED. SHIMS UP TO .03 INCHES IN THICKNESS ARE USUALLY REQUIRED FOR COUPLED OR GEARED MACHINES.
 - (2) "U" VARIES-----0.00 - .001
 - (3) "R" VARIES-----0.00 - .015
 - (4) TERMINAL BOX VARIES WITH H.P. FOR DIMENSIONS "AA", "AB", "AC", "AF", "X" AND "Y". SEE DRAWING NUMBER 609959-1.
 - (5) LEAD OUTLET FOR RE-045 AND TGF-2100 TACHS LOCATED ON HORIZ. CENTERLINE ON F-1 & F-2 SIDES.
- TERMINAL BOX CAN BE ROTATED FOR LEAD OUTLET AT TOP, SIDES OR BOTTOM.
TERMINAL BOX LOCATED ON OPPOSITE SIDE WHEN F-2, W-1, W-4, W-5, W-7.
OR C-1 MOUNTING IS SPECIFIED. BOX LOCATED ON TOP WHEN SPECIFIED.
BLOWER ASSEMBLY CAN BE LOCATED AT POSITIONS 1, 2, OR 4. EXCEPT
BLOWER ASSEMBLY AND TERMINAL BOX CAN NOT BE LOCATED AT THE SAME POSITION.
MOTOR WEIGHT MAY VARY 15% FOR NON-STANDARD RATINGS AND/OR ACCESSORIES.
IF MOUNTING CLEARANCE DETAILS ARE REQUIRED, CONSULT FACTORY.

ORIGINAL PAGE IS
OF POOR QUALITY

APPENDIX E

CENTRAL LUBRICATION MODULE -
TECHNICAL LITERATURE

Oil+Air Lubrication



1. Principle of oil+air lubrication

The oil+air lubrication is based on the principle that a liquid drop will be divided by an air flow, dispersed in streaks and transported into the direction of the air flow.

In practice, the drop will be transported in a narrow tube along the inner walls in the direction of the lubrication point. By an appropriate tube length (min. length 1 m) and a sufficient sequence of droplets it will be ascertained that a continuous, but extremely micro drop oil flow will arrive at the outlet. The oil remains at the friction point, whereas the air, which is – contrary to the oil mist lubrication – nearly oil-free, may escape unhindered into the open.

2. Range of application

The oil+air lubrication will be used at places where a small, finely dispersed oil flow must be led continuously to the friction point. This is, for instance, the case with high-speed anti-friction bearings which require an exact metering and adaptation to the construction of the bearing.

The same applies to the lubrication of gear drives to realize an economic dry sump lubrication.

It is also important for the lubrication of smaller conveyor chains, where an intermittent feeding of the lubricant is not possible.

3. Principles of the oil+air lubrication with high-speed anti-friction bearings in spindles serving as an example

3.1 Lubrication systems for anti-friction bearings

The oil+air lubrication is a minimum quantity lubrication. In many regions of the technical production there is the requirement to increase the speed of spindles and shafts supported by anti-friction bearings over and beyond the values quoted in the anti-friction bearing catalogs, e.g. for the bearings of grinding wheel spindles and milling spindles to increase the cutting speed. Apart from the constructive design of the bearings, decisive importance is attributed to the selection of the suitable lubrication system to meet this requirement.

The usual lubrication systems (for instance oil-bath lubrication), on which the values of anti-friction bearing catalogs are also based, will fail here, because by the hydrodynamic losses in the lubricant itself, the friction losses and thus the temperature will be increased over and above the permissible values.

With an oil circulating lubrication system, which is cooling at the same time, the temperature values could be reduced, but higher efficiency losses, increased installation costs and sealing-technical expenditure would be the consequence.

The diagram (fig. 1) shows that the most favorable values with regard to friction losses and temperature will be achieved by a minimum supply of oil.

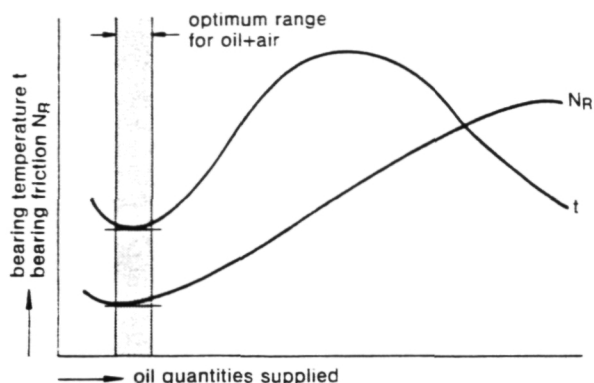


Fig. 1

The small quantities of lubricant fed may best be supplied in accordance with the principle of oil+air lubrication, as only according to this system these lubricant quantities may be exactly metered.

With the oil mist lubrication, however, it is hardly possible to supply individual bearings reliably and constantly with the required small lubricant quantity.

Well suited and many-sided used will be, on the other hand, the continuous grease lubrication.

The utilization of a grease lubrication is limited, however, to a speed parameter

$$n \times dm \text{ of approx. } 600\,000 \text{ mm} \times \text{min}^{-1},$$

where n = number of revolutions
and dm = mean diameter of bearing.

On top of the above, the grease change intervals will be, connected with the replacement of the spindle, extremely shortened, even when special greases are being used. The worked friction losses will be increased as a result of lacking cooling effect of the grease charge.

For higher speed parameters, the oil+air lubrication is thus the most suitable lubrication system, which, of course, can also be utilized for lower speed parameters.

3.2 Advantages of oil+air lubrication

- attainment of high-speed parameters for anti-friction bearings (up to approx. $1\,500\,000 \text{ mm} \times \text{min}^{-1}$)
- always fresh lubricant at the friction point
- small consumption of lubricant, approx. 10 % of an oil mist lubrication
- oil selection from a wide viscosity range
- use of oils with EP and adhesive additives
- omission of grease replacement times
- simplified bearing seals possible
- protection against contamination from the outside by the overpressure in the bearing itself, produced by the compressed air
- non-polluting, no oil mist
- low bearing temperature
- minor efficiency losses
- supply of every bearing with the quantity of lubricant required at the time

3.3 Lubricant quantities for anti-friction bearings

The lubricant quantity depends largely on the type of bearing, number of rows, width, etc. It is therefore recommended to discuss by all means the determination of the quantity with the maker of the bearing.

In technical literature, the following approximation formula is found for the determination of the approximate oil requirement:

$$Q = w \times d \times B,$$

where Q = quantity in mm^3/h ,

w = coefficient = 0.01

d = inner bearing diameter in mm

B = bearing width in mm.

In practice, however, the values determined with this formula had to be increased by four to ten times as much. This shows clearly that the lubricant quantity actually required for every bearing must be ascertained empirically for every case.

It is recommended to split up this lubricant quantity into 6 to 10 injection pulses per hour.

3.4 Requirements to the lubricant

Oils of ISO-grades VG 32 – VG 100 have proved to be very suitable. Especially for higher loads and low speeds, oils with EP-additives are recommended.

Oils with a lower viscosity than ISO VG 22 should be avoided, as with higher loads the load-carrying property might not be sufficient anymore and might impair the service life of the bearing.

The use of oils with higher viscosity is possible.

Oils with molybdate additives should, however, not be used, as with these oils there is the risk that molybdate is deposited at the nozzle throats and will choke them up. Moreover, by plating-on of molybdate particles, the bearing clearance may be critically reduced.

3.5 Compressed air

The air must be dry and filtered; filter rating $\leq 5 \mu\text{m}$. For water separation, a water separator as normally used in the compressed air program will be sufficient, if possible with semi-automatic drainage.

The air quantity required for proper transport of the oil in a tube of 2.3 mm inner diameter is approx. 1000 – 1500 NI/h . This value is applicable for oils of the viscosity grades ISO VG 32 – ISO VG 100. For oils of higher viscosity resp. oils with other adhesiveness, higher values should be placed into account.

The air pressure should be adjusted in such a way that under consideration of the pressure losses in the pipe and in the bearing, this air flow rate is achieved in every pipeline. The air pressure available at the unit inlet (compressed air mains) should be 6 bar.

3.6 Lubricant supply

(Criteria, bearing design, etc.)

The line, e.g. flexible plastic tube 4×0.85 , where the transport of the oil may well be seen, may be laid in descending or ascending direction. Minimum length of this line is 1 m. Max. length may well be 10 m. If the distance between unit and bearing will be less than 1 m, the tube must be laid as helical coil.

With very long tubes it is recommended that the supply tube is laid in a helical form with approx. 5 coils as close as possible to the bearing. The central axis of the helix should be either horizontal or inclined up to an angle of 30° to the horizontal.

In the lower part of the helical coil, oil from the helical coil should accumulate after cutting out the compressed air, so

that the bearing is supplied with oil within a short time after compressed air is supplied again.

Alterations of the inner cross section, especially at bends, are to be avoided. If they will be unavoidable, gradual reductions must be provided.

In case of tube connections (as few as possible) care is to be taken that no oil is lost or accumulating.

The feeding of lubricant into the bearings depends entirely on the design of the bearing and the constructional features of the bearing (see fig. 2).

With single-row bearings, the lubricant should be fed into the bearing from the side. The nozzle opening should be in the height of the inner ring; in no case, the nozzle is to be pointed directly onto the ball cage. With bearings, which exert a pump effect into one direction (e.g. angular contact ball bearings), the oil must be supplied in this direction. If at all possible, the oil is to be fed to the bearing by means of a special nozzle, the length of which depends on the size of the bearing. The diameter of the nozzle is between 0.5 and 1 mm.

If double-row cylindric roller bearings are used, the oil shall be sprayed from one side into the bearing at the height of the outer race. It will then be distributed almost evenly to both rows.

For anti-friction bearings with an outer diameter between 150 and 280 mm, the installation of a second nozzle is recommended, for even larger bearings adequately more.

The air pressure quoted above is normally sufficient to penetrate the air turbulences arising from high-speed bearings. If in particular cases higher pressures are required, they will not at all affect the function of the entire system.

To avoid the development of an oil sump in the lower part of the bearing, a drain of the oil supplied is to be provided. The diameter of this borehole should be at least 5 mm.

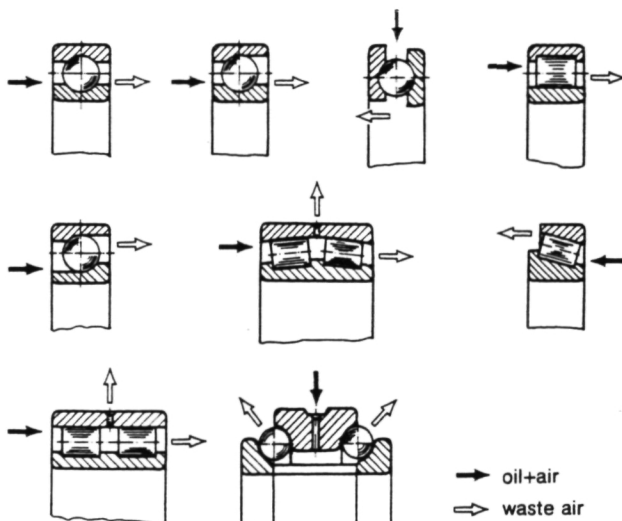


Fig. 2
Feeding of oil+air to the rolling elements

4. Oil+air lubrication systems

The following components are required for an oil+air lubrication system:

- pressure regulating valve for air
- pressure gauge for the air pressure
- pressure switch for min. air pressure
- oil+air metering unit with built-in piston distributors
- compact unit

with gear pump and the set of valves required for pressure relief and pressure regulation, with oil pressure switch, float switch, with control unit IG 38 or IGZ 51/S 6

or

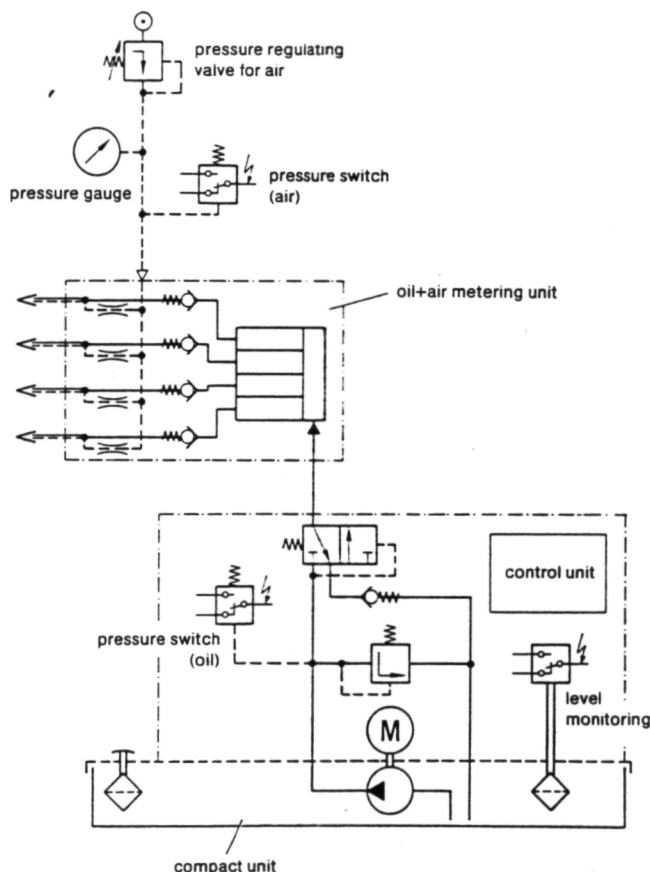
- gear pump unit

with the set of valves required for pressure relief and pressure regulation, with float switch.

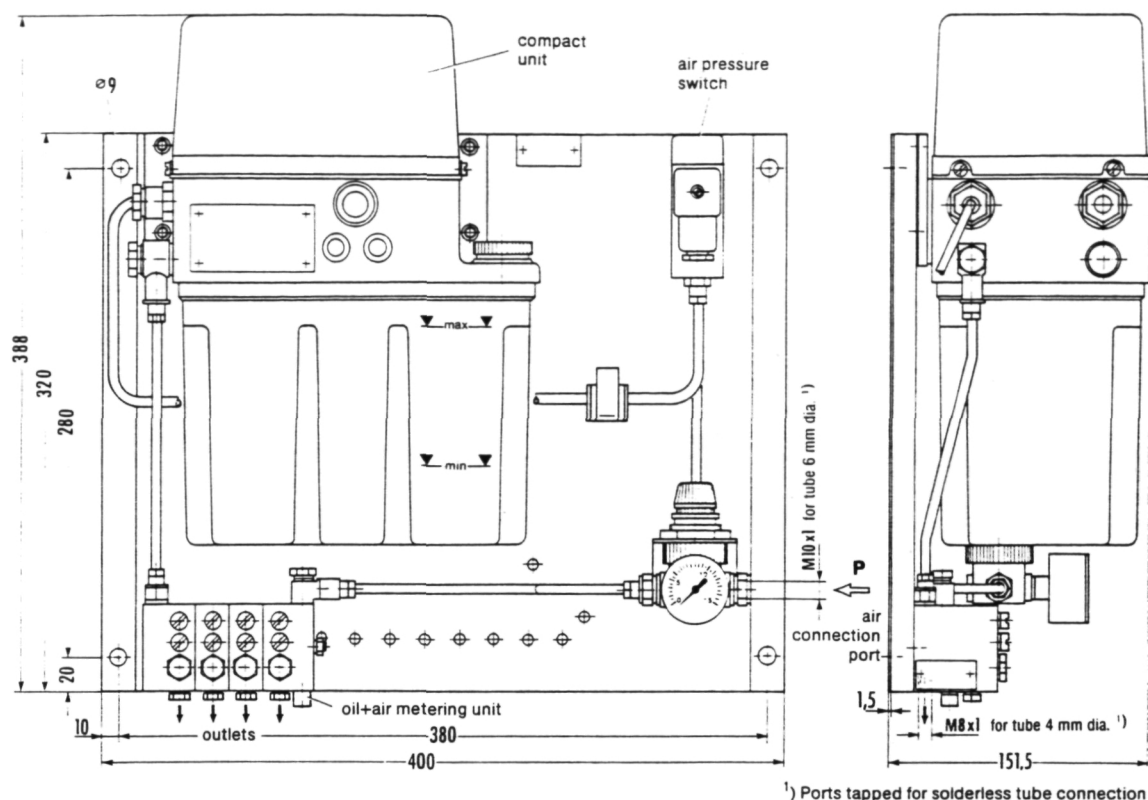
Here, control unit and oil pressure switch are to be installed separately.

These components may either be assembled to a unit (type OLA) or may be ordered individually.

Individual ordering presents itself, if the complete unit cannot be mounted directly to the machine.



Oil+air lubrication unit, type OLA, mounted completely on base plate



Technical data

Type OLA1 with compact unit 122 345 309 and control unit IG 38
Type OLA5 with compact unit 122 445 322 and control unit IGZ 51/S6

output	0.2 l/min
with an operating viscosity of 110 mm ² /s (cSt) and a back pressure p = 5 bar	
max. pressure	28 \pm 1 bar
corresponds to the actual value of the built-in pressure regulating valve	
effective reservoir capacity	2.7 liters
permissible operating viscosity	40 to 200 mm ² /s (cSt)
ambient temperature	from +10 to 40 °C
power consumption	120 W
voltage (please quote when ordering)	220 V, 50/60 Hz or 110 V, 50/60 Hz
type of enclosure	IP 43
cable gland	Pg 11

float switch,	type of contact	NO-contact
oil pressure switch,	type of contact	NO-contact
	switching pressure	22 \pm 1 bar

Control unit IG 38	for time-dependent control	interval setting range 1, 2, 4, 8, ... 2048 min.
Control unit IGZ 51/S6	for time- and load-dependent control (switchable)	interval setting range 1, 2, 3, ... 999 x 10 ³ min/pulses

Oil+air lubrication units are available with 3, 4, 5, 6, 7 and 8 outlets.

Order code OLA . - 0 .

	number of outlets desired
	1 for compact unit (122 345 309) with control unit IG 38 (time-dependent)
	5 for compact unit (122 445 322) with control unit IGZ 51/S6 (time- and load-dependent)

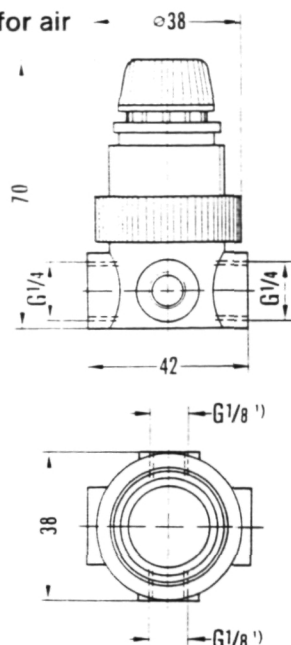
Order example: Oil+air unit with control unit IG 38 and 4 outlets:

Ref. No. OLA 1 - 04

plus additional statement of voltage required

If there will be more than 8 outlets required, a second oil-air metering unit with separate air feed is to be provided.

Pressure regulating valve for air

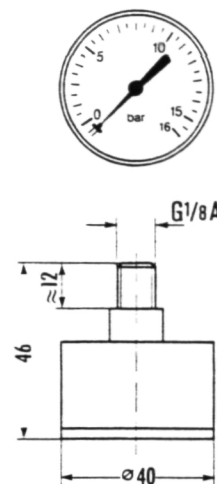


Ref. No. 231 900 025

max. primary pressure 28 bar
max. temperature 80 °C

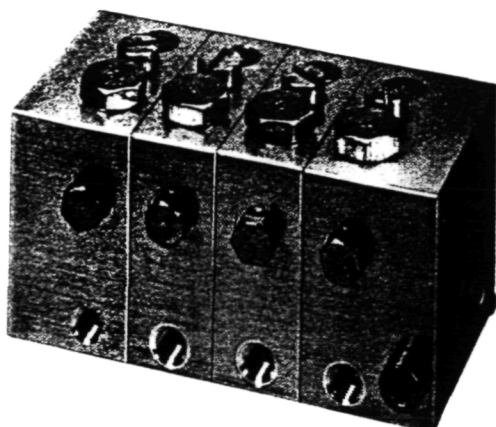
¹⁾ connection port for pressure gauge

Pressure gauge for compressed air



Ref. No. 169 101 606

indicating range 0 to 16 bar



Oil+air metering unit

The oil+air metering unit is an assembly of sections.

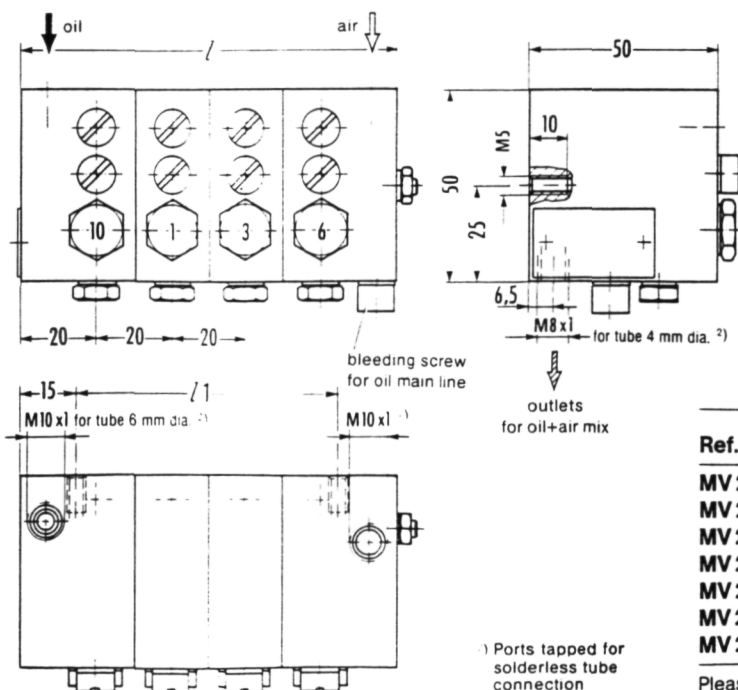
The metering unit consists of an oil inlet section, an air inlet section and up to 6 intermediate sections.

For more than 8 lubrication points, a second metering unit – with separate air supply – is to be provided.

Every sections is fitted with piston distributors as well as with feeding boreholes for oil and air.

Every outlet must be connected with one lubrication point.

Metered quantities can be chosen from 0.01; 0.03; 0.06 and 0.1 cm³ per outlet. Please quote desired metered quantities when ordering.



Technical data

min. air pressure 3^{+0.5} bar

min. oil pressure

for metered quantity 0.01 cm³ 17 bar

for metered quantities 0.03; 0.06; 0.1 cm³ ... 13 bar

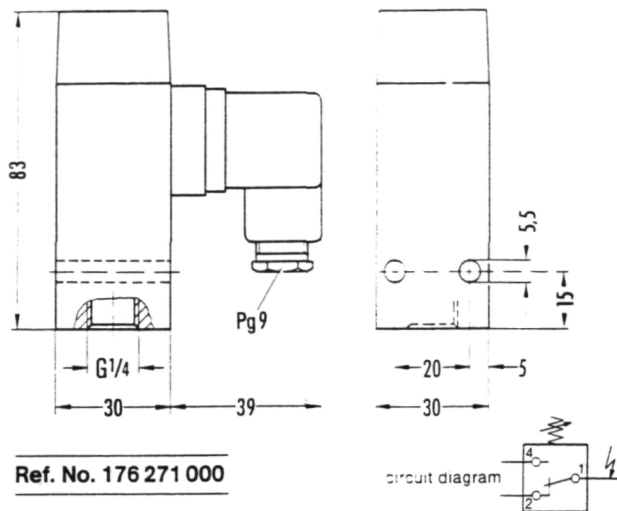
Mounting position:

oil + air outlet ports either at top or bottom.

Ref. No.	Number of outlets	Metered quantity per outlet in cm ³	Dimensions /	/1
MV 202	2		60	30
MV 203	3		80	50
MV 204	4	optionally	100	70
MV 205	5	0.01; 0.03;	120	90
MV 206	6	0.06; 0.1	140	110
MV 207	7		160	130
MV 208	8		180	150

Please quote metered quantities desired when ordering.

Pressure switch for air

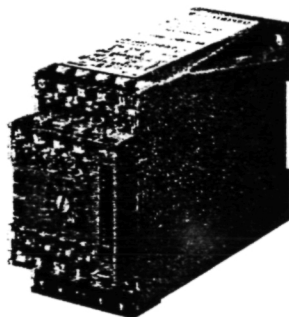


Ref. No. 176 271 000

Technical data

switching pressure (adjustable)	from 1 to 10 bar
reset differential (fixed)	10 %
switching rate	200/min
max. voltage	250 V
breaking capacity	
with resistive load 6 A at 24 V d. c. and 0.5 A at 220 V a. c.	
with inductive load 6 A at 24 V a. c. and 3 A at 220 V a. c.	
type of enclosure	IP 65

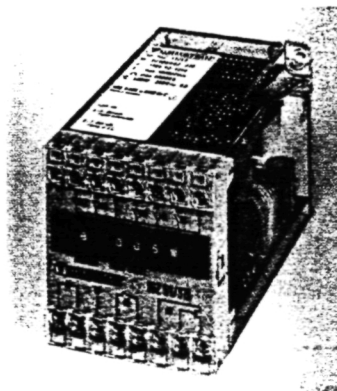
Electronic control units



Ref. No. IG 38

for time-dependent control

interval setting range	1, 2, 4, 8, ... 2048 min.
voltage ¹⁾	220 V, 50/60 Hz and 110 V, 50/60 Hz



Ref. No. IGZ 51/S6

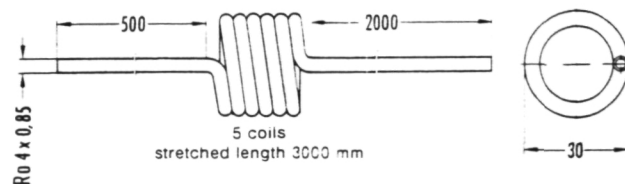
for time- and load-dependent control (switchable)

interval setting range	1, 2, 3, ... 999 x 10 ³ min/pulses
voltage ¹⁾	220 V, 50/60 Hz and 110 V, 50/60 Hz

¹⁾ Please quote when ordering

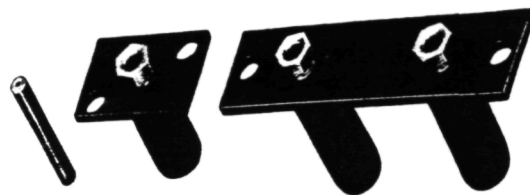
Helical coil tube

To connect the unit with the friction point, it is advisable to use a flexible plastic tube 4 x 0.85. The last piece should be formed as helical coil.



Ref. No. 828 090 004

Selection of nozzles



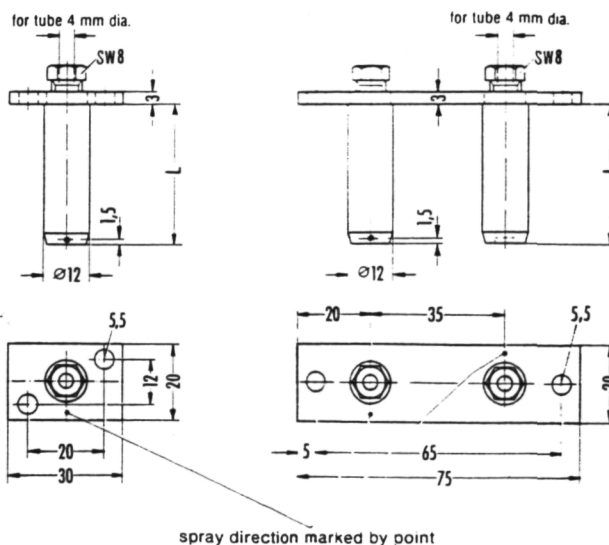
The nozzle forms depend to a large extent on the field of application.

For simple tasks, e. g. spray lubrication of chains, tooth flanks of gears, slideways and for the wetting of work surfaces, nozzle P-89.29 is well suited.

Ref. No. P-89.29



The following nozzles are suited for the lubrication of anti-friction bearings with radial feeding:



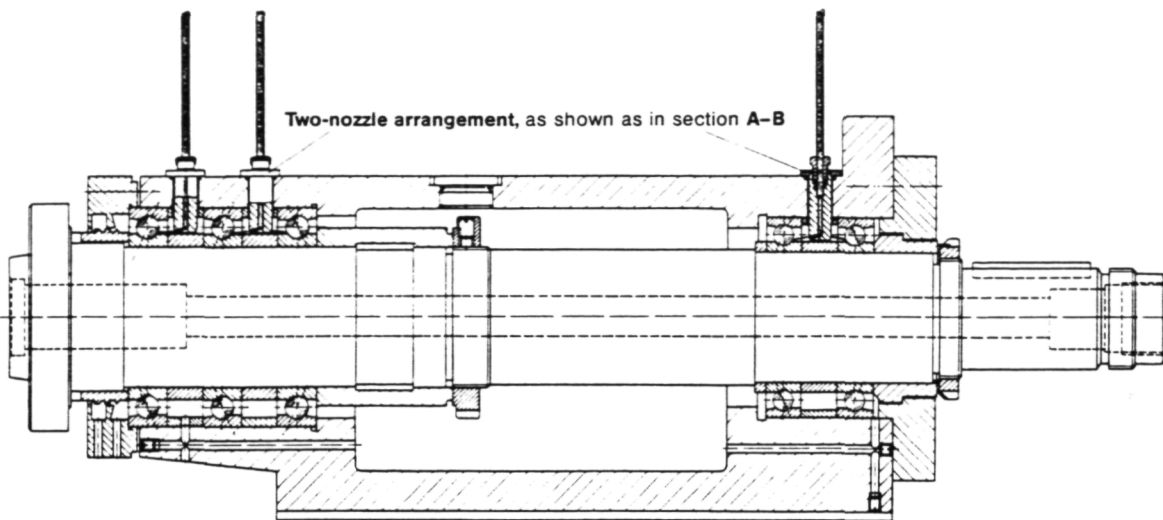
Ref. No. 169 000 101

L = length desired

Ref. No. 169 000 102

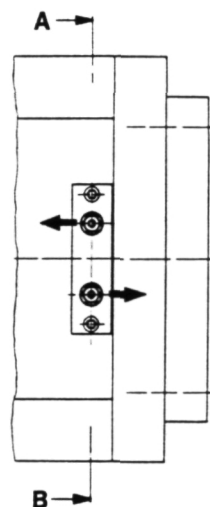
SW = width across flats

Example: spindle bearing

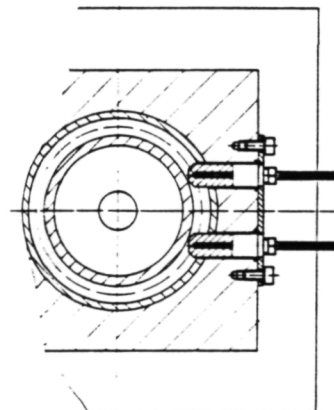


spindle speed: $1000-3000 \text{ min}^{-1}$
speed parameter: $n \times d_m = 345\,000 \text{ mm} \times \text{min}^{-1}$

One nozzle sprays
into the left bearing,
the other one
into the right one.

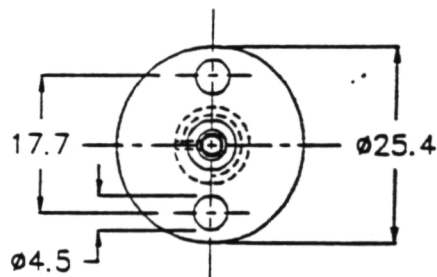
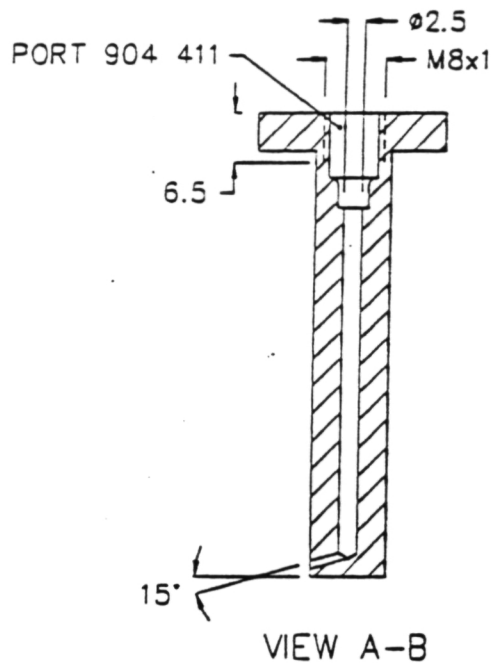
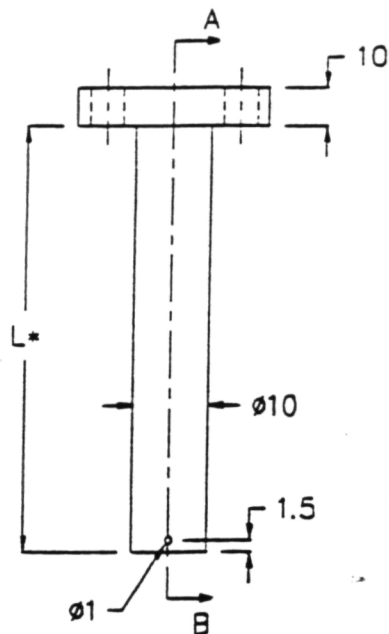


radial oil+air feed
section A-B



DAVE SHIRLEY
SALES ENGINEER
VOGEL LUBRICATION SYSTEMS
205-853-7086 BIRMINGHAM
804-380-8585 HOME OFFICE

* 'L' TO BE SPECIFIED BY THE CUSTOMER
 FOR 'L' LESS THAN 15MM, USE 169 000 100/V3
 MATERIAL $\phi 1$ IN BRONZE ROUND
 ALL DIMENSIONS ARE IN MM'S
 ALL TOLERANCES ± 1 MM



PART# 169 000 100/V1		VOGEL LUBRICATION SYSTEMS OF AMERICA NEWPORT NEWS, VA		VOGEL®	
FILENAME N1000012					
REPL'D BY		DESCRIPTION OIL-AIR NOZZLE		Centralized Lubrication	
REPL'T FOR					
DATE 11-09-89	SCALE	CUST		EUROPEAN PROJECTION	
CHK'D	1 : 1				
DONE BY M W TAYLOR	SIZE A	MM 0 25 50 75		NUM. 1	
SHEET 1	OF 1	IN 0 1 2 3		DATE 3/92	
				NAME MT	

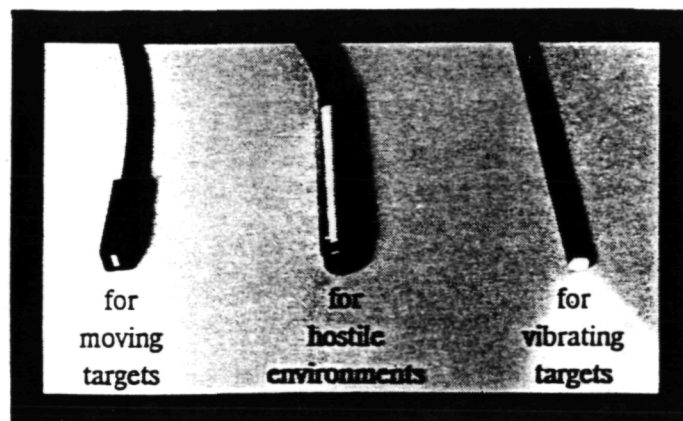
APPENDIX F

INSTRUMENTATION DETAILS -
TECHNICAL LITERATURE

HIGH PERFORMANCE **FIBER OPTIC DISPLACEMENT SENSORS**

SERIES 88

FOR HIGH RESOLUTION/CLOSE RANGE APPLICATIONS



88RC

88F

88N

- RC (Reflectance Compensated) models for non-contact displacement measurements on moving targets provide an output signal unaffected by target surface reflectance variations.
- F models are the patented FIBERTOUC[®]H sensor; the only contact displacement sensor with high frequency capability.
- N models for non-contact displacement measurements of vibrating targets provide an output signal that is proportional to proximity and reflectance of the target surface.



PHILTEC[®]

P.O. BOX 359 • ARNOLD, MD 21012 • (301) 757-4404

SERIES 88 SENSORS

SERIES 88 high performance fiber optic displacement sensors utilize bundled glass fibers to transmit to and receive light from target objects. In general, the intensity of received light reflected off a target surface varies proportionately with target motion and surface conditions. RC and FIBERTOUCH® models have been developed to eliminate the effects of variable surface and environmental conditions.

SERIES 88 sensors provide analog output signals and are packaged in small industrially rugged enclosures to facilitate their use in the manufacturing and processing environments. They are comprised of:

- a sensor tip (integral or detachable)
- a fiber optic cable
- an optoelectronic amplifier

The user supplies DC power (+8V to +25V) and a suitable readout device. Amplifier size for most models is 2.75" x 2.64" x 4.75". Output signals are nominally 0 to +5 VDC. Standard fiber optic cables are PVC/monocoil — flame retardant spring steel covered with PVC, crush/kink resistant. Temperature range is -50°F (-45°C) to 225°F (105°C). An optional flexible stainless steel interlocking hose offers maximum tensile strength and broadest range of operating temperatures -50°F (-45°C) to 525°F (275°C). Special high temperature non-contact sensor tips are available for continuous operation up to 800°F. Non-standard sensor tip and cable configurations are available on custom orders. A digital panel meter can also be provided for direct readout in volts or engineering units.

RC MODELS

Gross inaccuracies result from variations of target reflectance when uncompensated fiber optic displacement sensors are used to measure the motion of rotating or moving parts, because their output is sensitive to reflectance as well as to target motion. The model RC sensors are Reflectance Compensated fiber optic displacement transducers providing an output signal independent of target surface reflectance.

Four models are available: 88RC, 88RCE, 88RCD and 88RCX. The RC models offer high sensitivity. RCE models offer extended range. RCD models feature in-phase reflectance compensation and high sensitivity. RCX models feature the greatest operating range and standoff capability.

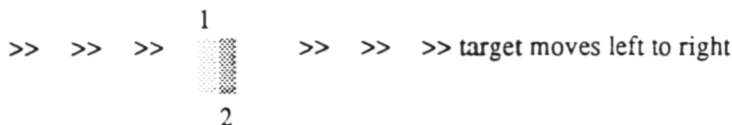
These sensors are suitable for measurement applications involving stationary or moving targets. They have a superior range of reflectance correction, 25 to 1, which permits successful operation over a wide variety of target materials such as ceramics, composites, metals, papers, paints, and plastics.

SPECULAR AND DIFFUSE REFLECTORS

Model RC sensors perform superbly with specular reflecting materials (i.e., finely ground, mirrored, polished, shiny or glossy surfaces) where light is reflected at the same angle at which it illuminates a target. With diffuse reflectors (i.e., dull or flat finishes or rough surfaces), special calibration may be required due to the random scattering of reflected light from such targets.

OPERATING PRINCIPLE

Model RC sensors are built with two parallel fiber bundles in the face of the sensor:



The two sections lie one behind the other along the direction of motion when the sensor is oriented as indicated here. This is the recommended orientation for best results, because all portions of a target surface that pass under the first sensing section shall also pass under the second section.

With the RC, RCE and RCX sensors, a reflectance compensated signal is created by deriving the ratio output of the two sections. Since the two sensor sections are side-by-side, this form of reflectance compensation is called "out-of-phase compensation".

Out-of-phase reflectance compensation is accurate so long as the target area underneath the two sensor sections can be assumed to be of uniform reflectance (along the direction of motion). This assumption holds true in a great many applications, both static and dynamic.

DISCONTINUITIES

Model RC sensors are most accurate where reflectance variations are negligible inside the sensing area along the direction of target motion.

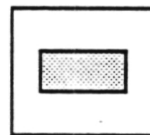
An abrupt reflectance change passing under the face of the sensor will cause an error in the ratio output when one sensor section "sees" light and the other "sees" dark. Abrupt reflectance changes are associated with edges of parts as well as with printed characters on labels for example. Unwanted voltage spikes arise in dynamic applications due to these effects.

With the model RCD sensor, a variable control is provided for delaying the acquisition of the signal from the leading fiber section. The purpose of the delay is to electronically position the two sensor sections into precise phase alignment. Optimized delay minimizes or eliminates those voltage spiking errors due to reflectance discontinuities.

SENSOR TIP PACKAGING OPTIONS

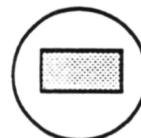
STANDARD

The standard 88RC series tip configuration has a 1/8" x 1/16" active fiber bundle packaged in a 1/4" SQ x 1" L brass housing.



OPTIONAL

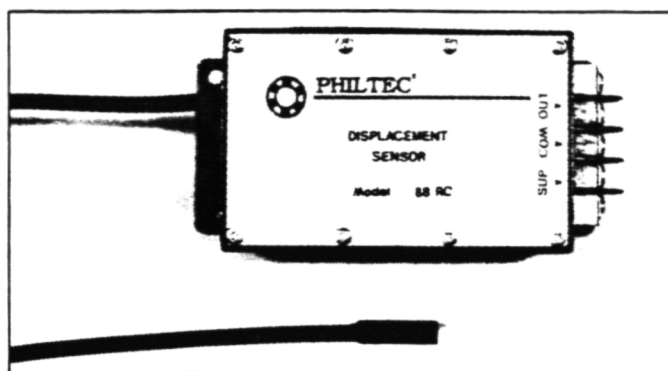
The 88RC series can optionally be provided in 3/16" DIA x 3" L brass tubing as well as in a 5/16" - 24 x 1" L threaded package. Tubing lengths from 1/2" up to 12" can be specified.



88RC and 88RCE SENSORS

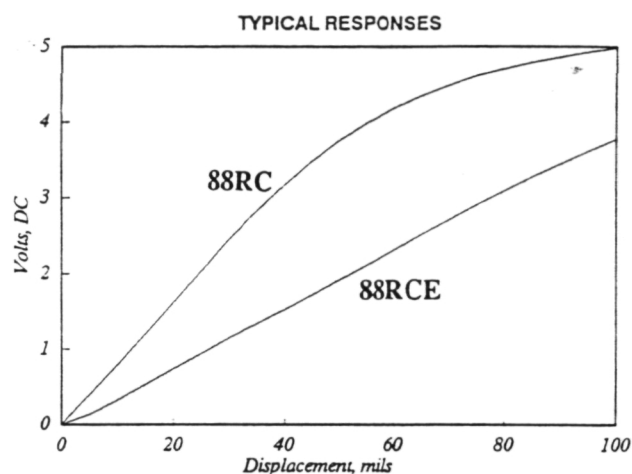
FEATURES

- Non-contact sensing
- Reflectance Compensation
- Resolutions to 1 microinch
- Bandwidths to 200 KHZ
- Linear Ranges to 70 mils
- Intrinsically Safe



APPLICATIONS

- ▶ PRECISION SPINDLE RUNOUT
- ▶ BEARING/ROTOR DYNAMICS
- ▶ PART PROFILING
- ▶ THICKNESS
- ▶ VIBRATION STUDIES
- ▶ NON-CONDUCTIVE PARTS MEASUREMENTS

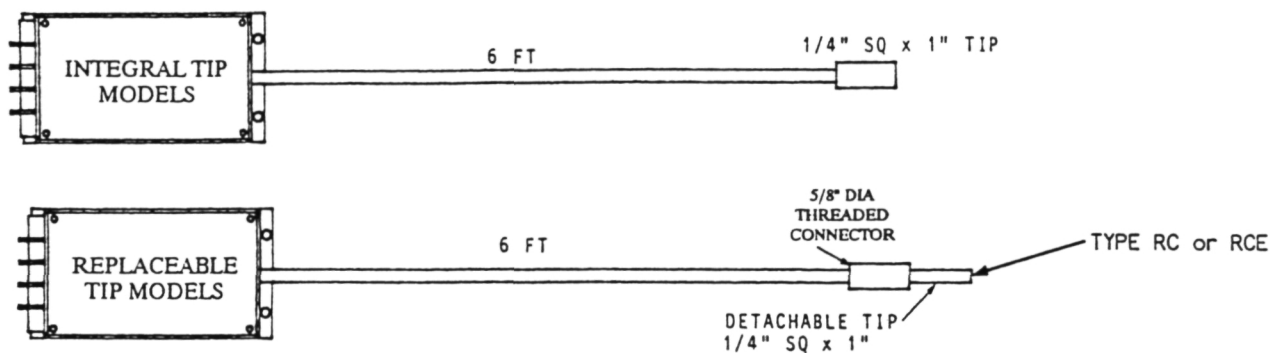


SPECIFICATIONS

		MODEL #	L88RC	88RC	H88RC	L88RCE	88RCE	H88RCE
Light source	LED, 880nm	Frequency Range, DC-()HZ	100	20K	200K	100	20K	200K
Input Voltage	+8 to +25 VDC	Linear Range, mils	25	25	25	70	70	70
Input Current	100 ma max	Nominal Standoff, mils	20	20	20	45	45	45
Output Voltage	0 to +5 VDC	Sensitivity, uIN/MV	12	12	12	24	24	24
Output Current	Full load, 5 ma max	Resolution, p-puIN/√HZ	0.5	0.5	0.5	1	1	1
		Resolution, rms uIN	1	13	40	2	26	80
Max Operating Temp	500° F (Tip) 140° F (Amplifier)	Fiber Bundle Size	1/8" x 1/16" Standard					
Amplifier Stability	< 0.1% Full Scale							

CONFIGURATIONS

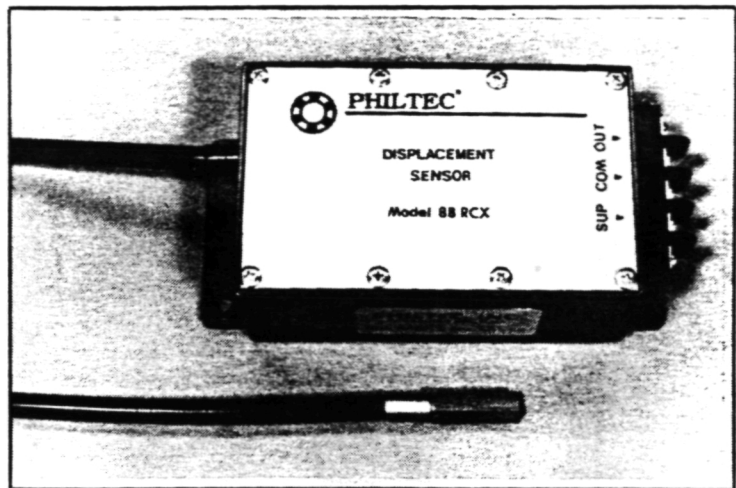
Series 88RC sensor tips are sheathed in a 1/4" square x 1" long brass housing with a 6 FT. integral fiber optic cable to the amplifier. Replaceable tip models are also available as shown below.



88RCX SENSORS

FEATURES

- Non-contact sensing
- Reflectance Compensation
- Analog and Logic Outputs
- Resolution to 0.4 mils
- 500 mil Operating Range
- 100 mil Linear Range
- Intrinsically Safe

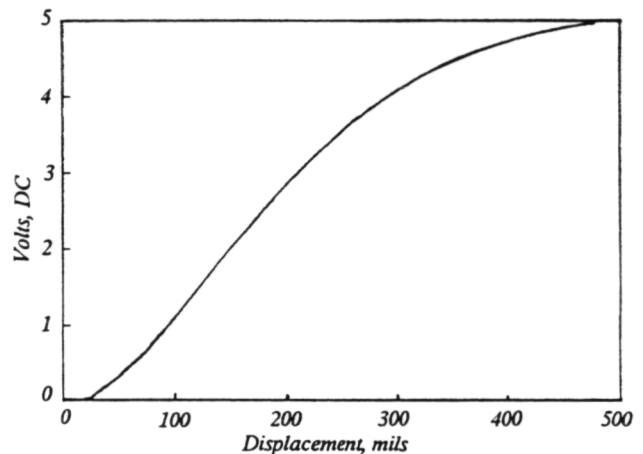


The model 88RCX sensor has the greatest operating range (0 - 1/2") in the RC series. It can be used as a precision analog displacement transducer with a linear range of ± 50 mils at a standoff of 150 mils. It also features a 5 Volt digital TTL compatible logic bit that can be set to change logic state at any point within the operating range of the device. The output state is at 5 volts close to a target and at 0 volts far away. The transition from one output state to another can be completed within 0.001" of target travel.

APPLICATIONS

- ▶ ROBOTICS
- ▶ SHEET STOCK GAGING
- ▶ PART PROFILING
- ▶ THICKNESS GAGING
- ▶ VIBRATION STUDIES
- ▶ NON-CONDUCTIVE PARTS MEASUREMENTS

Model 88RCX TYPICAL RESPONSE



SPECIFICATIONS

		MODEL #	188RCX	88RCX	H88RCX
Light source	Visible Laser Diode	Frequency Range, DC-()HZ	100	20K	200K
Input Voltage	+8 to +25 VDC	Linear Range, mils	100	100	100
Input Current	100 ma max	Nominal Standoff, mils	150	150	150
Output Voltage	0 to +5 VDC	Sensitivity, uN/MV	50	50	50
Analog Output Current	Full load, 5 ma max	Resolution, p-puN/√HZ	200	200	200
		Resolution, rms inch	.0004	.005	.016
Max Operating Temp	500° F (Tip) 140° F (Amplifier)	Fiber Bundle Size 3/32" x 3/16"			
Amplifier Stability	< 0.1% Full Scale	Optical Power Output < .2 milliwatts			
Digital Output, TTL Compatible	0/5 Volts				

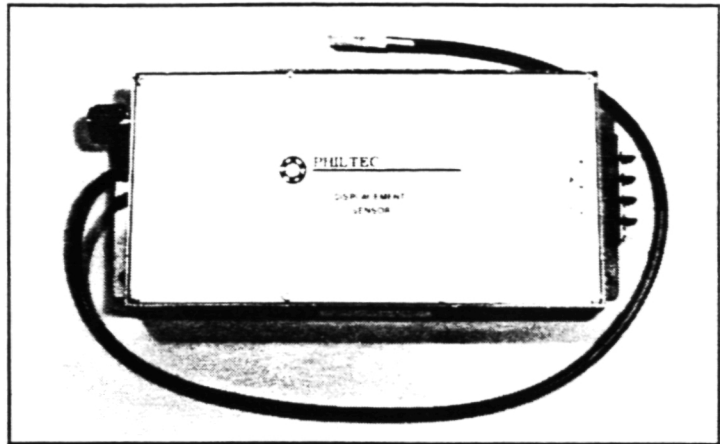
CONFIGURATIONS

88RCX sensor tips are sheathed in a 1/4" square x 1" L housing with a 6 FT. integral fiber optic cable to the amplifier.

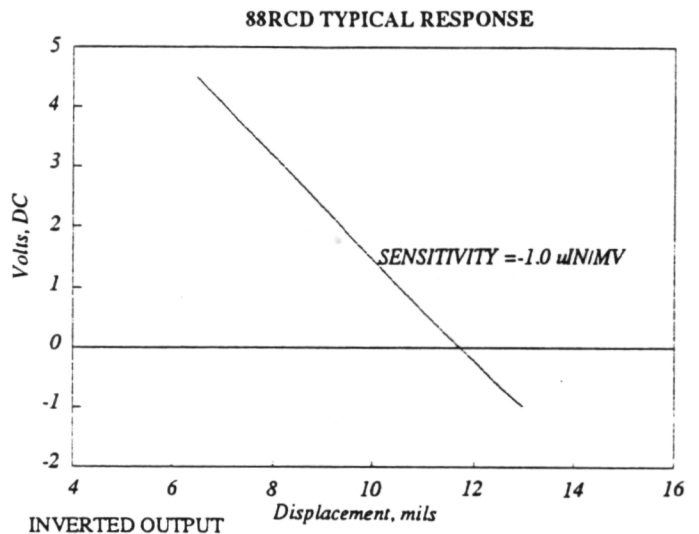
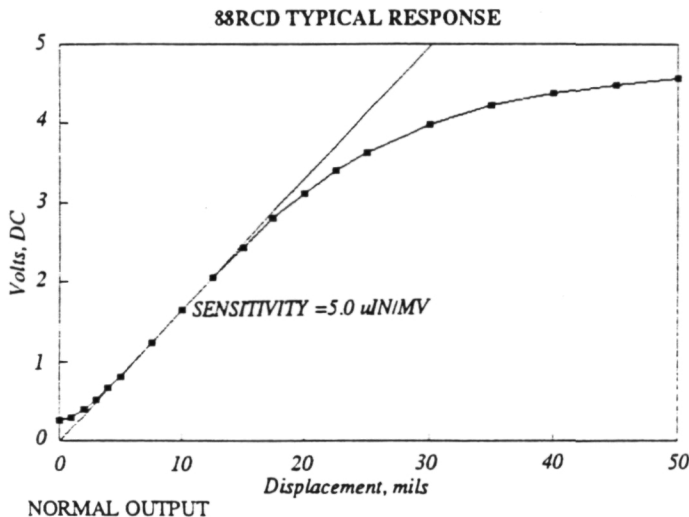
88RCD SENSORS

FEATURES

- In-Phase reflectance compensation
- Fast recovery time
- Non-contact sensing
- Small size
- Zero offset adjustment
- Intrinsically safe



The Model 88RCD sensor is a fiber optic displacement sensor with in-phase reflectance compensation. It minimizes voltage spiking errors due to abrupt changes in target color or reflectance that arise from fast moving discontinuous targets such as electric motor commutator bars. The width of the sensor is .025". A variable delay control is provided for phase adjustment. With optimized delay, the effective width of the sensor is cut in half.



The normal zero-five volt output response is shown on the left. The sensor is equipped with an inverted output having a voltage offset capability. A typical inverted output response is shown on the right.

SPECIFICATIONS

Light Source:	LED, 880nm	Frequency Response:	200 KHZ (with minimum delay)
Input Voltage	+8 to +25 VDC	Nominal Sensitivity:	-1.0 μ IN/MV (Inverted Output) +5.0 μ IN/MV (Normal Output)
Input Current	100ma max	Nominal Standoff:	10 MILS
Output Voltage	0 to +5 VDC	Operating Range:	5 MILS
Analog Output Current:	Full Load, 5ma max	Noise Ripple, PK-PK:	DC - 200 KHZ, 30 MV DC - 20 KHZ, 10 MV DC - 100 HZ, .1 MV
Max Operating Temp:	500° F (Tip) 140° F (Amplifier)	Fiber Bundle Dimensions:	.025" x .125"
Amplifier Stability	< 0.1% Full Scale		

CONFIGURATIONS

88RCD sensor tips are sheathed in a 1/4" square x 1" long brass housing with a 36" integral fiber optic cable to the amplifier.

N MODELS

The Series 88N are low cost high performance sensors that can be used in a wide variety of applications from the production floor to laboratory environments, where small amplitude displacement measurements of vibrating targets are required.

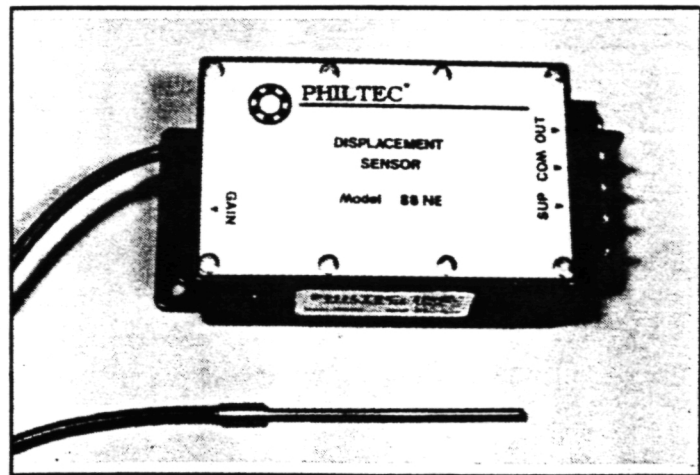
The sensor tip contains a mixed bundle of transmit and receive fibers. The amplitude of received light reflected from a target surface varies proportionately with the target's motion. The amplitude of received light also varies proportionately with the reflectance of the target surface. A gain adjustment is provided for calibration to various target surfaces.

Superior noise characteristics permit resolution to submicroinch levels. They are also versatile, having three regions of operation: a near side, a far side and a peak.

88N and 88NE SENSORS

FEATURES

- Non-contact Sensing
- Sub-microinch Resolution
- Bandwidths to 200 KHZ
- Operating Range to 1"
- Linear Ranges to 3/16"
- Intrinsically Safe

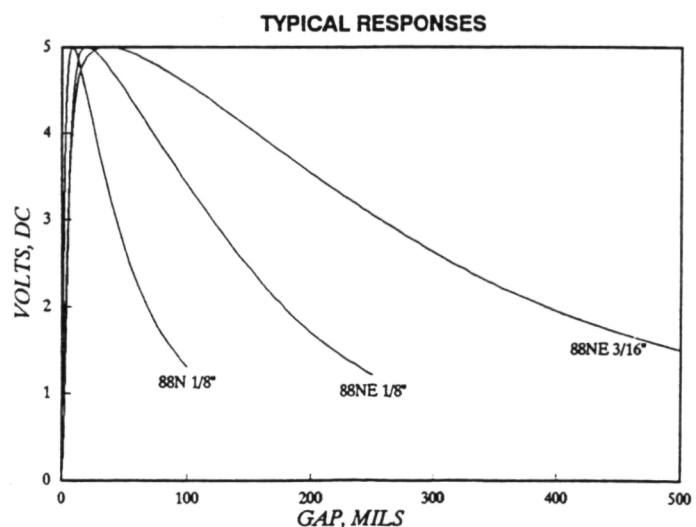


The output responses of three standard sensors are shown here. The 1/8" diameter 88N provides the greatest slope sensitivity. The 3/16" diameter 88NE provides the greatest operating range. The slope and linear range of the far side of N or NE Sensors is proportional to the diameter of the fiber bundle.

The slope and linear range of the near side is a function of individual fiber diameter and distribution within the bundle. Correspondence with the factory is invited for custom or non-standard applications.

APPLICATIONS

- ▶ ULTRASONIC WELDING
- ▶ COMPUTER DISK MAGNETIC HEAD TRACKING
- ▶ STRUCTURAL DEFORMATION
- ▶ BEARING VIBRATIONS
- ▶ VALVE STEM MOTIONS
- ▶ ACOUSTIC SPEAKER VIBRATIONS



OPERATING RANGE

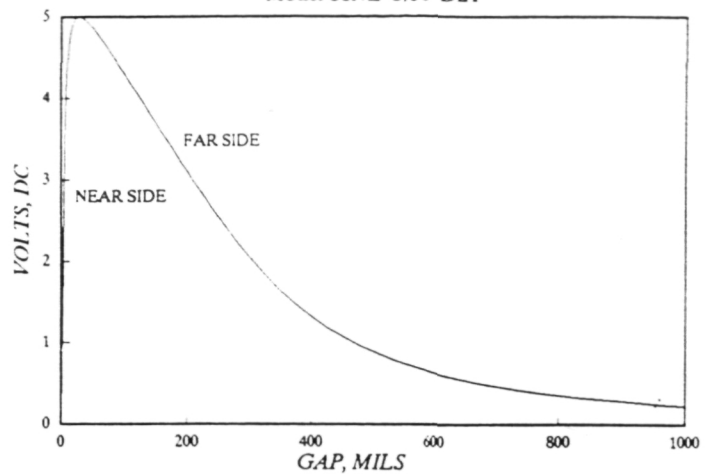
The usable operating range extends well beyond the linear range on the far side.

Operation in the near and far side regions gives outputs sensitive to target motion as well as target reflectance.

Operation on the peak yields a signal insensitive to motion and responsive only to surface reflectance and texture variations.

GREATEST OPERATING RANGE

Model 88NE 3/16" DIA

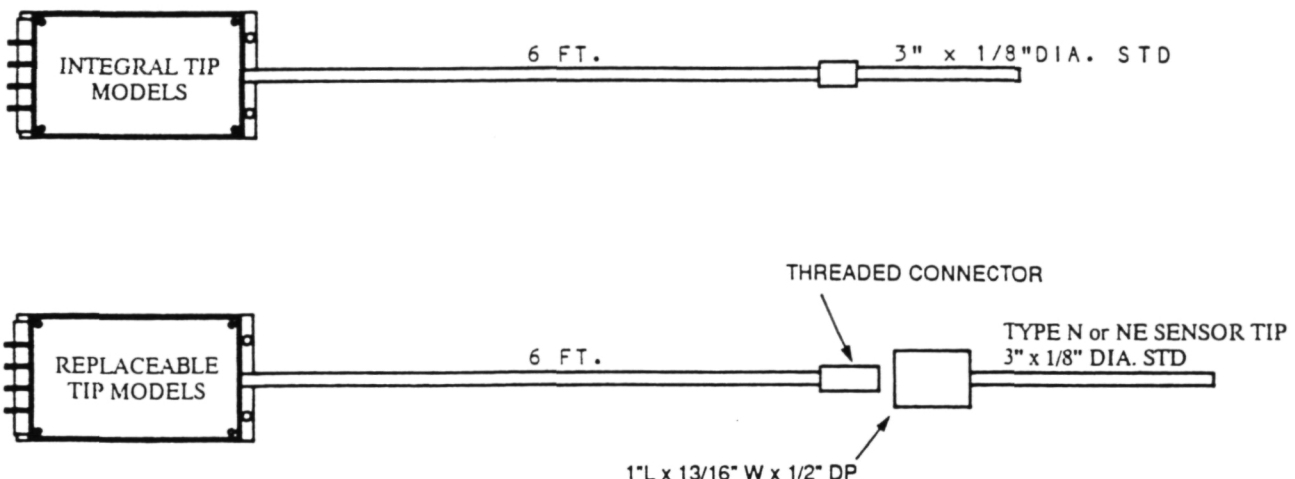


SPECIFICATIONS

		MODEL #	L88N	88N	H88N	L88NE	88NE	H88NE	L88NE	88NE	H88NE
Light Source	LED, 880nm	Tip Diameter, inch	.125	.125	.125	.125	.125	.125	.1875	.1875	.1875
Input Voltage	+8 to +25 VDC	Fiber Bundle Diameter, inch	.0625	.0625	.0625	.0625	.0625	.0625	.145	.145	.145
Input Current	100ma max	Frequency Range, DC-()HZ	100	20K	200K	100	20K	200K	100	20K	200K
Output Voltage	0 to +5 VDC	Operating Range, mils	150	150	150	400	400	400	1000	1000	1000
Output Current	Full Load, 5ma max	Linear Range, mils, Near Side	1.5	1.5	1.5	3	3	3	3	3	3
Amplifier Stability	< 0.1% Full Scale	Far Side	30	30	30	70	70	70	180	180	180
Max Operating Temp	525 F (Tip) 140 F (Amplifier)	Sensitivity, uN/MV, Near Side	0.7	0.7	0.7	1.5	1.5	1.5	1.5	1.5	1.5
	Resolution	Far Side	20	20	20	45	45	45	100	100	100
		p-p nanoinch/ $\sqrt{\text{HZ}}$, Near Side	5	5	5	15	15	15	35	35	35
		p-p nanoinch/ $\sqrt{\text{HZ}}$, Far Side	150	150	150	450	450	450	1000	1000	1000
		rms uIN Near Side	.04	0.5	1.5	0.1	1.0	3.0	0.1	1.0	3.0
		rms uIN Far Side	1	10	30	2	20	60	3	45	150

CONFIGURATIONS

Series 88N sensor tips are sheathed in stainless steel tubing 3" long with a 6 FT integral fiber optic cable to the amplifier. Replaceable tips are also available for all models as shown below.



F MODELS

FIBERTOUCH[®] is a sealed fiber optic sensor for the measurement of displacement of vibrating objects in harsh environments.

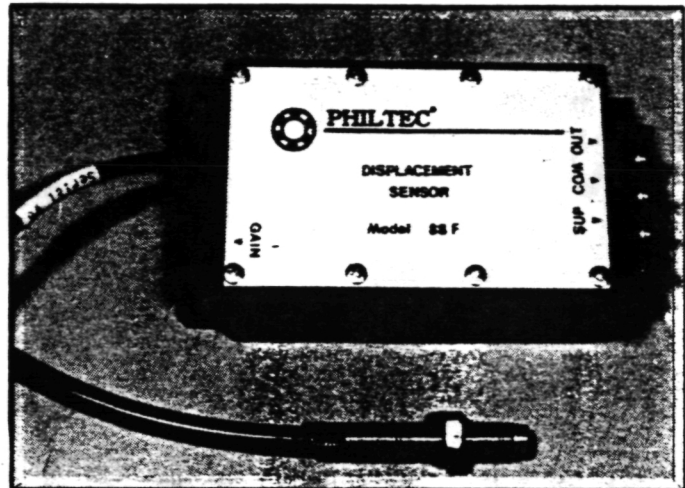
Non-contact displacement sensors provide high frequency capability but they are subject to fouling problems. Contact displacement transducers are non-fouling but have poor frequency response. The Fibertouch sensor allows non-fouling high frequency contact displacement measurements to be achieved.

88F SENSORS FIBERTOUCH[®]

FEATURES

- Contact Sensing
- DC - 10 KHz Bandwidth
- Sub-Microinch Resolution
- Intrinsically Safe
- Non-Fouling

U.S. Patent No. 4,814,603
Foreign Patents Pending



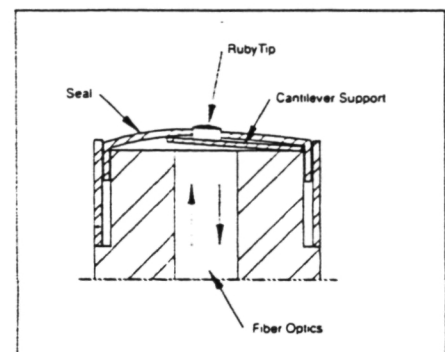
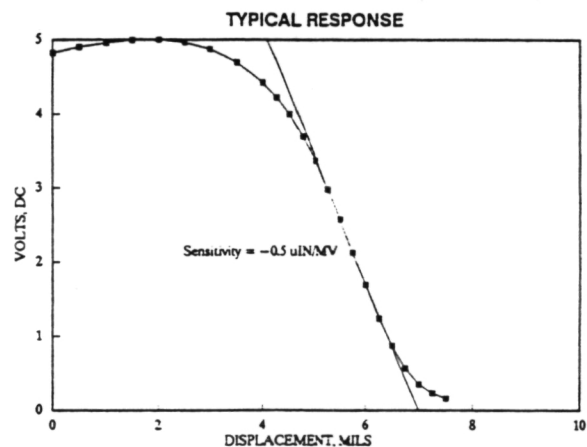
A typical Fibertouch output response is shown. The output is set at the factory to be approximately 4 1/2 volts when the sensor is not in contact with a target. After initial contact is made, a displacement of about 6 mils brings the sensor into its linear operating range.

APPLICATIONS

- ▶ BEARING VIBRATIONS
- ▶ STRUCTURAL DEFLECTIONS
- ▶ VIBRATION STUDIES

OPERATING PRINCIPLE

The basic elements of the sensor are shown in cross-section. A crowned ruby tip bonded to a reflective cantilever beam set above a bundle of glass fibers precisely follows target motion over the bandwidth DC - 10 KHz. A diaphragm seal protects the optical path from fouling problems. The fiber bundle contains transmit and receive fibers to reflect and capture light from the underside of the beam. The DC output of the sensor varies as the beam angle changes with target motion.

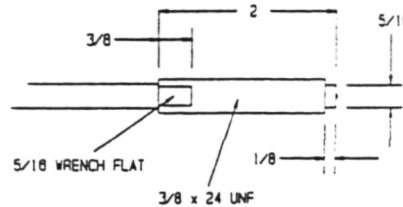


SPECIFICATIONS

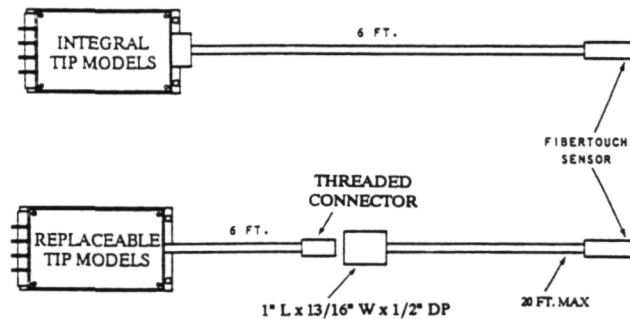
		MODEL #	L88F	88F
Input Voltage	+8 to +25 VDC	Contact Force (At 2 VDC), oz.	20	20
Input Current	100ma max	Linear Range, mils	1.5	1.5
Output Voltage	0 to +5 VDC	Frequency Response, HZ	100	10K
Output Current	Full Load, 5ma max	Sensitivity, uIN/MV	0.5	0.5
Amplifier Stability	< 0.1% Full Scale			
Max Operating Temp	300 F (Tip)	Resolution, p-p nanoinch/ $\sqrt{\text{HZ}}$	5	5
	250 F (Cable)	Resolution, rms nanoinch	30	300
	140 F (Amplifier)			

CONFIGURATIONS

Fibertouch is supplied in a 2" long threaded stainless steel housing as shown here. Other lengths can be made upon request. The sensor diameter can not be changed.



Fibertouch is available with or without a replaceable sensor tip as shown below. The replaceable tip is comprised of the standard Fibertouch sensor itself, a flexible length of fiber optic cable, and a quick disconnect coupling.



PHILTEC, INC.
P.O. Box 359
Arnold, MD 21012

BULK
RATE
PERMIT
#216
ARNOLD,
MD
21012

**N MODEL SENSORS**

We have recently added two new sizes to our sensor series 88N. The tables below give the pertinent size and operational specifications for these five standard products.

TIP SIZES AVAILABLE

MODEL	UNITS	88N	88N	88NE	88NE	88NE
OUTER DIAMETER	INCH	1/32	1/8	1/8	5/32	3/16
FIBER DIAMETER	INCH	.020	.0625	.101	.125	.168
TIP LENGTH	INCH	1.5	3	3	3	3
OPTICAL PEAK	MILS	6	12	25	25	25

FAR SIDE
SPECIFICATIONS

LINEAR RANGE	MILS	12-18	20-45	50-125	60-160	95-245
NOM. STANDOFF	MILS	15	35	90	110	170
SENSITIVITY	uIN/MV	6	20	50	65	100
RESOLUTION						
DC - 100 HZ	uIN	1.5	3	7.5	8	10
DC - 20 KHZ	uIN	15	30	75	80	150
DC - 200 KHZ	uIN	60	120	300	325	600

NEAR SIDE
SPECIFICATIONS

LINEAR RANGE	MILS	1-2	1-2.5	2-4	2-4	2-4
NOM. STANDOFF	MILS	1.5	1.5	3	3	3
SENSITIVITY	uIN/MV	.63	.74	1.1	1.1	1.1
RESOLUTION						
DC - 100 HZ	uIN	.15	.10	.15	.10	.10
DC - 20 KHZ	uIN	2	1	2	2	2
DC - 200 KHZ	uIN	7	5	7	6	7

7200 Proximity Transducer Systems

5 mm and 8 mm



Accurate, reliable measurements

The 7200 5 mm and 8 mm Proximity Transducer Systems are noncontacting, gap-to-voltage transducer systems that measure static as well as dynamic distances between the probe tip and the observed target. The general application is any requirement for an accurate, non-contacting displacement measurement. However, the most common use is for shaft position and vibration measurements on rotating and reciprocating machinery. They are designed for use with virtually any machine type including gas and steam turbines, compressors, pumps, centrifuges, electric motors and generators. The systems offer 80 mils (2 mm) of linear measuring range and are compatible with API 670 requirements.

A system consists of a probe with integral coaxial cable, an extension cable, and Proximitors®. All 7200 proximity transducer systems are compatible with 3300 and 9000 Monitoring Systems.

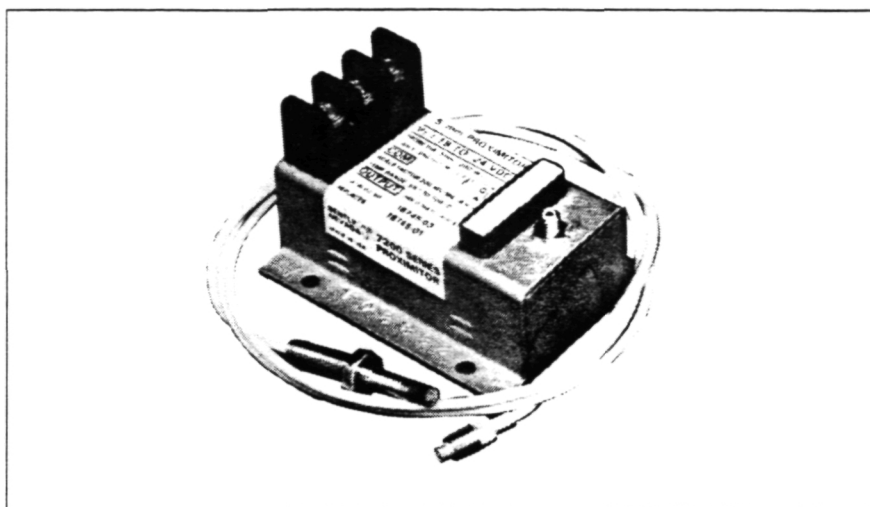
Applications

The 7200 5 and 8 mm Systems have a frequency response of 0 Hz (DC) to 10 kHz and can be used to make the following types of measurements:

- Radial vibration for indicating bearing condition and such machine malfunctions as rotor imbalance and misalignment.
- Axial thrust position for determining thrust bearing wear or potential bearing failure.
- Shaft average radial position, for determining attitude angle, an indicator of rotor stability.
- Vibration amplitude and phase angle for plotting diagnostic information in Polar and Bodé formats.
- Eccentricity to measure the amount of rotor bow.

How a proximity transducer system works

Operating on the eddy current principle, the proximity probe senses the distance between the probe tip and the observed surface. The Proximitors generates a radio frequency signal, which is radiated through the probe tip



7200 Proximity Transducer System

into the observed surface. Eddy currents are generated in the surface, and the loss of strength in the return signal is detected by the Proximitors, which conditions the signal for linear display on a monitor.

Improved proximity probes

An improved 8 mm version of the 7200 System is now standard which includes Bently Nevada's Cable Loc™ feature. This new technique of securing the coaxial cable to the probe tip provides the strongest junction yet offered by Bently Nevada and increases the durability of the probe during installation and usage.

Two new cable length options are now available on 8 mm probes. They are 5 metres and 9 metres of integral cable. Since the entire lead-length is built into the probe, an extension cable is not used with these length options.

Nine probe configurations are available to accommodate English and metric thread requirements (See Table 1). The 5 mm probes are constructed of fiberglass. The 8 mm probes are constructed of polyphenylene sulfide, (PPS), a high performance plastic capable of withstanding unusually harsh, wet and/or chemical environments.

Both transducers are suitable for use in a confined space and offer 80 mils (2 mm) of linear range with a scale factor of 200 mV/mil (8 V/mm)

Extension cables

The combination of probe with integral lead and extension cable is designed to achieve a system length of either five or nine metres from probe tip to Proximitors. Probes are available with integral leads of various lengths to match the average extension cable lengths. Probes and cables of the same length, and Proximitors with the same part number, are completely interchangeable.

For added protection, stainless steel armor is available. It provides improved resistance to physical abuse.

Proximitors

The 5 mm and 8 mm systems use the same type of Proximitors. Both 5 and 9 metre Proximitors are available. A three-conductor, shielded cable provides the signal output and power source input between 7200 Proximitors and Bently Nevada monitors. Proximitors can be located up to 1,000 feet from standard Bently Nevada monitors without degradation of performance.

Hazardous locations

Most Bently Nevada 7200 Transducers are certified by CSA, BASEEFA and FM for use in specific hazardous locations. Refer to Data Sheet L1035 "Bently Nevada Systems for Hazardous Locations" for more details.

7200 Proximity Transducer Systems

5 mm and 8 mm

5 mm and 8 mm Proximity Probe Configurations

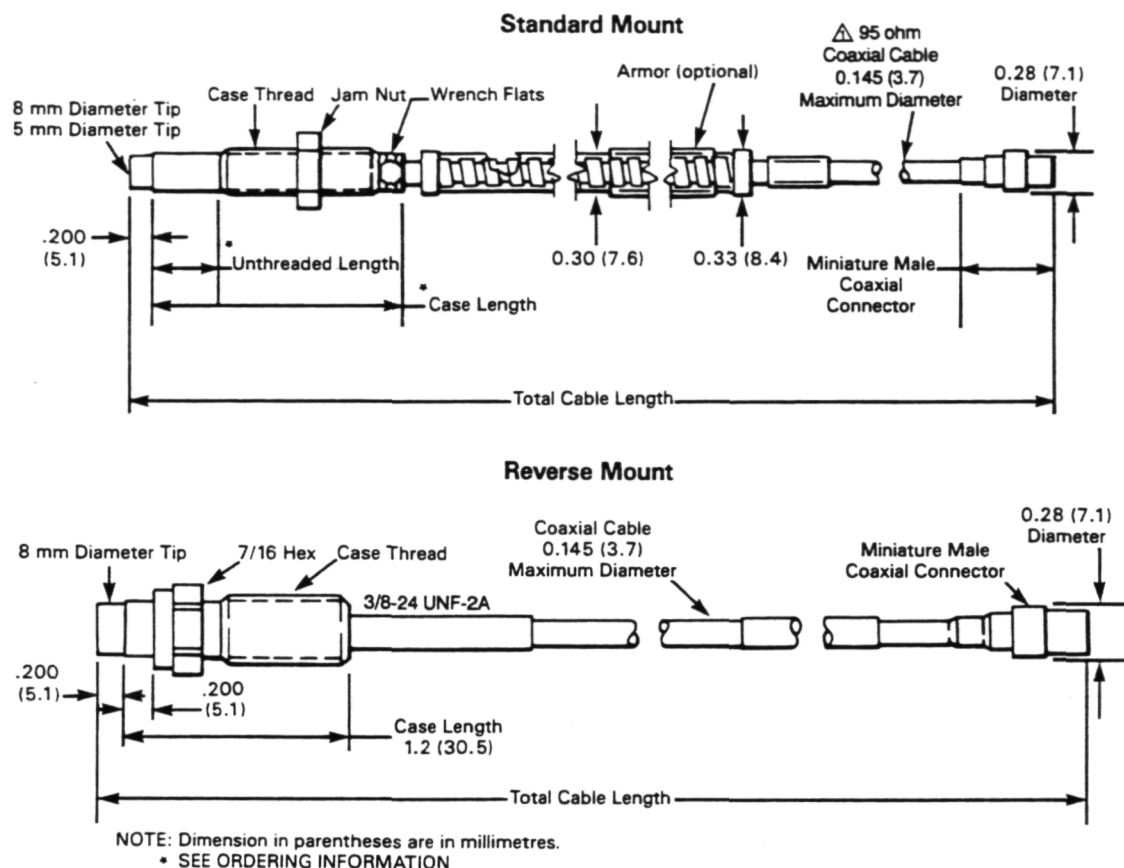


FIGURE 1
Maximum diameter for 21500 and 21501 probes is 0.111 in. (3.4 mm).

Specifications

Specifications were determined with a -24 Vdc power supply, 10 kΩ load, and an AISI 4140 steel target at +72°F (+22°C).

INPUT

Power: -17.5 Vdc to -26 Vdc at 12 mA maximum consumption.

OUTPUT

Calibrated Range: 80 mils (2.0 mm).
Begins at approximately 10 mils (0.25 mm) from probe face.

Scale Factor: 200 mV/mil (7.87 V/mm), ±4% (measured in increments of 10 mils over the calibrated range) if calibrated as a system. Within ±9.5% including interchangeability errors.

Linearity: Within 0.8 mils (0.02 mm) of a 200 mV/mil straight line if calibrated as a system. Within 2.3 mils (0.06 mm) of a 200 mV/mil straight line including interchangeability errors.

Frequency Response: 0 to 10 kHz (0 to 600,000 cpm); -5% at 10 kHz (600,000 cpm).

Temperature Sensitivity: Typically -3% change in scale factor at +150°F (+65°C) at 50 mils gap (1.27 mm).

ENVIRONMENTAL LIMITS

Operating Temperature:

Proximitors: -60°F to +212°F (-51°C to +100°C).

Probe and Extension Cable: -30°F to +350°F (-34°C to +177°C).

Relative Humidity: To 95%, noncondensing.

Corrosion Resistance (for 8 mm probes only): Probe operation is not affected by direct contact to the following: air, water, lube oil, ammonium hydroxide, sulfuric acid (10%), MEK (methyl-ethylketone) or DMF (Dimethylformamide).

System Weight: 1.3 lbs.(0.59 kg).

7200 Proximity Transducer Systems

5 mm and 8 mm

TABLE 1
Probe Part Number Option Descriptions

TIP CONSTRUCTION		CASE		
PART NO. □□□□	DIAMETER	CONFIGURATION TYPE	THREADS	LEAD ARMOR
*21500-	5 mm	Standard	1/4-28	No
*21501-	5 mm	Standard	1/4-28	Yes (stainless steel)
21504-	8 mm	Standard	3/8-24	No
21505-	8 mm	Standard	3/8-24	Yes (stainless steel)
21508-02-12	8 mm	Reverse	3/8-24	No
22810-	8 mm	Standard	M10 × 1	Yes (stainless steel)
22811-	8 mm	Standard	M10 × 1	No
*22812-	5 mm	Standard	M8 × 1	Yes (stainless steel)
*22813-	5 mm	Standard	M8 × 1	No

* Maximum case length for all M8 × 1 probes is 100 mm; and for 1/4-28 probes is 4 inches. Also, maximum overall length for 5 mm probes is 1 metre.

PHYSICAL

For Probes: See Figure 1 and Table 1.

Proximator:

Size:

Height: 2.00 inches (50.8 mm)
maximum.

Length: 3.12 inches (79.2 mm).

Width: 2.38 inches (60.5 mm).

Weight: 7.9 ounces (.22 kg).

Example: $\boxed{04}$ = 0.4 inches

Metric thread configuration:

Maximum unthreaded length:

230 mm $\boxed{23}$

Minimum unthreaded length:

0.0 mm $\boxed{00}$

Example: $\boxed{06}$ = 60 mm

B □ Overall Case Length Option*

Order in increments of 0.4

inches $\boxed{04}$ for English thread,

10 mm $\boxed{01}$ for metric threads.

English thread configurations:

Maximum case length:

9.6 inches $\boxed{96}$

Minimum case length:

0.8 inches $\boxed{08}$

Example: $\boxed{24}$ = 2.4 inches

Metric thread configuration:

Maximum length:

250 mm $\boxed{25}$

Minimum length:

20 mm $\boxed{02}$

Example: $\boxed{04}$ = 40 mm

C □ Total Length Option*

05 0.5 metre (20 inches).

Tolerance: +.13 metre, -.05 metre
(+ 5 inches, -2 inches).

10 1.0 metre (39 inches).

Tolerance: +.25 metre, -.10 metre
(+ 10 inches, -4 inches).

50 5 metre (195 inches).

Tolerance: +.6 metre, -.5 metre
(+ 24 inches, -20 inches).

90 9 metre (351 inches).

Tolerance: + 1.0 metre, -.9 metre
(+ 39 inches, -35 inches)

D □ Connector Option

00 Without connector.

02 With miniature male coaxial
connector.

8 mm Reverse Mount Probe

A B C D

21508 - 02 - 12 - □□ - □□

Option Description

C □ Total Cable Length Option

05 0.5 metre (20 inches).

Tolerance: +.13 metre, -.05 metre
(+ 5 inches, -2 inches).

10 1.0 metre (39 inches).

Tolerance: +.25 metre, -.10 metre
(+ 10 inches, -4 inches).

50 5 metre (195 inches).

Tolerance: +.6 metre, -.5 metre
(+ 24 inches, -20 inches).

90 9 metre (351 inches).

Tolerance: + 1.0 metre, -.9 metre
(+ 39 inches, -35 inches)

D □ Connector Option

00 Without connector.

02 With miniature male coaxial
connector.

Ordering Information

5 mm and 8 mm Standard Mount Probe

A B C D

□□□□ - □□ - □□ - □□ - □□

Option Description

□□□□ Probe Part Number Option

Select from Table 1.

A □ Unthreaded Length Option ①

Order in increments of 0.4

inches $\boxed{04}$ for English thread,

10 mm $\boxed{01}$ for metric threads.

English thread configurations:

Maximum unthreaded length:

8.8 inches $\boxed{88}$

Minimum unthreaded length:

0.0 inches $\boxed{00}$

Extension Cable

A B

21747 - □□□ - □□

Option Description

A □□ Cable Length Option ②

040 4.00 metres (157 inches).③

045 4.50 metres (177 inches).③

080 8.00 metres (315 inches).

085 8.50 metres (335 inches).

B □ Armor Option

00 Without armor.

01 With armor.

7200 Proximity Transducer Systems

5 mm and 8 mm

Proximitior

18745-□□

- 03 For combined probe and extension cable system length of 5 metres (16.4 feet).
- 04 For combined probe and extension cable system length of 9 metres (29.6 feet).
- ① *Unthreaded length must be at least 0.8 inches (20 mm) less than case length.*
- ② *Extension cable physical length equals the electrical length, $\pm 10\%$.*
- ③ *For use with the 18745-03 five-metre Proximitior only.*

WORLDWIDE SALES AND SERVICE

United States of America: Phoenix, Arizona □ Los Angeles, California □ San Diego, California □ San Francisco, California
Denver, Colorado □ St. Petersburg, Florida □ Atlanta, Georgia □ Chicago, Illinois □ Fort Mitchell, Kentucky □ Baton Rouge, Louisiana
Boston, Massachusetts □ Chester, New Jersey □ Buffalo, New York □ Charlotte, North Carolina □ Tulsa, Oklahoma □ Portland, Oregon
Philadelphia, Pennsylvania □ Pittsburgh, Pennsylvania □ Dallas, Texas □ Houston, Texas

International: Argentina □ Australia □ Brazil □ Canada □ Chile □ Columbia □ Egypt □ France □ Germany □ Greece
India □ Indonesia □ Italy □ Japan □ Korea □ Kuwait □ Malaysia □ Mexico □ The Netherlands □ New Zealand □ Nigeria □ Norway
Pakistan □ People's Republic of China □ Peru □ Portugal □ Qatar □ Saudi Arabia □ Singapore □ South Africa □ Spain □ Sweden
□ Taiwan □ Turkey □ United Arab Emirates □ United Kingdom □ Venezuela

Corporate Office: P.O. Box 157 • Minden, Nevada, U.S.A. • Telephone: (702) 782-3611 • Fax: (702) 782-9253 • Telemail: 7400983 BNC UC

MicroPROX® Proximity Transducer System

Used for REBAM®: Rolling Element Bearing Activity Monitor

Machines with rolling element bearings have traditionally been equipped with case-mounted velocity Seismoprobes® or accelerometers to measure vibration or perform diagnostics. With the advent of REBAM, a third type of vibration measurement is now available.

REBAM allows you to observe a rolling element bearing at its source, rather than on the outside machine case where true bearing activity can be concealed. This proven method of measurement gives advanced warning of impending bearing failure more quickly and allows diagnostic work to be performed more easily. Since the REBAM system is measuring direct outer ring deflection, false vibrations and harmonics from surrounding sources do not disrupt the measurement.

The REBAM System uses a high-gain, low-noise eddy current proximity transducer that is installed in the bearing housing observing the bearing outer ring, which contains the outer race. The REBAM transducer measures the very small deflection of the outer ring as the rolling elements pass the area observed by the transducer. These deflections are measured in terms of displacement and are typically in the range of 4 to 300 microinches (0.1 to 8 micrometres). They contain direct information on the bearing condition and loading being applied to the bearing.

Application

The REBAM System provides a direct and very sensitive method to determine the condition of rolling element bearings. It offers a very high signal-to-noise ratio, as compared with casing mounted accelerometer or velocity measurements. REBAM also provides rotor vibration information which can be used to analyze rotor related malfunctions such as imbalance and misalignment.

Other applications include field and laboratory measurements in the micro-inch range that require a high gain output.



REBAM® MicroPROX®

MicroPROX®

REBAM is based on the high sensitivity eddy-current MicroPROX proximity transducer system. The MicroPROX transducer system is able to make dynamic displacement measurements as small as 4 microinches (0.1 micrometre) with a scale factor of 2 volts per mil or 2 millivolts per microinch (78.7 millivolts per micrometre).

The MicroPROX system makes it possible to measure deflections of the bearing outer ring as the rolling elements pass above or beneath it. Spalls in the rolling elements and races, degraded lubrication conditions and loose bearing to housing fits can be detected.

The MicroPROX system uses standard 7200 5 mm and 8 mm proximity probes and extension cables with optional total cable lengths of 1 or 5 metres, for continuous on-line measurements.

The REBAM System uses a specially designed Bently Nevada 9000 Monitor. It processes the MicroPROX transducer system vibration signal and provides reliable continuous monitoring.

For more information, refer to Applications Notes on *Predictive Maintenance Through the Monitoring and Diagnostics of Rolling Element Bearings* (AN044) and *REBAM® Part 1: An Effective Way To Monitor and Analyze Rolling Element Bearing Condition* (AN047).

Specifications

Specifications were determined with a -24 Vdc power supply, 10 k Ω load, and an AISI 4140 steel target at +72°F (+22°C).

ELECTRICAL

Power: -17.5 Vdc to -26 Vdc.

Frequency Response: 0 to 10 kHz (0 to 600,000 cpm); -3dB at 10 kHz.

Sensitivity: 2 V/mil (2 mV/microinch or 78.7 mV micrometre).

Calibrated Range: 8 mils (203 micrometres) nominal.

Noise Floor: Less than or equal to 4 mV.

ENVIRONMENTAL LIMITS

Temperature Range:

Operating: -60°F to +212°F
(-51°C to +100°C).

Relative Humidity: To 95%, noncondensing.

PHYSICAL

Height: 2.00 inches (51 mm).

Length: 3.12 inches (79 mm).

Width: 2.38 inches (60 mm).

Weight: 6.4 ounces (182 grams).

Ordering Information

MicroPROX

40892-01 1.0 metre system.

40892-02 5.0 metre system.

To order extension cables and proximity probes, use standard 7200 5 mm or 8 mm transducer system components.

For ordering information on the REBAM monitor, contact your nearest Bently Nevada sales representative.

APPLICATIONS NOTE

Predictive Maintenance
Through the Monitoring
and Diagnostics of Rolling
Element Bearings

BENTLY 
NEVADA

P.O. BOX 157
MINDEN, NEVADA, USA 89423
PHONE: (702) 782-3611
TELEX: 7400983 BNC UC

Introduction

The predictive maintenance philosophy of using vibration information to lower operating costs and increase machinery availability is gaining acceptance throughout industry. Since most of the machinery in a predictive maintenance program contains rolling element bearings, it is imperative to understand how to monitor and diagnose problems associated with them. Bently Nevada has adopted a two-part philosophy with regard to rolling element bearing monitoring and diagnostics: (1) the monitor system will provide adequate warning to avert catastrophic machine failures and (2) diagnostic data will be available so that when warning is given, the bearings will have visible damage. This philosophy should be kept in mind during the following discussion.

Rolling Element Bearing Characteristics

Any discussion of monitoring and diagnostics for rolling element bearings would not be complete without a comparison with the techniques used for fluid film bearings. The construction of a fluid film bearing is such that the shaft is supported by a fluid film during operation. By design, the shaft can experience motion relative to the bearing. Because of this freedom of motion, the industry-accepted vibration measurement for a fluid film bearing machine is a shaft relative measurement, i.e., proximity probe.

A rolling element bearing, by design, has extremely small clearances which do not allow a significant amount of shaft motion relative to the bearing (Figure 1). Forces from the shaft are transferred through the rolling elements to the bearing outer race and then ultimately to the bearing housing. Because of this transmission, a casing (bearing housing) measurement is normally acceptable for monitoring machines with rolling element bearings. However, as explained later in this discussion, a method called REBAM® is available from Bently Nevada Corporation that allows vibration measurements directly at the bearing outer ring, which contains the outer race. This direct measurement greatly enhances bearing vibration data, and in some cases, this is the

only measurement that can provide adequate vibration information.¹ Shaft relative vibration measurements (i.e., proximity probe) are also useful when clearances increase during failure and for observation of rotor problems that are not related to bearings. A classical characteristic of rolling element bearings is the generation of specific vibration frequencies based on the bearing geometry, number of rolling elements and the speed at which the bearing is rotating (Appendix A).² These "bearing-related" frequencies, typically in the range from 1 to 7 times the element passage rate (EPx), are generated even by a new bearing, but the amplitudes are very small. Element passage rate is defined as the rate at which the rolling elements pass a point on either the inner or outer bearing race. As a bearing fails, these bearing-related frequencies (Prime Spike) will increase in amplitude. Observation of these bearing-related signals is used to diagnose rolling element bearing-related vibration problems and to determine what has failed in the bearing. This precise diagnosis may aid the analyst's credibility, but from a plant manager's viewpoint, it is not as necessary to identify **what** in the bearing is failing, as it is **essential** to determine **when** the bearing must be replaced to avert a machine failure. The methodology for using the bearing-related frequencies to achieve the plant manager's goal is outlined later in this discussion.

Vibration Characteristics of Rolling Element Bearings

The vibrations produced by machines with rolling element bearings occur in three frequency regions. (See example on page 8 for calculation of monitor filter ranges for rolling element bearing applications).

1. Rotor Vibration Region

Rotor-related vibrations normally occur in the range of $1/4$ to 3 times shaft rotative speed ($1/4X - 3X$) and are best measured in terms of velocity or displacement. Many rolling element bearing failures are the direct result of a rotor-related malfunction (e.g., unbalance, misalignment, or rotor instability). Rotor-related malfunctions must be corrected to eliminate bearing overloading and subsequent failure. Most general purpose equipment with speeds from 1200 to 3600 rpm generate rotor-related vibration signals between 10 and 500 Hz (600 cpm to 30 kcpm). It is, therefore, imperative for diagnostics to monitor this frequency range in order to determine when/if a bearing failure is caused by a rotor related malfunction. Without this data, the rotor-related malfunction would remain undetected and bearings will continue to fail and need periodic replacement.

2. Prime Spike Region

The second vibration frequency region to monitor for machines with rolling element bearings is the Prime Spike (element passage) region. As previously mentioned, a rolling element bearing generates characteristic frequencies based on its geometry and speed. Prime Spike is a term used by Bently Nevada to describe a vibration frequency range which includes those bearing frequencies that are generated by the rolling elements traversing either an inner or outer race flaw. This frequency range is normally 1 to 7 times the element passage rate (1-7 EPx). Vibrations in this range can be measured effectively in terms of acceleration, velocity or displacement. Field studies indicate that approximately 90% of all bearing failures are related to either an inner or outer race flaw. The other 10% are related to either a rolling element flaw or a cage flaw, both of which generate frequencies that appear in the rotor vibration region. By establishing a frequency band around the predominant bearing failure frequencies

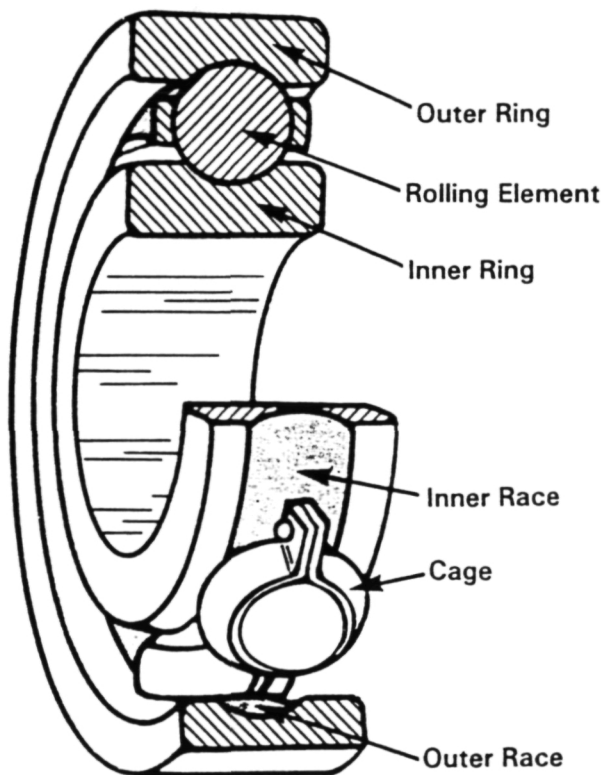


FIGURE 1

and filtering out the rotor-related vibration frequencies, it is possible to gain improved monitoring of bearing condition. A computer analysis of 428 different bearings shows that the Prime Spike Region (1-7 EPx) covers the bearing frequencies of many rolling element bearings.

3. High Frequency (Spike Energy) Region

The third region is the high frequency (Spike Energy) region.³ This region covers frequencies from 5 kHz to approximately 25 kHz and is measured in terms of acceleration. If high frequency region measurements are used for bearing failure detection, they should be used as a supplement to measurements made in the rotor-related and Prime Spike regions. High frequency measurements have two primary uses:

1. High frequency signals occasionally provide an early indication of a bearing problem at the prefailure stage. Care must be exercised because "self-peening" of bearing flaws results in decreasing readings in this frequency region as a bearing failure progresses.
2. High frequency signals are useful to help detect certain other machine malfunctions such as cavitation, rubs, steam or gas leaks, valve problems, blade passage or gear mesh problems. High frequency vibration energy attenuates very rapidly with distance from the source. This can be both bad and good. Bad, in that one needs to be very close to the source to obtain data; good, in that the localized nature of the vibration can be used to isolate the source of a problem.

Based on observation of many rolling element bearings in the field by Bently Nevada Corporation, and many of our customers, most of the information on the performance of rolling element bearings and warning of their failure occurs in the Prime Spike Region (1-7 EPx). Information about **rotor behavior** generally occurs in the region between $1/4X$ and $3X$ times rotative speed. Information at very high frequencies (8 EPx and higher to the megahertz region) may contain very early warning information, as well as other data concerning machinery condition (e.g., rubs, gear noise, cavitation, valve noise, etc.). However, the **principal** and **vital** data for rolling element bearings is contained in the Prime Spike Region (1-7 EPx).

Causes of Failure in Rolling Element Bearings

A rolling element bearing has a finite life and **will** fail due to fatigue, even if operated under ideal design conditions.

Rolling element bearing manufacturers realize this fact and have developed design life limits (L_{10}/B_{10}) to let users know how long a bearing should last when installed and operated within design limits. L_{10}/B_{10} is defined as the rating life of a group of apparently identical rolling element bearings operating under identical loads and speeds with a 90% reliability before the first evidence of fatigue develops. Unfortunately, most "real world" installations are not under ideal conditions and the bearings prematurely fail well before reaching their design life. Most premature bearing failures can be attributed to one or more of the following causes:

1. Excessive loading
 - a. Steady-state (e.g., misalignment or static load)
 - b. Dynamic (e.g., unbalance or rotor system instability)
2. Improper lubrication (insufficient or excessive)
3. External contamination
4. Improper installation
5. Incorrect sizing (e.g., wrong design)
6. Exposure to vibration while not rotating (false brinelling)
7. Passage of electric current through the bearing

When analyzing premature rolling element bearing failures, it is important to not only determine that the bearing is failing, but also to determine the underlying cause of that failure. The above list shows the major causes of premature bearing failure and can be used as an initial guide to determine the reason for

a bearing failure. To ensure success, elimination of premature bearing failures must be a major goal of any predictive maintenance program.

A rolling element bearing progresses through three failure stages:

1. Prefailure
2. Failure
3. Near Catastrophic/Catastrophic

NOTE: Each of these different failure stages exhibit specific vibration characteristics which require specific diagnostic/monitoring techniques.

Prefailure Stage—During the prefailure stage, the bearing is in the earliest stages of failure. It develops hairline cracks or microscopic spalls that are not normally visible to the human eye. During this stage there may be an increase in the high frequency (> 7 EPx) vibration produced by the bearing. If temperature or Prime Spike vibration measurements are taken during this stage, the levels will be normal. At this stage, the bearing usually has a significant amount of safe operating life left and it is not economical to replace it at this time.

Failure Stage—During the failure stage, the bearing develops flaws that are visible to the human eye. At this stage, the bearing usually produces audible sound and the temperature of the bearing will rise. Vibration amplitudes in the "bearing related" range (Prime Spike) reach easily detectable levels. Once the failure stage is reached, it is necessary to either change the bearing or increase the frequency of monitoring to estimate how long the bearing will safely operate before causing a catastrophic machine failure. This stage is considered the economical time at which to replace the bearing.

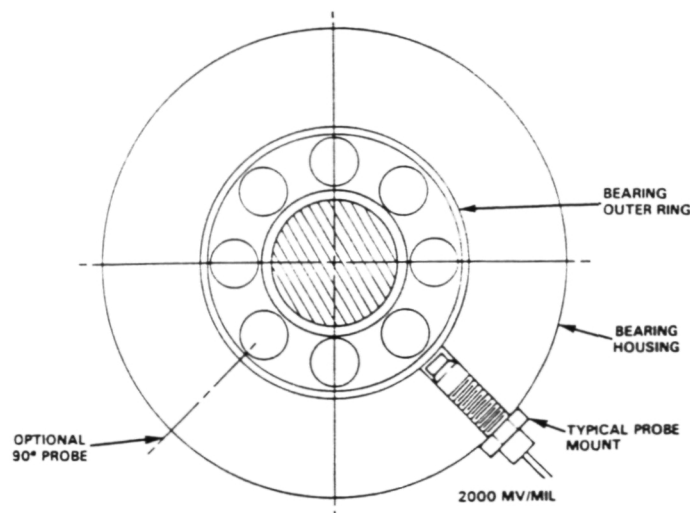
If the bearing is not removed during the failure stage, it will eventually enter the final progression of failure, the near catastrophic/catastrophic stage.

Near Catastrophic/Catastrophic Stage—When the bearing enters this stage, rapid failure of the bearing is **imminent**. Audible noise produced by the bearing significantly increases and the bearing temperature increases until the bearing overheats. Rapid wear causes the bearing clearance to increase, which then allows significant shaft motion relative to the bearing. Since a rolling element bearing is designed to **restrict** shaft motion, it can be very dangerous to allow the bearing to reach this stage due to the probability of creating a rub within the machine. Bearing-related (Prime Spike) vibration amplitude levels will show significant increases in this stage. High frequency vibration data may be unreliable in this stage and caution should be used in its interpretation. Due to "self-peening" of the bearing flaws, high frequency amplitude levels often **decrease** during this stage and it can **appear** that the bearing is in an earlier stage of failure. The occurrence of this "self-peening" phenomena is especially true for low speed machines.

Transducers and Instrumentation for Vibration Measurement and Monitoring of Rolling Element Bearings

1. REBAM Instrumentation System

REBAM is an acronym for Rolling Element Bearing Activity Monitor. The REBAM system uses a high-gain, low-noise eddy current proximity transducer that is installed in the bearing housing observing the bearing outer ring (Figure 2). The bearing outer ring contains the outer race. The REBAM transducer measures the very small (microinch/micrometre) deflection of the outer ring as the rolling elements pass the area observed by the transducer. These deflections are measured in terms of



TYPICAL REBAM* PROBE MOUNT

*ROLLING ELEMENT BEARING ACTIVITY MONITOR

FIGURE 2

displacement. The operating frequency range for the REBAM transducer system is from 0 Hz (DC) to 10 kHz (0 to 600 kcpm). The REBAM system is a direct and very sensitive method of rolling element bearing measurement. It offers a very high signal-to-noise ratio, as compared to casing-mounted acceleration or velocity measurements.

Through the use of electronic filters, the REBAM vibration signal is separated into rotor vibration and Prime Spike regions as previously discussed. The REBAM Prime Spike values occur in the range of 20 to 50 microinches (0.5 to 1 micrometres) peak-to-peak when the bearing is in good condition and increases to 100 to 300 microinches (3 to 8 micrometres) peak-to-peak when deterioration of the contacting surfaces occurs.⁴ A common practice is to take reference data to determine its "normal" level when the bearing is in a known good condition. Alert and Danger alarm levels are then typically set at three and ten times the "normal" level for the bearing. Field tests confirm that by using these alarm levels, adequate failure protection is usually provided.⁵

2. Shaft Relative Instrumentation System

Shaft relative measurements (i.e., eddy current proximity transducer) have been accepted industry-wide as the primary measurement for vibration monitoring and diagnostics of fluid-film bearing machines. However, a proximity probe based system can be used effectively to monitor rolling element bearing performance and it also provides rotor-related vibration information for the machine. The typical operating frequency range for an eddy current proximity transducer is from 0 Hz (dc) to 10 kHz (0 to 600 kcpm). As is the case with the REBAM transducer, the proximity probe vibration signal can be separated with electronic filters into the rotor vibration and prime spike regions. As previously discussed, this signal separation provides the information necessary to effectively analyze and monitor rolling element bearing machinery.

3. Casing Vibration Instrument Systems

Rolling element bearing condition can be monitored by using casing measurements. Overall velocity or displacement, Prime Spike velocity, and the high frequency

acceleration region can be used. Bently Nevada can provide accelerometer or velocity transducer-based systems to monitor rolling element bearing condition. Overall casing velocity or displacement provides a means for determining the general mechanical condition of rolling element bearing machinery.

For a velocity transducer based system, the frequency range used is from 10 Hz to 1 kHz (600 cpm to 60 kcpm). For an accelerometer based system, the frequency range used is from 10 Hz to 2.5 kHz (600 cpm to 150 kcpm). This frequency range includes the rotor vibration frequency region and overlaps the lower end of the Prime Spike frequency region. This range gives very good indication of rotor-related malfunctions and it is also somewhat sensitive to bearing-related problems.

As stated previously, the Prime Spike region is used by Bently Nevada to monitor the rolling element bearing-related frequencies (inner/outer race defects). By filtering out the rotor-related vibration signals (i.e., 1X, 2X, etc.), it is possible to get better signals related to the rolling element bearing condition. The Prime Spike frequency region includes the fundamental element passage frequency (EPx) and harmonics up to 7 EPx.

If an accelerometer-based system is used, Prime Spike and high frequency measurements are available. However, due to the noise susceptibility problems previously mentioned, the high frequency measurements should be used only as a possible early indicator of impending rolling element bearing problems. The high frequency range used by Bently Nevada is from 5 kHz to 25 kHz (300 kcpm to 1500 kcpm). High frequency measurements are useful when diagnosing certain machine malfunctions previously mentioned.

The following alarm threshold guidelines were established for the three diagnostic techniques based on field tests conducted by Bently Nevada:

1. Overall velocity: 0.3 in./sec. (7.7 mm/s) pk.
2. Prime spike region: 0.1 to 0.15 in./sec. (2.5 to 3.8 mm/s) pk.
3. High frequency region: 3 to 4 g pk.

NOTE 1: These high frequency levels, as measured with the Bently Nevada Trendmaster accelerometer, are typically 10 times higher in amplitude in this region than competing units.³

NOTE 2: These alarm threshold levels for balance-of-plant equipment should be considered as an **initial guide only**. The levels may need adjusting up or down, depending on how an individual monitored machine behaves.

When using casing measurement systems, two key factors should be considered: (1) signal amplitude versus transmission distance and (2) the measurement's susceptibility to noise. The farther away a vibration measurement is made from the vibration source, the more the signal will be attenuated. Most rolling element bearing machines have joints between machine parts which further attenuates the signals. Figure 3 shows that there is a sharp vibration signal attenuation at each joint. The closer the measurement is made to the machine vibration source, the better the measurement. For a rolling element bearing, it is suggested to be within 1 to 2 inches (25 to 50 mm) from the bearing. Another fact that must be considered is a comparison of the various transducer systems' signal-to-noise ratios. System signal-to-noise ratio is defined as the ratio of the amplitude of a desired signal at any point to the amplitude of noise signals at that same point. A comparison of the signal-to-noise ratios for the various transducer systems is shown in Figure 4. If not carefully considered, these two factors can have a large negative impact on the success of using casing measurements for monitoring.

Bibliography

1. Hansen, J. Steven and Harker, Roger G., "A New Method for Rolling Element Bearing Monitoring in the Petrochemical Industry," Presented at the Vibration Institute Seminar, New Orleans, Louisiana, June 1984.
2. Foiles, Bill, "Rolling Element Bearing Frequencies," Edited by Bently Nevada Corporation.
3. Applications Note, "Bently Nevada Trendmaster - Superior Performance from a Hand-held Accelerometer," Bently Nevada Corporation, September 1986.
4. Laws, C. W., "Condition Monitoring of Rotating Machines," Presented at the Institute of Measurement and Control, London Section Technical Meeting, January 1985.
5. Spencer, Donald B. and Hansen, J. Steven, "A Better Way to Monitor Bearings," Hydrocarbon Processing, January 1985.

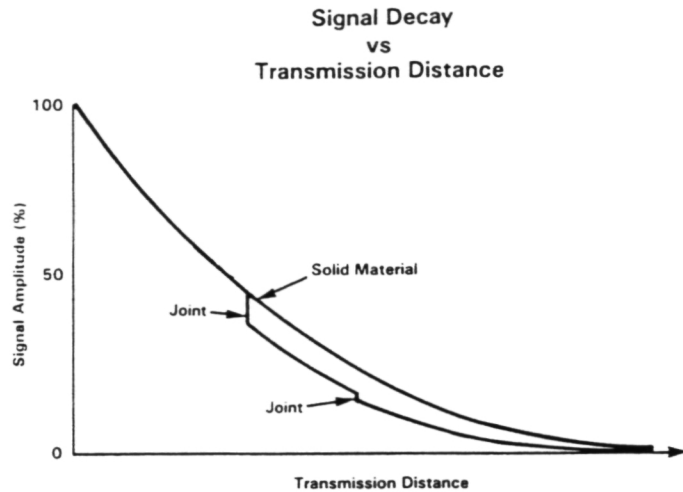


FIGURE 3

NOTE: It has been observed that traversing an interface (water jackets, double cases, etc.) can attenuate the signal by as much as a factor of ten (20 dB).

Transducer System Comparative Signal-To-Noise Ratios

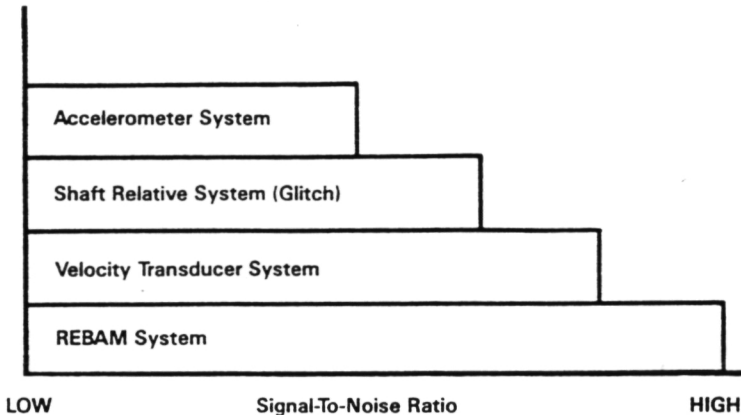


FIGURE 4

Summary

Based on the Bently Nevada two-part philosophy of (1) providing adequate warning to avert machine failures and (2) removing bearings only when they are likely to have visible evidence of an impending failure, the following conclusions are drawn:

1. Rotor vibration and Prime Spike displacement (obtained from permanently-installed REBAM probes) or overall velocity and Prime Spike velocity (obtained from a casing-based measurement), are the primary techniques used to monitor rolling element bearings. These measurements should be used to determine when to remove the bearing.
2. High frequency measurements are to be used only as a **possible indicator** of impending rolling element bearing failure and should generally not be used as the primary indicator to determine when to replace the bearing.

Rolling Element Bearing Frequencies

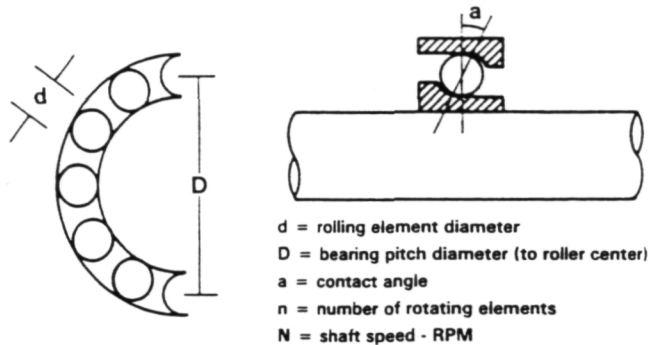
These calculated frequencies are essentially of academic interest, because (1) it frequently occurs that any flaw on any element rapidly generates secondary flaws on other elements and (2) knowledge of the existence and extent of a flaw is vital; however, the element that it is on is not too important because the entire rolling element bearing is normally replaced and not just the damaged portion.

Rolling element bearings find many uses in today's machinery. They can be found in motors, slow-speed rollers, gas turbines, pumps, and many other machines. Some of the reasons rolling element bearings are used are: low starting friction, low operating friction, ability to support loads at low (even zero) speed, lower sensitivity to lubrication (compared to fluid film bearings, thus a simpler lubrication system can often be used), and the ability to support both radial and axial loads in the same bearing. When some of these factors are important, rolling element bearings may be in use.

By themselves, rolling element bearings have very little damping, so whenever a machine with rolling element bearings traverses a balance resonance, large vibration can result. Also, compared to fluid film bearings, which generally have a long life, rolling element bearings have a limited fatigue life due to the repeated stresses involved in their normal use.

Rolling element bearings, regardless of type (ball, cylindrical, spherical, tapered, or needle) consist of an inner and outer race separated by the rolling elements, which are usually held in a cage (see Figure 1). Mechanical flaws may develop on any of these components. Using the basic geometry of a bearing, the fundamental frequencies generated by these flaws can be determined.

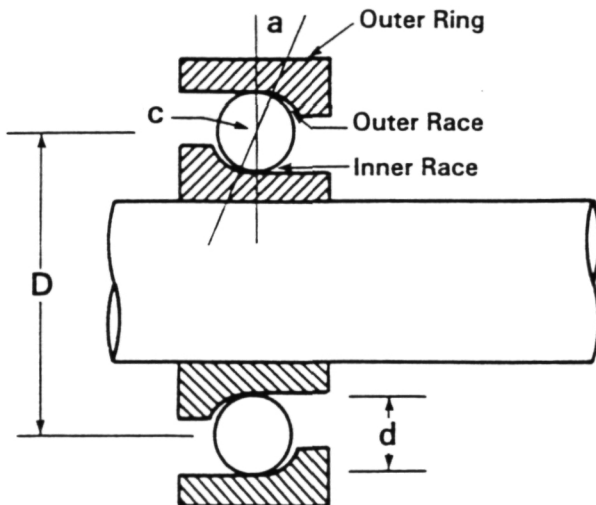
These frequencies may, and often do, include sum and difference frequencies. Often they are modulated by the speed of the equipment.



Frequency Component (CPM)

Cage Frequency	$(N/2)[1 - (d/D)\cos a]$
Roller Spin	$(N/2)(D/d)[1 - (d/D)\cos a]^2$
2x Roller Spin	$N(D/d)[1 - (d/D)\cos a]^2$
Outer Race Defect	$(N/2)n[1 - (d/D)\cos a]$
Inner Race Defect	$(N/2)n[1 + (d/D)\cos a]$

Figure 2. Frequencies when outer race is fixed
(Frequencies are exact if no slippage, or load changes occur).



- c = ball center
- d = rolling element diameter
- D = bearing pitch diameter (to roller center)
- a = contact angle

Figure 1. Basic rolling element bearing geometry
(Assuming no slippage, or change in bearing geometry with load).

For most applications, the outer race is fixed and does not rotate. However, in some instances, just the outer race or both races rotate. For the case of the outer race fixed, Figure 2 contains a summary of the main bearing frequencies.

Derivation of Bearing Frequencies

The basic geometry for rolling element bearings can be seen in Figure 1. Balls (rolling elements) passing over a flaw on the outer race or the inner race generate the inner and outer roller pass frequencies. These frequencies can be derived from the bearing geometry assuming there is no slippage or dimensional change with load. Rolling element flaws or a defect in the cage can generate the roller spin frequencies; a flaw in a roller can generate a 2X roller spin frequency by hitting both the inner and outer races with each roller rotation. Any of a combination of flaws can generate or be modulated by the cage frequency, the frequency with which the rollers revolve as a set. What follows is a derivation of the primary rolling element bearing frequencies when both races are allowed to rotate, and the simplified form when the outer race does not rotate.

Primary Rolling Element Bearing Frequencies (Both Races Rotating)

Notation as in Figure 1

- N_o = outer race angular speed
- N_i = inner race angular speed (= shaft rotative speed)
- n = number of rotating elements
- a = contact angle
- D = bearing pitch diameter
- d = rolling element diameter

The following fact is used in the derivation:

Linear velocity = (angular velocity) x (radius).

Since the outer race radius is $[D/2 + (d/2) \cos a]$, the velocity at a point on the outer race is

$$V_o = N_o [D/2 + (d/2) \cos a]$$

or

$$V_o = 1/2 N_o (D + d \cos a) \quad (1)$$

Similarly, the velocity of a point on the inner race is

$$V_i = 1/2 N_i (D - d \cos a) \quad (2)$$

The velocity of the center of a rolling element is

$$V_c = 1/2 (V_o + V_i)$$

So,

$$V_c = 1/2 [1/2 N_o (D + d \cos a) + 1/2 N_i (D - d \cos a)] \quad (3)$$

The angular frequency of the cage is

$$N_c = \frac{V_c}{D/2} \quad (4)$$

or

Cage Frequency

Both races allowed to rotate:

$$N_c = 1/2 \{N_o [1 + (d/D) \cos a] + N_i [1 - (d/D) \cos a]\} \quad (5)$$

For the outer race fixed:

$$N_c = 1/2 N_i [1 - (d/D) \cos a] \quad (5')$$

The frequency of a single rolling element passing a point on the outer race is:

$$N_o/c = N_o - N_c \\ = N_o - 1/2 \{N_o [1 + (d/D) \cos a] + N_i [1 - (d/D) \cos a]\}$$

so,

$$N_o/c = 1/2 |N_o - N_i| [1 - (d/D) \cos a] \quad (6)$$

NOTE: In the above equation and all following equations, the mathematical sign $||$ stands for the absolute value of the enclosed quantity. The absolute value is always a positive number.

Outer Race Ball Pass Frequency

Both races allowed to rotate:

$$n N_o/c = 1/2 n |N_o - N_i| [1 - (d/D) \cos a] \quad (7)$$

With the outer race fixed (neglecting negative signs), this reduces to:

$$n N_o/c = 1/2 n N_i [1 - (d/D) \cos a] \quad (7')$$

Similarly, the frequency of rollers passing the inner race is

$$n N_i/c = n(N_i - N_c)$$

or

Inner Race Ball Pass Frequency

Both races allowed to rotate:

$$n N_i/c = 1/2 n |N_i - N_o| [1 + (d/D) \cos a] \quad (8)$$

With the outer race fixed, this reduces to:

$$n N_i/c = 1/2 n N_i [1 + (d/D) \cos a] \quad (8')$$

The roller spin frequency, N_r , is the angular velocity of an individual rolling element.

Equating velocities on the outer race with those of a contacting point on a rolling element, one obtains the following:

$$V_o = 1/2 N_o (D + d \cos a)$$

and the velocity of a rolling element at the outer race,

$$V_o = 1/2 N_r (d) + 1/2 N_c (D + d \cos a)$$

Equating the two,

$$N_o (D + d \cos a) = N_r (d) + N_c (D + d \cos a) \quad (9)$$

Solve for N_r , the roller spin frequency.

Roller Spin Frequency

Both races allowed to rotate:

$$N_r = 1/2 D/d |N_o - N_i| \{1 - [(d/D) \cos a]^2\} \quad (10)$$

With the outer race fixed:

$$N_r = 1/2 D/d (N_i) \{1 - [(d/D) \cos a]^2\} \quad (10')$$

Summary

The fundamental rolling element bearing frequencies have just been derived with both races allowed to rotate. Figure 2 presents these frequencies with the outer race fixed, not rotating; this is most often the situation. In addition to these calculated rolling element frequencies, the bearing natural frequency can be generated. This frequency can be determined best by testing, not calculation. Knowing these frequencies gives both measurement and diagnostic information. The expected frequency ranges inform us as to the proper measurement system, and they enable us to isolate bearing-related frequencies for diagnostics.

A Practical Example of How to Establish the Required Filter Ranges for a Rolling Element Bearing Application

The following information must accompany any order for rolling element bearing monitors in order to establish the proper filter ranges for the rotor vibration and prime spike regions:

Bearing manufacturer and manufacturers bearing number
type of bearing (e.g., Angular contact ball, Cylindrical roller, etc.)

N = Shaft Speed RPM (or speed range if applicable)

n = Number of Rolling Elements

d = Rolling Element Diameter

D = Bearing Pitch Diameter (roller center to roller center)

a = Contact Angle

A good rule for setting the 1 to 7 times EPx is to use the outer race defect rate to set the 1EPx and the inner race defect rate to set the 7EPx cutoff of the filter.

Example:

SKF = N306 Single Row Cylindrical Roller

N = 3600 RPM

n = 11

d = 0.394 Inch

D = 2.007 Inch

a = 0 Degrees

$$\begin{aligned}1EPx &= (N/2) (n) ((1 - (d/D) (\cos a))) \\&= (3600/2) (11) ((1 - (.394/2.007) (\cos 0))) \\&= (1800) (11) (0.80) \\&= 15,899 \text{ RPM}\end{aligned}$$

$$\begin{aligned}7EPx &= (7) (N/2) (n) ((1 + (d/D) (\cos a))) \\&= (7) (3600/2) (11) ((1 + (.394/2.007) (\cos 0))) \\&= (7) (1800) (11) (1.20) \\&= 165,810 \text{ RPM}\end{aligned}$$

Therefore for this particular machine and bearing arrangement the rotor vibration and Prime Spike regions are respectively:

1/4 N to 3N = 900 RPM to 10,800 RPM (Rotor Vibration)

1EPx to 7EPx = 15,899 RPM to 165,810 RPM (Prime Spike)

BENTLY NEVADA

WORLDWIDE SALES AND SERVICE

United States of America: Phoenix, Arizona ☐ Los Angeles, California ☐ San Diego, California ☐ San Francisco, California

St. Petersburg, Florida ☐ Charlotte, North Carolina ☐ Atlanta, Georgia ☐ Chicago, Illinois ☐ Kansas City, Kansas

Baton Rouge, Louisiana ☐ Boston, Massachusetts ☐ Chester, New Jersey ☐ Buffalo, New York ☐ Cincinnati, Ohio ☐ Tulsa, Oklahoma

Portland, Oregon ☐ Philadelphia, Pennsylvania ☐ Pittsburgh, Pennsylvania ☐ Dallas, Texas ☐ Houston, Texas

International: Argentina ☐ Australia ☐ Brazil ☐ British Columbia ☐ Canada ☐ Chile ☐ Columbia ☐ Egypt ☐ France

Germany ☐ Greece ☐ India ☐ Indonesia ☐ Italy ☐ Japan ☐ Korea ☐ Kuwait ☐ Malaysia ☐ Mexico ☐ The Netherlands ☐ New Zealand

Nigeria ☐ Norway ☐ Pakistan ☐ People's Republic of China ☐ Qatar ☐ Quebec ☐ Saudi Arabia ☐ Singapore ☐ South Africa ☐ Sweden

Taiwan ☐ Turkey ☐ United Arab Emirates ☐ United Kingdom ☐ USSR ☐ Venezuela

Corporate Office: P.O. Box 157 • Minden, Nevada, U.S.A. • Telephone: 702-782-3611 • Telex: 7400983 BNC UC • Fax: 702-782-9253

© 1989 Bently Nevada Corporation

Verde GeoScience

Petrophysics & Rock Mechanics

Ultrasonic Transducers & Software

Test Systems & Instrumentation

Verde GeoScience

Petrophysics, Materials Testing, Ultrasonics, and Instrumentation

Karl B. Coyner, Ph.D.
Geophysicist

RR #1 Box 117
Tunbridge, Vermont 05077 USA
Phone or Fax: 802-889-3403

Verde GeoScience provides material testing and engineering services, instrumentation, and software to companies and individuals interested in measuring or predicting the acoustical, mechanical, electrical, thermal, and flow-related properties of rocks, sediments, soils, and other materials. These services are routinely required by those involved in geotechnical engineering, reservoir engineering, well-logging, geology, geophysics, seismic stratigraphy, mining, construction, and civil, mechanical, and materials engineering. The company is capable of single-task measurement services or more extensive involvement in engineering, research, or consortia projects. Verde GeoScience is actively working on projects for petroleum and related oil-field service companies, academic institutions, government laboratories, and consortia in the United States, Europe, Canada, and Japan.

Petrophysics & Rock Mechanics

The laboratory at Verde GeoScience provides accurate and precise petrophysical measurements on consolidated and unconsolidated cores, fluids, and other materials at elevated pressures and temperature. Projects usually require a combination of the following standard measurements and procedures:

- Compressional (P) and shear (S) wave velocities, dynamic moduli, and seismic wave attenuation
- Triaxial deformation: compressive strength, Young's modulus, and Poisson's ratio
- Density, porosity, and permeability
- Pore volume compressibility and bulk modulus
- Electrical resistivity and magnetic susceptibility
- Thermal expansion and thermal conductivity
- Resonant bar and hysteresis loop (phase angle) moduli and attenuation
- Strain amplitude and frequency effects on velocities, moduli, and attenuation
- Sample coring and thin section preparation
- CT scans and sample photography

Ultrasonic Transducers & Software

Verde GeoScience designs and manufactures Compound Ultrasonic Transducers™ and instrumentation for the precise determination of compressional and shear wave velocities and attenuations in rock, sediment, concrete, soil, and other materials. A novel feature of the standard transducer is the ability to independently propagate either of two polarized shear waves (S1 and S2) in addition to a compressional (P) wave. This combination enables the routine acquisition of all signals at any test condition, simplifying the measurement of dynamic moduli and elastic anisotropy. The transducers are manufactured in a variety of sizes and frequencies, and are available as individual units or as an integral part of our benchtop and high pressure test systems. Special designs are available for high temperature requirements. We are also experienced in configuring transducers for use in other load frames and pressure vessels that may already exist in your facility. In addition to our transducers, Verde GeoScience has developed instrumentation and software that combines a pulser-receiver and oscilloscope with a computer to enable complete ultrasonic measurements of velocity, attenuation, and dynamic moduli.

Test Systems & Instrumentation

Verde GeoScience also designs and manufactures innovative test systems for petrophysical measurements and material evaluations. These test systems are based on years of experience and knowledge accumulated in making the measurements for which they are designed; system performance, therefore, is assured. Key features include flexibility and adaptability, allowing multiple measurements to be made as a function of axial load, pressure, and temperature. The ultrasonic test system incorporates matched, high quality compound ultrasonic transducers for determining P and S wave velocities and attenuations. This system is available in a benchtop and high pressure versions with either manual or automatic control of confining and pore fluid pressures to 20,000 psi (140 MPa) and temperature capability to 130 °C. High pressure systems can also be used to measure pore volume compressibility, bulk modulus, permeability from 1 nDarcy to 500 mDarcy's, electrical resistivity, and triaxial deformation, which includes Young's modulus, Poisson's ratio, and compressive strength. Verde GeoScience includes with its systems a versatile data acquisition and control software package that is easily customized to automate measurement protocols and to facilitate data analysis. Complete or partial systems may be ordered. We would be pleased to consider your requests, offer suggestions, and prepare a proposal suited to your requirements and budget.

Verde GeoScience is committed to providing personalized, high quality core measurement services to our customers at a reasonable price. We offer the large variety of core measurements outlined below. The listed prices are for individual measurements on small projects. Larger projects and combinations of measurements are generally given a discount. We would be pleased to consider your special requests, offer suggestions, and design or conduct a measurement program suited to your requirements.

Compressional and Shear Wave Velocities, Anisotropy, Dynamic Elastic Moduli, and Attenuation

Ultrasonic compressional and shear wave velocities and attenuation are normally measured on 1 or 1.5 inch (25 or 38 mm) diameter samples using broad bandwidth transducers with center frequencies of either 500 kHz or 1 MHz. The transducers propagate a compressional wave and two orthogonally polarized shear waves along the sample axis; the two shear waves characterize seismic anisotropy in this direction. Confining and pore fluid pressures may be specified to 20,000 psi (138 MPa), and the jacketed sample may be completely or partially saturated with brine, gas, hydrocarbons, or other pore fluids. Verde GeoScience can assist in the selection of pore fluids and pressures. Measurements at high temperature are highly dependent on sample consolidation, pore fluid, and ultimate temperature; these measurements, therefore, are quoted separately. The measurements are summarized in a full report that includes a description of experimental procedure, tabulated velocities, calculated dynamic moduli (bulk, shear, and Young's moduli), porosity, grain density and bulk density, plus complete documentation of the digital waveforms and arrival time picks. For consolidated, intact samples the precision of the velocities is within 1%. If requested, a discussion section and interpretation of results may also be included. In addition to velocities, ultrasonic P and S wave attenuations can also be determined with a spectral ratio technique that compares the frequency content of measured signals to an aluminum standard. The charge for this is in addition to that for velocity measurements.

Ultrasonic Velocities

Ambient Temperature

Room pressure	\$65
One confining and pore fluid pressure (to 20,000 psi/138 MPa)	\$250
Each additional confining and pore fluid pressure	\$20

High Temperature

Measurements to 130°C or higher are available.	Call
--	------

Ultrasonic Attenuations

Determined utilizing spectral ratios; price per sample	\$100
--	-------

We recommend measurements at 5 confining pressures to characterize sample velocities. The total cost is:

First pressure	\$250
Additional pressures	4 x \$20 = \$80
Total	\$330

The quoted prices are applicable to consolidated samples and include sample preparation. For semi-consolidated and fractured samples or sediments a surcharge may be necessary for the specialized techniques required in preparation and measurements. Additional sample sizes can be accommodated at other transducer center frequencies; higher confining and pore fluid pressures are also available.

Verde GeoScience

Resonant Bar Modulus and Attenuation

\$1000/mode

The sample is prepared as a thin bar and is driven to resonance in either extensional, flexural, or torsional modes using a benchtop apparatus. The attenuation of the sample is calculated from the width of the resonant frequency peak. The center frequency of the resonant peak is used to calculate Young's modulus (extensional mode) and shear modulus (flexural and torsional modes). Repeated measurements at overtone frequencies are used to determine modulus and attenuation at multiple frequencies between approximately 1 kHz and 100 kHz, depending on the sample. Measurements may be carried out in a variety of saturation conditions.

Low Frequency and Strain-Amplitude Dependent Attenuation

Call

The stress-strain response of the sample to low frequency sinusoidal loading is used to determine the strain amplitude and frequency dependence of Young's modulus and extensional attenuation at frequencies near 1 Hz. Measurements may be carried out in a variety of saturation conditions.

Triaxial Deformation: Compressive Strength, Young's Modulus, and Poisson's Ratio

Triaxial deformation experiments are normally carried out on samples with a length to diameter ratio of approximately 2. The sample is instrumented with either strain gages or LVDT gage rings, and deformation is measured as a function of axial load to determine strength and modulus. The sample may be unconfined or jacketed with confining and pore fluid pressures to 20,000 psi (138 MPa). Measurements at elevated temperatures are also available.

Unconfined

\$300

Confining and pore fluid pressures to 20,000 psi (138 MPa)

\$400

Pore Volume Compressibility & Static Bulk Modulus

\$300

Pore volume compressibility and porosity at pressure are calculated from measurements of pore fluid volume expelled from the sample as a function of confining pressure; sample bulk modulus is calculated from external sample deformation measured with strain gages or LVDT gage rings.

Porosity, Bulk Density, and Grain Density

\$50

Permeability

Gas permeability measured at ambient conditions

\$50

Gas permeability at confining pressures to 20,000 psi (138 MPa)

\$125

Constant flow liquid permeability (greater than 1 milliDarcy) measured at a single confining and pore fluid pressure

\$300

Transient pulse liquid permeability (less than 1 milliDarcy) measured at a single confining and pore fluid pressure

\$900

Electrical Resistivity & Formation Factor

2-electrode technique; measurements as a continuous function of frequency between 10 Hz and 10 kHz, depending on sample and fluid resistivity, at confining and pore fluid pressure to 20,000 psi (138 MPa)

\$175

2-electrode technique; elevated temperatures to 250 °C

\$300

Magnetic Susceptibility

\$35

Thermal Expansion and Thermal Conductivity

Call

CT Scan & Sample Photography

\$150

Thin Section

\$20

Sample Preparation:

No charge

Compound Ultrasonic Transducer TM

Verde GeoScience's Compound Ultrasonic TransducersTM accurately measure the compressional and shear wave velocities and attenuations of materials subjected to rigorous petrophysical and mechanical testing. Each transducer contains a novel arrangement of one compressional (P) and two polarized shear (S1 & S2) elements to enable the independent propagation or reception of broad bandwidth, pulse-like signals at any point during an investigation. A pair of matched transducers are normally used to transmit and receive signals through samples of rock, soil, ice, and concrete; individual transducers can also be used, however, in a pulse-echo mode. The transducers may be used with ultrasonic equipment available from Verde GeoScience or other commercial sources. Various configurations are available for benchtop, high pressure, high temperature, and immersed applications.

Features

A novel arrangement of compressional and two polarized shear elements are contained within a single transducer. Individual signals are selected by a control signal that originates from either a manual control box or a computer digital I/O port. Compressional and shear wave properties are routinely determined with a single set of rugged transducers. Dynamic moduli (Young's modulus, Poisson's ratio, shear and bulk modulus) are calculated from the combined compressional and shear measurements.

In addition to a compressional wave, two independent and orthogonally polarized shear waves are propagated, allowing instant assessment of shear wave anisotropy and reducing the number of measurements required for fully characterizing anisotropy.

Ultrasonic crystal elements are highly damped, producing a broadband signal with superior resolution and bandwidth; sharp, well-defined signals are propagated through the sample, allowing precise determination of compressional and shear wave arrivals and windowing of signals for spectral analysis.

Transducers are available in a variety of frequencies and configurations for benchtop, high pressure, and high temperature applications. They can be customized to fit into existing pressure vessels and loading frames, enabling the inexpensive integration of ultrasonic measurement capabilities.

Compound Ultrasonic Transducer TM

Specifications

Element Diameter:	1.0 inch (25.4 mm)
Nominal Center Frequencies:	125 kHz, 250 kHz, 500 kHz, 1 MHz, and 2 MHz
Sample Diameters:	0.5, 0.75, 1.0, 1.5, 2.0, 3.0, and 4.0 inch 13, 20, 25, 38, 50, 75, and 100 mm
Control Signal:	± 5 Volt, 16 mA
Connector:	Bendix PT02A8-3P or .040" (1 mm) diameter Be-Cu pins (2)
Cable:	1 meter coaxial and 1 meter single-conductor control cable

Proper transducer selection depends on sample size, acoustical characteristics, and measurement goals. For many consolidated rocks a 1 inch diameter by 1 inch long (Ø 25mm x 25mm) sample is adequately measured with 1 MHz transducers. Larger samples, semi-consolidated sediments, and concrete require lower frequencies. Please call us with your requirements.

The Compound Ultrasonic TransducerTM is highly damped in order to produce wide bandwidth, pulse-like signals. For a nominal center frequency of 1 MHz significant energy is contained at frequencies from 600 kHz to 1.2 MHz. Transducers are supplied with a calibration certificate which includes plots of spectra and signals propagated through 6061 aluminum or other designated standards.

Models

Standard unit; Bendix connector; if intended for immersed applications, specify fluid
Model # CUT-B-X-Y

High Pressure unit; pressures and axial loads to 20,000 psi (138 MPa); high pressure Be-Cu pins
Model # CUT-HP-X-Y

X is frequency in kHz; standard frequencies are: 125, 250, 500, 1000, and 2000 kHz; Y is sample diameter in inches (in) or millimeters (mm) ; standard sizes are 0.5, 0.75, 1.0, 1.5, 2.0, 3.0, and 4.0 inches, and 13, 20, 25, 38, 50, 75, and 100 millimeters; other frequencies and sizes can also be specified.

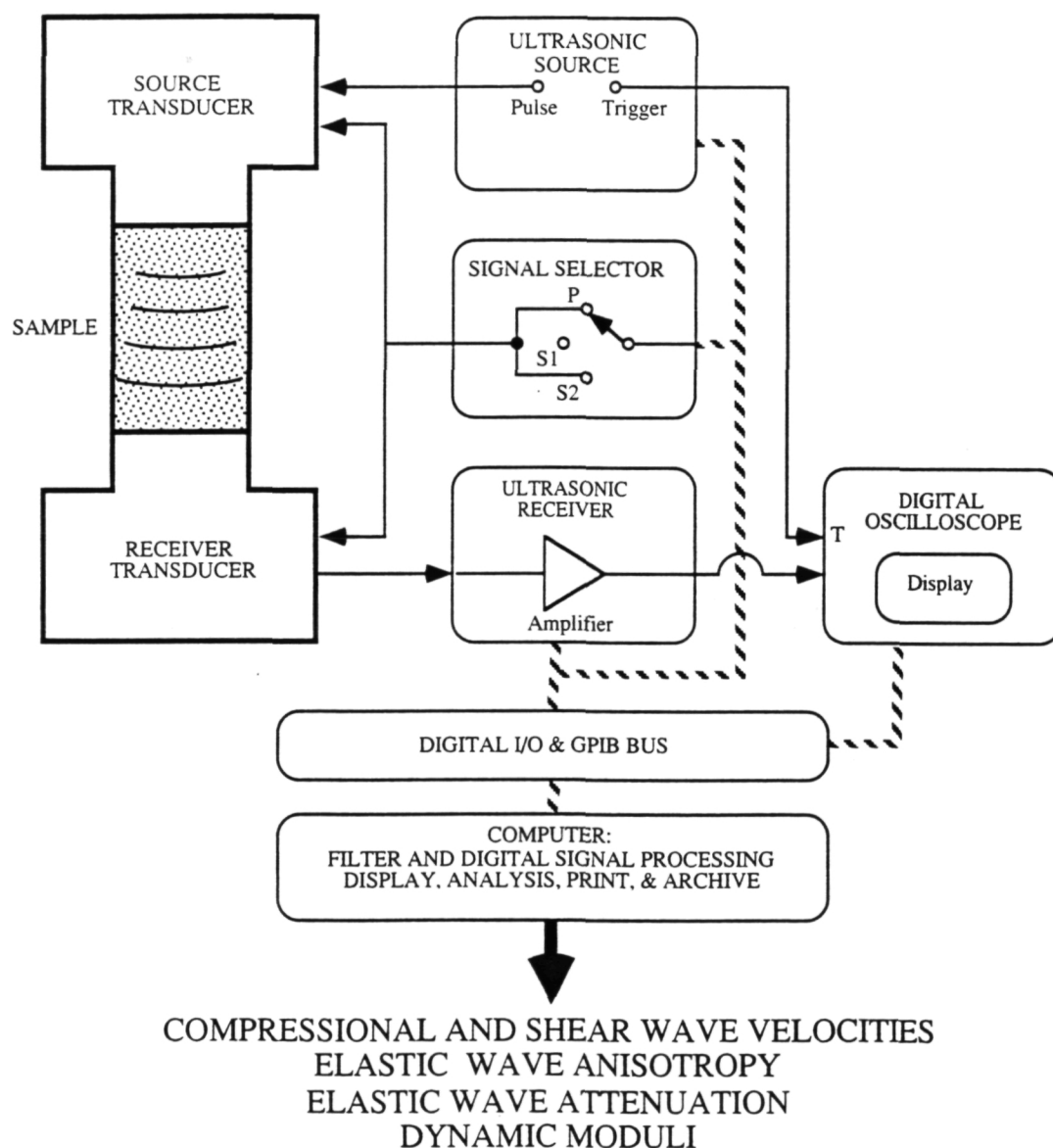
Control Box
Model # CUT-CB-voltage
specify voltage: 115 or 230 VAC; 50-60 Hz

High temperature models are custom designed and manufactured: please call with your requirements.

Also available from Verde GeoScience are complete measurement systems that integrate transducers with an ultrasonic pulser-receiver, digital oscilloscope, computer interface, and velocity and attenuation analysis software. Verde GeoScience also offers measurement and analysis services, plus engineering, design, and manufacturing assistance for specialized requirements.

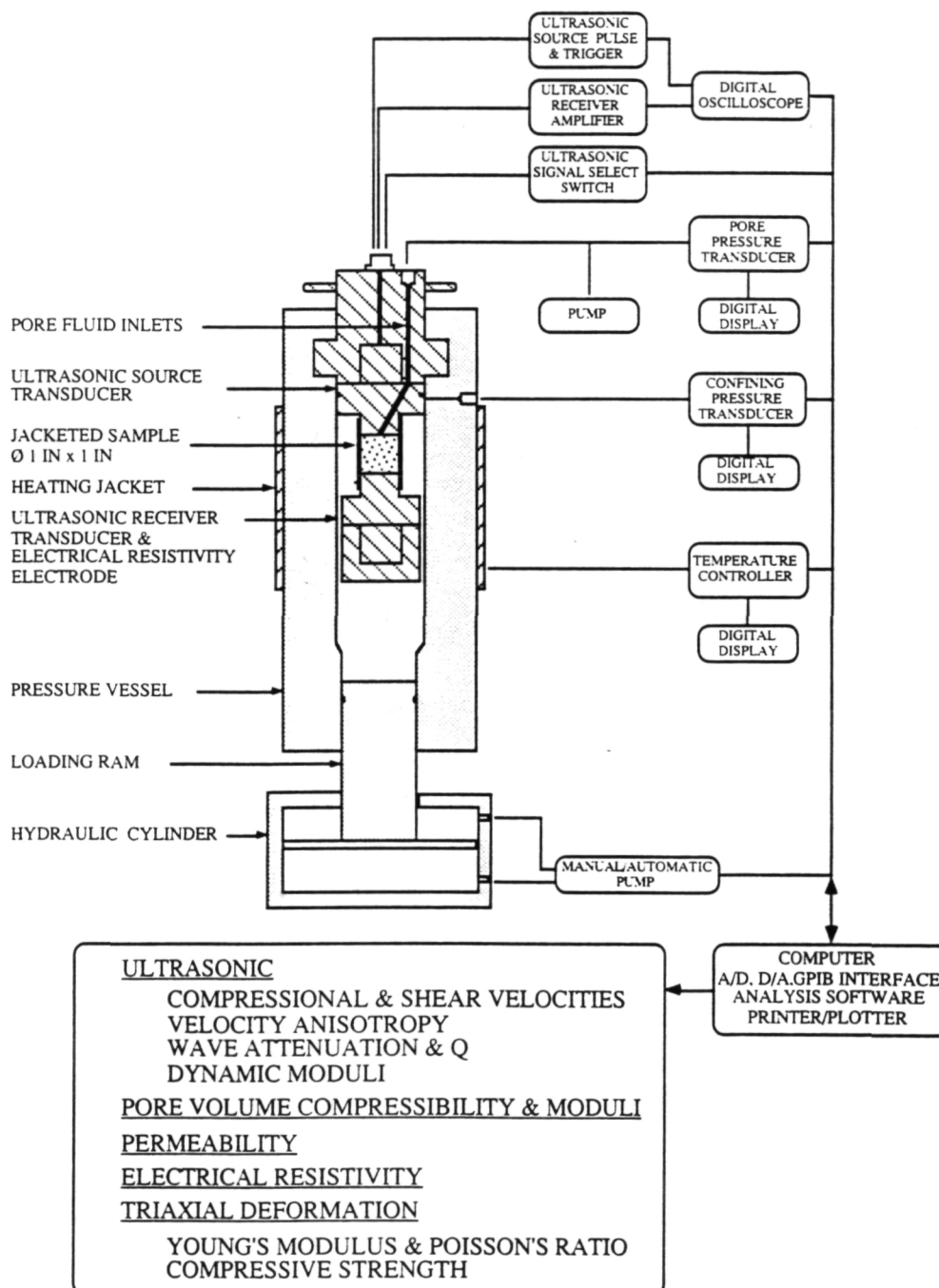
Test Systems - Ultrasonic

Verde GeoScience designs and manufactures innovative test systems for petrophysical measurements and materials evaluation. Ultrasonic test systems are based on the integrated components schematically shown below, all or part of which may be ordered from the company. Verde GeoScience has developed an unparalleled ultrasonic analysis software package that supports virtually all digital oscilloscopes with a GPIB interface. Test systems are normally customized to the customer's requirements and budget. Specifications include sample sizes, pressures, temperatures, other desired measurement capabilities, and different combinations of automatic and manual features. A basic and inexpensive benchtop version is ideal for applications where high pressure is not required, and is wonderfully suited for educational demonstration of the fundamental properties of elastic wave propagation, including compressional and shear wave velocities, attenuation, and anisotropy as a function of saturation and lithology.



Test Systems - High Pressure

Verde GeoScience's advanced petrophysical properties measuring system is schematically shown below. The test system measures the fundamental elastic wave properties as a function of confining pressure, pore pressure, temperature, and applied axial load. Flexibility and adaptability are key design features, however, and the systems can also be configured to measure bulk properties, permeability, resistivity, and triaxial deformation. Pressures and axial load can be optionally specified for manual or automatic operation. A versatile data acquisition and control software package that is used in the laboratory of Verde GeoScience is included with all systems.



CN31 (0) (2)
TURNER J/PUBLICATION
MARSHALL SPACE FLIGHT CENTER
HUNTSVILLE AL
DELETIONS OR CHANGES 544-4494
RETURN ADDRESS CN22D 000002444

WYLE
LABORATORIES

P.O. Box 077777, Huntsville, AL 35807-7777
Phone (205) 837-4411, Fax (205) 830-2109